THE ROLE OF CANOE/AFADIN IN *DROSOPHILA* MORPHOGENESIS

Jessica K. Sawyer

A dissertation submitted to the faculty of the University of North Carolina at Chapel Hill in partial fulfillment of the requirements for the degree of Doctor of Philosophy in the Department of Biology.

Chapel Hill
2010

Approved by:

Dr. Mark Peifer
(advisor)

Dr. Victoria Bautch

Dr. Bob Goldstein

Dr. Bob Duronio

Dr. Alan Fanning

ABSTRACT

JESSICA K. SAWYER: The Role of Canoe/Afadin in *Drosophila* Morphogenesis
(Under the Direction of Mark Peifer)

Morphogenesis is the amazing process of forming tissues and organs to build an animal. Coordinating cell-cell adhesion and cell shape change are both essential for morphogenesis. Adherens junctions(AJs) are thought to form mechanical attachments between cells by linking the cytoskeletons of neighboring cells via the cadherin-catenin complex. This linkage was long thought to be direct, but recent evidence called this into question. The nectin-afadin complex has also been proposed to mediate linkages between AJs and the cytoskeleton. In my dissertation research, I investigated the role of Canoe(Cno)/Afadin in *Drosophila* morphogenesis.

First, I found that Cno is not required for the establishment of adhesion or polarity. However, loss of Cno impairs morphogenesis from the start. Cno is required for the first step of gastrulation, a process requiring apical constriction. Apical constriction initiates, but is incomplete. In the absence of Cno, the actomyosin network disconnects from AJs, uncoupling cell shape change and actomyosin constriction. Cno is also required for the elongation of the body axis, a process requiring cell intercalation. Planar polarity of junctional proteins along the dorsal-ventral(DV) axis and cytoskeleton proteins along the anterior-posterior(AP) axis is thought to be an important driving force for intercalation and axis elongation. In the absence of Cno, axis elongation is slowed.

Planar polarity of junctional proteins, but not cytoskeletal proteins is enhanced. Cno is planar polarized on the AP axis with cytoskeletal proteins, suggesting that Cno restrains planar polarity by facilitating connections between AJs and the actomyosin network along the AP axis.

I next investigated where Cno acts to regulate AJ-actomyosin linkages. Cno localizes to AJs and is enriched at tricellular junctions with a subpool of actin, suggesting these structures may play key roles in apical constriction and in restraining planar polarity. Cno has multiple direct interactions with AJ proteins, but is not a core part of the cadherin-catenin complex. Cno does not require either the cadherin-catenin complex or the nectin Echinoid for its cortical localization. Instead, Cno localizes to AJs by a Rap1 and actin-dependent mechanism. Taken together, these data suggest that Cno is required to regulate AJ-actomyosin linkages during dynamic morphogenesis.

ACKNOWLEDGEMENTS

So some people helped me. In fact, a lot of wonderful people helped me on my journey through graduate school. The faculty, postdocs, and students are all enthusiastic, fun, and intelligent, making the Biology Department at UNC a great place to do science. I would like to thank my advisor, Mark, for giving me so many opportunities to grow as a scientist. I would also like to thank my fantastic committee: Vicki, Bob D., Bob G., and Alan. Their enthusiasm and support for my project and me personally has been invaluable. I would also like to thank all the members of Peifer lab past and present, who have made the lab a great place to be. I especially want to thank Tony, a former postdoc, who helped me immensely when I was getting my project started and is still a great resource and colleague. I want to thank Steph, Kelly, and Nathan who all did their rotations with me and still decided to join the lab. They have been great friends and colleagues. I would like to thank Doug, a former undergraduate researcher, for all his hard work and his friendship. I would like to thank my parents, Brian and Paulette, for their unconditional support of my career path and me (and for the Fisher Price microscope that got me started). Finally, I would like to thank my husband Jacob for his love, support, and patience (and the times he helped me sort flies). I can't imagine a better person to have taken this journey with and I look forward to seeing where the future takes us.

TABLE OF CONTENTS

LIST OF TABLES

Tables

LIST OF FIGURES

Figures

CHAPTER 1

CHAPTER 2

ABBREVIATIONS

αcat	α-catenin
AJ	Adherens Junction
AP	anterior-posterior
aPKC	Atypical Protein Kinase C
Arm	Armadillo/β-catenin
Baz	Bazooka
Cno	Canoe
Crb	Crumbs
cytoD	cytochalasin D
DEcad	*Drosophila* E-cadherin
DIC	Differential Interference Contrast
Dlg	Discs large
DMSO	Dimethyl sulfoxide
DV	dorsal-ventral
Ecad	E-cadherin
Ed	Echinoid
GBE	germband elongation/extension
GFP	Green Fluorescent Protein
Mira	Miranda

moe-GFP	moesin-GFP
MT	microtubule
MZ	maternal and zygotic
Nrt	Neurotactin
PCR	Polymerase Chain Reaction
Pyd	Polychaetoid
RA	Ras association
SEM	Scanning Electron Microscopy
zipGFP	Zipper(Myosin II heavy chain)-GFP
ZO-1	zonula occludens-1

CHAPTER 1

MORPHOGENESIS: THE ORIGAMI OF LIFE

Preface

Origami is the art of taking of a plain sheet of paper and creating a beautiful form. In development we all begin as a disorganized group of cells with no defined shape. The role of morphogenesis is to shape and organize cells as they divide and grow, ultimately creating a cohesive form. Cell-cell adhesion and cell shape change are two essential parts of morphogenesis, but how are these two processes coordinated? My dissertation research addresses this question.

As an introduction, I am including a portion of a review chapter I wrote with my advisor, Mark Peifer, and a former postdoctoral fellow, Tony J. Harris. Together we wrote a chapter entitled, "How the cytoskeleton helps build the embryonic body plan: models of morphogenesis from *Drosophila*", for the journal *Current Topics in Developmental Biology* in 2009 (Harris et al., 2009). In this review we discuss the dynamic nature of epithelial morphogenesis, for which *Drosophila* is an ideal model system. I have included the two sections of the review I wrote, which are relevant to my dissertation research.

Internalizing mesoderm: Actomyosin contractility drives apical constriction

Internalization of the ventral furrow cells (mesoderm) and posterior midgut (endoderm) are the first steps in Drosophila gastrulation (reviewed in (Lecuit and Lenne, 2007; Leptin, 1999). The ventral furrow involves a stripe of cells along the ventral midline that is 18 cells wide and 60 cells long. These cells will invaginate and form a tube in the interior of the embryo. Eventually, cells in the tube will disperse into a single layer of cells beneath the ectoderm and become mesoderm (Costa et al., 1993). This process of internalization is characterized by four distinct phases. First, cells apically flatten and display random cell constrictions. Second, cells spanning a 12-cell width begin apically constricting in a coordinated fashion, resulting in a bend in the epithelium. As cells constrict, small membrane protrusions/blebs form on the apical surface, which may be a response to, or possibly aid in, the reduction of the apical surface area. At the same time, cells elongate along the apical–basal axis to 1.7 times their original length. Additionally, their nuclei shift basally and their basal surfaces expand. Third, after the ventral furrow cells have reached their maximum length, they begin to shorten back to their original length, while remaining constricted apically. This shortening results in a wedge shape and may help to move the furrow beneath the epidermis. Finally, the lateral epidermis on either side of the furrow covers the tube of mesoderm, separating it from the overlaying ectoderm (Costa et al., 1993; Leptin et al., 1992; Sweeton et al., 1991). Almost 20 years ago, apical constriction of ventral furrow cells was proposed to be a result of contraction of the actin cytoskeleton underlying the apices of the cells (Young et al., 1991). A pathway that instructs cells to constrict has begun to emerge, starting with specification and ending with cell shape change (Fig. 1A). First, specification and

internalization of the mesoderm is controlled by the transcription factors Twist and Snail. Both genes are required for mesodermal fates. Loss of function of these genes results in elimination of ventral furrow formation and an expansion of lateral fates into the ventral domain (Costa et al., 1993). Twist and Snail have many transcriptional targets, including some involved in triggering constriction. One is the secreted ligand Folded Gastrulation (Fog), and Concertina (Cta), a G protein a12/13 subunit, acts downstream of this ligand (Costa et al., 1994; Morize et al., 1998). However, the G-coupled receptor for Fog remains a mystery. RhoGEF2, a regulator of the Rho family GTPases, acts downstream of Fog–Cta signaling and links the signaling pathway with the cytoskeletal machinery (Barrett et al., 1997; Rogers et al., 2004). Expression of dominant-negative Rho1 results in ventral furrow defects similar to *fog* and *cta*, suggesting that RhoGEF2 mostly likely activates Rho1 to initiate cell shape change (Barrett et al., 1997). The transmembrane protein T48, a RhoGEF2-binding partner regulated by Twi, appears to function in parallel to Fog–Cta signaling to recruit Rho-GEF2 apically for activation (Kolsch et al., 2007). The existence of parallel pathways is supported by the fact that mutations in *fog*, *cta*, or *T48* lead to uncoordinated constriction of cells, but the ventral furrow eventually forms (Costa et al., 1994; Dawes-Hoang et al., 2005; Kolsch et al., 2007; Sweeton et al., 1991). In contrast, loss of RhoGEF2 severely disrupts apical constriction and the ventral furrow never forms (Barrett et al., 1997; Hacker and Perrimon, 1998). Interestingly, ectopic expression of Fog leads to ectopic apical constrictions in the embryo (Costa et al., 1994); however, in embryos lacking RhoGEF2, ectopic expression of Fog fails to produce ectopic constrictions (Barrett et al., 1997).

How do these proteins affect the contractile machinery? Further research suggests that pathway activation affects apical localization of RhoGEF2 and/or Myosin II. In wild-type ventral furrow cells, RhoGEF2 and Myosin II are first localized basally at the tips of cellularization furrows. At gastrulation onset they are relocalized apically and cells begin to constrict (Kolsch et al., 2007; Nikolaidou and Barrett, 2004). T48 and Cta each mildly affect the localization of RhoGEF2, but if both proteins are absent RhoGEF2 does not become apically localized (Kolsch et al., 2007). *cta* mutants have reduced and patchy accumulation of apical Myosin II, resulting in constriction of some, but not all, cells in the furrow (Nikolaidou and Barrett, 2004). Ventral furrow cells lacking RhoGEF2 fail to accumulate Myosin II apically in all cells and are therefore unable to constrict (Nikolaidou and Barrett, 2004), suggesting it is at the convergence of the constriction signals.

Constriction involves assembly of both actin and Myosin II. Apical actin organization appears to be regulated by Abelson (Abl) kinase, a nonreceptor tyrosine kinase, and also affects the formation of the ventral furrow (Fox and Peifer, 2007). In *abl* mutants, furrow constriction is uncoordinated, but cells are eventually internalized, like *fog* and *cta* mutants. Interestingly, the localization of actin is disrupted in *abl* mutants, while it is not in *cta* mutants. However, in *RhoGEF2* mutants, the localization of F-actin is disrupted. This suggests that RhoGEF2 and Abl work in parallel to regulate actin localization in the ventral furrow. Enabled (Ena), an actin regulator, is a known target for Abl in other processes. Ena localization to AJs is normally downregulated in the ventral furrow cells. In *abl* mutants, Ena is not downregulated, resulting in ectopic, disorganized apical actin. Consistent with Ena downregulation being critical, reduction of *ena* in an *abl*

mutant background suppresses the *abl* ventral furrow phenotype (Fox and Peifer, 2007). This suggests that through Ena, Abl helps to regulate actin so coordinated constriction can take place.

Once in place, how does a contractile cytoskeleton create cell shape change? Cells must both create and resist forces for coordinated cell shape changes to occur within a tissue. One hypothesis for apical constriction was the purse string model, where actin filaments localized in rings at cell junctions slide together with the help of Myosin II to reduce the apical area of all the cells in concert (Costa et al., 1993; Young et al., 1991). However, apical actin and Myosin II are not restricted to rings at AJs, but instead cover the entire apical surface. Recent work provided detailed insights into the process, revealing that apical constriction in the ventral furrow is created by pulsed contractions of this actomyosin apical network (Martin et al., 2009). High-resolution live microscopy of ventral furrow cells revealed cyclic formation of Myosin II coalescences over the apical surface of the cells. These coalescences occur within a larger Myosin II network that appears to shrink with each pulsed coalescence, and then remain in this smaller state, suggesting a ratchet model for apical constriction. Additionally, these coalescences are attached to AJs at discrete sites and bend the plasma membrane inward, resulting in coordinated apical constriction across the epithelial sheet (Martin et al., 2009). Indeed, if AJs are disrupted, Myosin II coalescences form, but no shape change occurs (Dawes-Hoang et al., 2005). The ratchet model is further supported by analysis of Myosin II localization in *twist* and *snail* mutant embryos. As mentioned above, apical constriction fails to occur in these mutants. Interestingly, in *twist* and *snail* mutants the localization of Myosin II becomes more concentrated at cell junctions (Martin et al., 2009). If the purse

string model were correct, cells should still be able to constrict with Myosin II localized at cell junctions, but they do not. However, it is possible that Myosin II is not properly activated at the junctions in *twist* and *snail* mutants. *twist* and *snail* differentially affected the formation of Myosin II coalescences. In *twist* mutants, Myosin II coalescences were reduced with few pulsed constrictions (Martin et al., 2009), while in *snail* mutants both the Myosin II coalescences and pulsed constriction were lost. In double-mutant embryos, both Myosin II coalescences and pulsed constriction were also absent, suggesting that Snail is required to initiate apical constriction.

Actomyosin contractility also drives formation of the posterior midgut invagination (PMGI), which internalizes the endoderm. This cup-like structure forms as the ventral furrow seals and germband extension begins. The cells that will invaginate surround the pole cells at the posterior end of the embryo, with 10 cells extending dorsally and ventrally from the pole cells and 5 cells on each lateral side (Costa et al., 1993). PMGI is surprisingly similar to ventral furrow formation and is governed by many of the same players. Again, the process begins with apical flattening, proceeds with coordinated constriction, lengthening of cells in the apical–basal axis, downward shift of nuclei, and basal expansion, and as apical constriction proceeds, the cells begin to shorten, deepening the overall cup structure. Loss of *fog* or *cta* function completely blocks posterior midgut invagination, while it only delays the invagination of the ventral furrow (Parks and Wieschaus, 1991; Sweeton et al., 1991). Posterior midgut formation is also disrupted in embryos lacking RhoGEF2 or expressing a dominant-negative form of Rho1 (Barrett et al., 1997). Posterior midgut cells also relocalize Myosin II to their apical ends (Young et al., 1991). Together, these results suggest actomyosin contractility plays

an important role in the apical constriction of the posterior midgut cells, as it does in the ventral furrow. However, other influences impact the PGMI. For example, the invagination has polarity, with more dorsal cells constricting before the more ventral cells (Sweeton et al., 1991). Internalization is also aided by the contraction of the dorsal side of the embryo, which pulls the posterior midgut cells, and extension of the germband, which pushes them and eventually seals the invagination into the interior of the embryo (Costa et al., 1993). It is also unclear how the contractile cytoskeleton behaves during the apical constriction of posterior midgut cells. It will be interesting to determine whether the purse string or ratchet model best fits the apical constriction of these cells.

Germband extension: Actomyosin contractility driving cell intercalation

The third event in gastrulation is germband extension (GBE), in which the ectoderm narrows in the dorsal–ventral (D–V) axis and lengthens in the anterior–posterior (A–P) axis. Because of the constraints of the eggshell, this pushes the posterior end of the embryo up and over the anterior end. Cell intercalation drives extension of the germband through a convergence and extension process (Lecuit and Lenne, 2007; Zallen, 2007). As mentioned above, the germband begins to elongate as the posterior midgut invaginates, and eventually seals it. The posterior two thirds of the embryo contains the cells that will become the germband. In about 2 h the germband elongates along the A–P axis, doubling its length, and shortens in the D–V axis, halving its width (Costa et al., 1993). Most studies of GBE have focused on the anterior part of the germband because the cells move more slowly and are thus easier to image. Moreover, most of the actual cell intercalation occurs in this region.

Early studies of cell behavior in the germband revealed cells shift their positions relative to one another (Irvine and Wieschaus, 1994). Cells intercalate primarily between dorsal and ventral neighbors, and rarely between anterior and posterior neighbors. Before the onset of GBE, cells are arranged in a hexagonal array, resembling a honeycomb. As GBE proceeds cells become disordered, resulting in four-cell arrays (Bertet et al., 2004) and multicellular rosettes (Blankenship et al., 2006; Zallen and Wieschaus, 2004). Polarized cell junction remodeling accompanies and may drive this polarized cell behavior. The simple four-cell arrays begin with a long cell–cell contact between A–P neighbors, while D–V neighbors are not in contact (this is referred to as a Type I junction). Next the contact between A–P neighbors shrinks, so that all cells in the group are touching (a Type 2, X-shaped junction). Type 2 junctions then resolve so that D–V neighbors form a long cell–cell contact and A–P neighbors are separated (a Type 3 junction), completing a cell–cell intercalation event (Bertet et al., 2004); Fig. 1B). In addition to four-cell arrays, the germband also assembles multicellular rosettes, where the vertices of 5–11 cells meet. However, the behavior of these structures is similar to four-cell arrays. Contacts between A–P neighbors shorten until multiple cells meet to form a structure resembling a cut pie. Then, contacts between D–V neighbors grow displacing A–P neighbors away from each other along the A–P axis (Blankenship et al., 2006; Zallen and Wieschaus, 2004; Zallen and Zallen, 2004); Fig. 1B). Planar polarized actomyosin activity is at work in the germband (Fig. 1B). Cells in the germband differentially localize proteins along their A–P and D–V boundaries. F-actin becomes enriched at the A–P boundary first, and then nonmuscle Myosin II follows (Blankenship et al., 2006; Zallen and Wieschaus, 2004). Significantly, Myosin II localizes at these

contacts as they constrict during cell intercalation (Bertet et al., 2004). Moreover, partial loss of Myosin II activity in Myosin II zygotic mutants produces slight defects in GBE; while inhibition of Rho kinase (Rok), which normally phosphorylates and activates Myosin II, severely affects GBE (Bertet et al., 2004). Thus, actomyosin activity appears to constrict cell–cell contacts between A–P neighbors to drive cell intercalation. In fact, computer models suggest constriction of cell borders in a polarized direction is sufficient to result in the elongation of a group of cells (Honda et al., 2008; Rauzi et al., 2008). Before GBE, the cells are not polarized and therefore all cell boundaries probably experience similar tension on the junctions. However, when Myosin II becomes enriched along the A–P boundary, this increases tension and shrinks that boundary. This change irreversibly changes the tension in the system, so cells resolve into Type 3 to return to a more static state. Nanodissection experiments that disrupted the actomyosin cytoskeleton, but maintained cell integrity, confirmed there is tension along the A–P boundary (Rauzi et al., 2008). Interestingly, the apical polarity protein Baz (PAR-3) is enriched at the D–V boundary along with the AJ proteins E-cadherin and Arm/β-catenin (Blankenship et al., 2006; Zallen and Wieschaus, 2004). Zygotic *baz* mutants do not completely elongate their germband (Zallen and Wieschaus, 2004), but the mechanism involved is unclear. Further, inmutants disrupting Baz (PAR-3) localization, A–P localization ofMyosin II and F-actin is unaffected (Zallen and Wieschaus, 2004), suggesting these proteins do not depend on each other for their polarized localization. However, disruption of the actin cytoskeleton enhances planar polarization of Baz (PAR-3) and AJ proteins (Harris and Peifer, 2007), suggesting that the actin cytoskeleton plays a role in preventing hyperpolarization of AJs, which might disrupt adhesion.

What directs the planar polarity of germband cells? Early studies revealed that A–P patterning, but not D–V patterning is essential for GBE (Irvine and Wieschaus, 1994). The A–P body axis in Drosophila is determined by sequentially restricted patterns of gene expression. Spatially restricted maternally contributed proteins provide positional cues to activate zygotic genes. The first zygotic genes activated are the gap genes, which provide regional information. In turn, the pair-rule genes are activated and define parasegments. Segment polarity genes further refine the anterior–posterior pattern within segments, and then finally, the homeotic genes define the identity of each segment. Interestingly, the pair-rule genes *even-skipped* (*eve*) and *runt* both are important for GBE. Loss of function or misexpression of Eve, Runt, or upstream A–P patterning genes disrupts GBE, suggesting these genes are required for polarizing cells so they are able to intercalate (Bertet et al., 2004; Irvine and Wieschaus, 1994; Zallen and Wieschaus, 2004). Moreover, mutants affecting A–P patterning disrupt the planar polarized localization of cytoskeletal and junctional proteins. These experiments suggest A–P patterning is the primary cue to set up polarity in germband cells to allow efficient cell intercalation. However, it is unclear how A–P patterning triggers planar polarized cell architecture and directed cell rearrangement. In vertebrates, planar cell polarity (PCP) genes are required for convergent extension, an analogous process (Goto and Keller, 2002). However, in Drosophila, the PCP genes frizzled and disheveled do not appear to play roles in GBE (Zallen and Wieschaus, 2004).

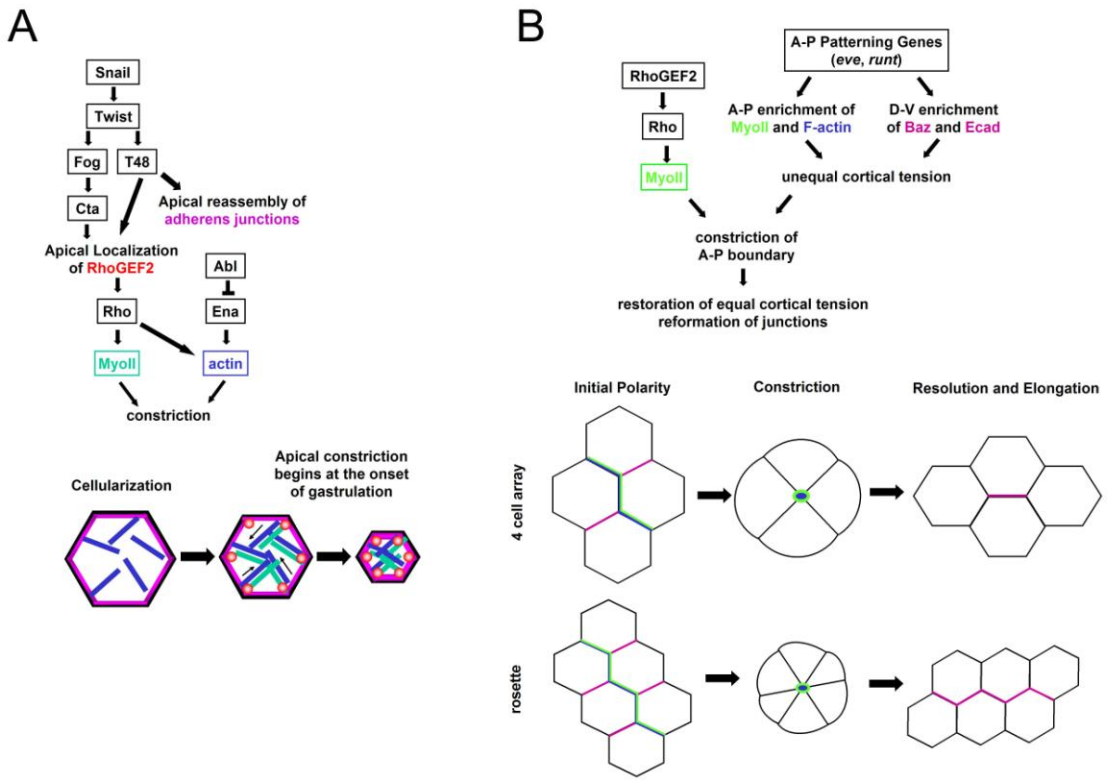

Figure 1. Morphogenesis of the ventral furrow and germband.
(A) Pathway to apical constriction in the ventral furrow. Transcription factors Twi and Snail specify the mesoderm and activate downstream effectors, T48, and Fog/Cta to apically localize RhoGEF2. RhoGEF2 signals through Rho to assemble Myosin II. RhoGEF2 also works in concert with Abl to establish an organized actin cytoskeleton. This leads to coordinated apical constriction in the ventral furrow. (B) Pathway to germband elongation. A–P patterning genes lead to the differential enrichment of actin/Myosin II and Baz (PAR-3)/DE-cad. This leads to unequal cortical tension. RhoGEF2 signals through Rho and Myosin II to constrict the A–P boundary. This allows the A–P neighbors to exchange positions with the D–V neighbors and leads to axis elongation. Colors in the model indicate differential enrichment of proteins, not total protein localization.

References

Barrett, K., M. Leptin, and J. Settleman. 1997. The Rho GTPase and a putative RhoGEF mediate a signaling pathway for the cell shape changes in Drosophila gastrulation. *Cell*. 91:905-15.

Bertet, C., L. Sulak, and T. Lecuit. 2004. Myosin-dependent junction remodelling controls planar cell intercalation and axis elongation. *Nature*. 429:667-71.

Blankenship, J.T., S.T. Backovic, J.S. Sanny, O. Weitz, and J.A. Zallen. 2006. Multicellular rosette formation links planar cell polarity to tissue morphogenesis. *Dev Cell*. 11:459-70.

Buszczak, M., S. Paterno, D. Lighthouse, J. Bachman, J. Planck, S. Owen, A.D. Skora, T.G. Nystul, B. Ohlstein, A. Allen, J.E. Wilhelm, T.D. Murphy, R.W. Levis, E. Matunis, N. Srivali, R.A. Hoskins, and A.C. Spradling. 2007. The carnegie protein trap library: a versatile tool for Drosophila developmental studies. *Genetics*. 175:1505-31.

Costa, M., D. Sweeton, and E. Wieschaus. 1993. Gastrulation in Drosophila: Cellular Mechanisms of Morphogenetic Movements. *In* The Development of Drosophila melanogaster. Vol. I. M. Bate and A. Martinez Arias, editors. Cold Spring Harbor Laboratory Press, New York. 425-466.

Costa, M., E.T. Wilson, and E. Wieschaus. 1994. A putative cell signal encoded by the folded gastrulation gene coordinates cell shape changes during Drosophila gastrulation. *Cell*. 76:1075-89.

Dawes-Hoang, R.E., K.M. Parmar, A.E. Christiansen, C.B. Phelps, A.H. Brand, and E.F. Wieschaus. 2005. folded gastrulation, cell shape change and the control of myosin localization. *Development*. 132:4165-78.

Fox, D.T., and M. Peifer. 2007. Abelson kinase (Abl) and RhoGEF2 regulate actin organization during cell constriction in Drosophila. *Development*. 134:567-78.

Goto, T., and R. Keller. 2002. The planar cell polarity gene strabismus regulates convergence and extension and neural fold closure in Xenopus. *Dev Biol*. 247:165-81.

Hacker, U., and N. Perrimon. 1998. DRhoGEF2 encodes a member of the Dbl family of oncogenes and controls cell shape changes during gastrulation in Drosophila. *Genes Dev*. 12:274-84.

Harris, T.J., and M. Peifer. 2007. aPKC controls microtubule organization to balance adherens junction symmetry and planar polarity during development. *Dev Cell*. 12:727-38.

Harris, T.J., J.K. Sawyer, and M. Peifer. 2009. How the cytoskeleton helps build the embryonic body plan: models of morphogenesis from Drosophila. *Curr Top Dev Biol*. 89:55-85.

Honda, H., T. Nagai, and M. Tanemura. 2008. Two different mechanisms of planar cell intercalation leading to tissue elongation. *Dev Dyn*. 237:1826-36.

Irvine, K.D., and E. Wieschaus. 1994. Cell intercalation during Drosophila germband extension and its regulation by pair-rule segmentation genes. *Development*. 120:827-41.

Kolsch, V., T. Seher, G.J. Fernandez-Ballester, L. Serrano, and M. Leptin. 2007. Control of Drosophila gastrulation by apical localization of adherens junctions and RhoGEF2. *Science*. 315:384-6.

Lecuit, T., and P.F. Lenne. 2007. Cell surface mechanics and the control of cell shape, tissue patterns and morphogenesis. *Nat Rev Mol Cell Biol*. 8:633-44.

Leptin, M. 1999. Gastrulation in Drosophila: the logic and the cellular mechanisms. *Embo J*. 18:3187-92.

Leptin, M., J. Casal, B. Grunewald, and R. Reuter. 1992. Mechanisms of early Drosophila mesoderm formation. *Dev Suppl*:23-31.

Martin, A.C., M. Kaschube, and E.F. Wieschaus. 2009. Pulsed contractions of an actin-myosin network drive apical constriction. *Nature*.

Morize, P., A.E. Christiansen, M. Costa, S. Parks, and E. Wieschaus. 1998. Hyperactivation of the folded gastrulation pathway induces specific cell shape changes. *Development*. 125:589-97.

Nikolaidou, K.K., and K. Barrett. 2004. A Rho GTPase signaling pathway is used reiteratively in epithelial folding and potentially selects the outcome of Rho activation. *Curr Biol*. 14:1822-6.

Parks, S., and E. Wieschaus. 1991. The Drosophila gastrulation gene concertina encodes a G alpha-like protein. *Cell*. 64:447-58.

Rauzi, M., P. Verant, T. Lecuit, and P.F. Lenne. 2008. Nature and anisotropy of cortical forces orienting Drosophila tissue morphogenesis. *Nat Cell Biol*. 10:1401-10.

Rogers, S.L., U. Wiedemann, U. Hacker, C. Turck, and R.D. Vale. 2004. Drosophila RhoGEF2 associates with microtubule plus ends in an EB1-dependent manner. *Curr Biol*. 14:1827-33.

Sweeton, D., S. Parks, M. Costa, and E. Wieschaus. 1991. Gastrulation in Drosophila: the formation of the ventral furrow and posterior midgut invaginations. *Development*. 112:775-89.

Young, P.E., T.C. Pesacreta, and D.P. Kiehart. 1991. Dynamic changes in the distribution of cytoplasmic myosin during Drosophila embryogenesis. *Development*. 111:1-14.

Zallen, J.A. 2007. Planar polarity and tissue morphogenesis. *Cell*. 129:1051-63.

Zallen, J.A., and E. Wieschaus. 2004. Patterned gene expression directs bipolar planar polarity in Drosophila. *Dev Cell*. 6:343-55.

Zallen, J.A., and R. Zallen. 2004. Cell-pattern disordering during convergent extension in Drosophila. *Journal of Physics: Condensed Matter*:S5073-S5080.

CHAPTER 2

THE DROSOPHILA AFADIN HOMOLOG CANOE REGULATES LINKAGE OF THE ACTIN CYTOSKELETON TO ADHERENS JUNCTIONS DURING APICAL CONSTRICTION

Preface

For the second chapter, I have included my first author paper that was published in the *Journal of Cell Biology* in 2009, entitled "The *Drosophila* afadin homolog Canoe regulates linkage of the actin cytoskeleton to adherens junctions during apical constriction". The other authors on the paper are: Nathan J. Harris, Kevin C. Slep, Ulrike Gaul, and Mark Peifer. Nathan J. Harris, a graduate student in Mark Peifer's laboratory, did all Rap1-related experiments. Kevin C. Slep, an assistant professor at UNC-Chapel Hill, performed the GST-Ecad immunoprecipitation with the Cno PDZ domain. Ulrike Gaul, a professor at Rockefeller University, kindly provided the cno^{R2} allele used in our studies. This work was done under the direction of Mark Peifer, a professor at UNC – Chapel Hill.

Abstract

Cadherin-based adherens junctions (AJs) mediate cell adhesion and regulate cell shape change. The nectin–afadin complex also localizes to AJs and links to the cytoskeleton. Mammalian afadin has been suggested to be essential for adhesion and polarity establishment, but its mechanism of action is unclear. In contrast, *Drosophila melanogaster's* afadin homologue Canoe (Cno) has suggested roles in signal transduction during morphogenesis. We completely removed Cno from embryos, testing these hypotheses. Surprisingly, Cno is not essential for AJ assembly or for AJ maintenance in many tissues. However, morphogenesis is impaired from the start. Apical constriction of mesodermal cells initiates but is not completed. The actomyosin cytoskeleton disconnects from AJs, uncoupling actomyosin constriction and cell shape change. Cno has multiple direct interactions with AJ proteins, but is not a core part of the cadherin–catenin complex. Instead, Cno localizes to AJs by a Rap1- and actin-dependent mechanism. These data suggest that Cno regulates linkage between AJs and the actin cytoskeleton during morphogenesis.

Introduction

Embryonic cells self-assemble tissues and organs. This morphogenesis process requires dynamic regulation of cell adhesion and cell shape change (Halbleib and Nelson, 2006), which are coordinated by cell–cell adherens junctions (AJs). AJs link neighboring cells to each other and to the apical actin cytoskeleton. Central to AJs are cadherins, which are transmembrane homophilic adhesion proteins. Their cytoplasmic tails bind

β-catenin (fly Armadillo [Arm]), which binds α-catenin (α cat). αCat can directly bind actin filaments. Each of these proteins is essential for cell adhesion and epithelial integrity, with loss leading to very early defects in embryogenesis (Larue et al., 1994; Cox et al., 1996; Müller and Wieschaus, 1996; Kofron et al., 1997; Torres et al., 1997). It was assumed that AJs directly link to actin via the catenins. However, things are more complex. Although E-cadherin (Ecad) binds both catenins and αcat binds actin, these interactions are mutually exclusive, and thus, cadherin–catenin complexes cannot bind actin (Drees et al., 2005; Yamada et al., 2005). However, many morphogenetic events require intimate interactions between AJs and the cytoskeleton, prompting us to explore other proteins that may regulate adhesion and linkage to actin.

One interesting candidate is the nectin–afadin complex. Nectins are transmembrane immunoglobulin domain proteins colocalizing with Ecad at AJs (Takahashi et al., 1999) and mediating homophilic and heterophilic adhesion (Sakisaka et al., 2007). The four mouse nectins complicate loss of function analysis, but expression of soluble nectin extracellular domain diminishes cell adhesion in culture (Honda et al., 2003). These and other data (Tachibana et al., 2000; Fukuhara et al., 2002) led the authors to suggest that nectins are "necessary and sufficient for the recruitment of Ecad to the nectin-based cell–cell adhesion sites and [are] involved in the formation of Ecadbased cell–cell AJs" (Honda et al., 2003).

Nectins are thought to associate with actin via the filamentous actin (F-actin)–binding protein afadin (AF6), which binds via its PDZ (PSD-95/Dlg/zona occludens-1 [ZO-1] homology) domain to nectin C termini and localizes to AJs (Mandai et al.,

1997). Afadin's structure suggests a scaffolding role (Fig. 1 A). It has two Ras association (RA) domains, forkhead-associated and dilute domains, and a C-terminal actin-binding domain. Rap1 is thought to be the preferred binding partner for the RA domains (Linnemann et al., 1999), and afadin and Rap1 are functionally linked (Kooistra et al., 2007). Afadin provides a potential direct link between nectins and actin, and afadin also associates with other actin-binding proteins, including αcat (Tachibana et al., 2000; Pokutta et al., 2002).

This raised the possibility that afadin plays an important role in adhesion. Afadin knockdown in MDCK cells reduced Ecad at AJs after Ca^{2+} shift, although, surprisingly, total cell surface Ecad and catenin association were unchanged (Sato et al., 2006). *Afadin*-null embryoid bodies have many AJ and tight junction proteins mislocalized (Komura et al., 2008), suggesting that afadin is important in establishing polarity and cell adhesion. Afadin knockout in mice resulted in embryonic lethality, with defects during and after gastrulation. These authors concluded that afadin is "a key molecule essential for structural organization of cell–cell junctions of polarized epithelia during embryogenesis (Ikeda et al., 1999)" or that loss of afadin "disrupts epithelial cell–cell junctions and cell polarity during mouse development (Zhadanov et al., 1999)." However, *afadin's* phenotype is much milder than those caused by loss of Ecad (Larue et al., 1994) or α -E-catenin (Torres et al., 1997), which disrupt the trophectoderm epithelium and block implantation.

Drosophila melanogaster has one afadin homologue, Canoe (Cno; Miyamoto et al., 1995), and at least one nectin, Echinoid (Ed), to which Cno binds (Wei et al., 2005). Cno also genetically interacts with and binds Rap1 (Boettner et al., 2003) and

Polychaetoid (Pyd; fly ZO-1; Takahashi et al., 1998). Surprisingly, experiments with Cno suggested a different model in which it is a scaffold for signal transduction proteins. *cno* genetically interacts with receptor tyrosine kinase/Ras, JNK, Notch, and Wnt pathways (Miyamoto et al., 1995; Takahashi et al., 1998; Matsuo et al., 1999; Carmena et al., 2006), but mechanisms by which Cno influences signaling remain unclear. As in mice, Cno regulates morphogenesis. Zygotic mutants have defects in cell shape change during dorsal closure (Jürgens et al., 1984; Takahashi et al., 1998; Boettner et al., 2003) and in asymmetric divisions and cell fate choice in the nervous system and mesoderm (Carmena et al., 2006; Speicher et al., 2008). However, these studies left intact maternally contributed wild-type Cno.

These data provide several alternate hypotheses for Cno–afadin function: at one extreme, it may be essential in cell adhesion, whereas at the other, it may transduce signals regulating cell shape change. *Drosophila* provides powerful tools to distinguish between these mechanistic hypotheses. In this study, we examine the consequences of completely eliminating Cno function from the onset of embryogenesis. Our data suggest that Cno regulates links between AJs and actin during apical constriction, providing one possible solution to the dilemma posed by Drees et al. (2005) and Yamada et al. (2005).

Results

Complete loss of Cno leads to severe morphogenesis defects

Cno plays important roles in dorsal closure, mesoderm, and neural development (see Introduction), but these studies only examined zygotic mutants. We hypothesized maternal Cno masked earlier roles. To eliminate maternal and zygotic Cno (cno^{MZ} mutants), we screened for new *cno* alleles on an FRT chromosome (*cno* is very close to

the FRT site), allowing us to remove Cno from the germline (Chou et al., 1993). *cno*^{R2} has an early stop codon (K211Stop) after the first RA binding domain (Fig. 1A), suggesting it is null. Maternal and zygotic *cno*^{R2} mutants lost Cno immunoreactivity with a C-terminal antibody (Fig. 1B vs. C; imaged on the same slide), confirming that there is not stop codon readthrough or re-initiation. While it is possible the remaining short protein fragment is produced, we think this is unlikely. First, nonsense mediated mRNA decay usually efficiently degrades mRNAs with such early stop codons (Gatfield et al., 2003; Muhlemann et al., 2008). Second, we could not detect a stable product of *cno*^{2}, with a much later stop codon (Q1310Stop; data not shown). Finally, a second independent early truncation has a similar phenotype (see following paragraph).

To assess how complete Cno loss affects morphogenesis, we examined cuticles secreted by epidermal cells (Fig. 1D). Zygotic *cno* mutant embryos die; 88% have defects in head involution but close dorsally (Fig. 1E), while 11% have defects in head involution and dorsal closure (Fig. 1F). Loss of maternal Cno is not fully rescued by zygotic wildtype Cno; ~30% of paternally rescued mutants die, with defects in head involution (data not shown). *cno*^{MZ} mutants (Fig. 1G) are much more severe than zygotic mutants, consistent with strong maternal contribution. Most *cno*^{MZ} embryos (83%) entirely lack ventral cuticle, secreted by ventral neurogenic epidermis, but retain dorsal cuticle, secreted by non-neurogenic dorsal epidermis (Fig. 1G). *cno*^{R10} MZ mutants (a second putative null; Q140STOP) had similar phenotypes (data not shown). The *cno*^{MZ} phenotype is not as severe as that of mutants completely lacking core AJ proteins *DEcadherin (DEcad*; Tepass et al., 1996) or *armadillo (arm=ßcatenin,* Cox et al., 1996; Müller and Wieschaus, 1996), in which only cuticle scraps are secreted (Fig. 1H). This

suggests Cno is not essential for epithelial integrity. However, *cno*^{MZ} mutants mimic mutants retaining maternal DEcad but zygotically mutant (Tepass et al., 1996; Fig. 1I), which lose AJ function as maternal DEcad is depleted. This is consistent with Cno modulating adhesion during later morphogenesis.

Cno is not essential for AJ assembly and is only required for AJ maintenance in some tissues

To further test Cno's roles in AJs, we assessed AJ protein localization in *cno*^{MZ} mutants. We first examined AJ assembly. During cellularization, DEcad first localizes to basal junctions near the invaginating actomyosin front and then relocalizes to apical spot AJs; as the germband extends, these smooth out into belt AJs (Tepass and Hartenstein, 1994; Harris and Peifer, 2004). Initial AJ assembly in *cno*^{MZ} was indistinguishable from wild type (Arm and αcat also assembled correctly; Fig. 2, A vs. B and C vs. D; and Fig. S1, A–F; unpublished data), and AJ proteins became apically enriched (Fig. 2 F). Apical actin also appeared normal, colocalizing with DEcad (Fig. 2, A' vs. B' and C vs. D). This is in striking contrast to the loss of junctional DEcad and polarized F-actin in *arm* mutants (Fig. 2, E and E'; Cox et al., 1996). Maturation of spot AJs to belt AJs (Fig. S1, A–F) also proceeded normally. Finally, AJ protein levels were normal at these stages (Fig. 3, 0–4 h; Decad 102%, Arm 111%, and αcat 90% of wild type; mean of three experiments). Two Cno-binding proteins, Pyd and Ed, localize to AJs from the start, and both localize normally in *cno*^{MZ} mutants (Fig. S1, G–J). These data suggest that Cno is not essential for AJ assembly or initial maturation.

In many embryonic cells, Cno is also not essential for AJ maintenance. In *cno*^{MZ}, AJs and cell shapes remain normal in amnioserosa (Fig. 2 I, arrows) and dorsal epidermal

cells (Fig. 2, I [arrowheads] and J vs. K) through germband retraction. However, in a subset of ectoderm, AJs are not maintained normally. As the germband extends, ectodermal cells initiate mitosis; as they divide, they round up, and apical AJ protein accumulation is reduced (Fig. 2, L and N, arrows). As they exit mitosis, AJs reassemble, and cells become columnar again. In cno^{MZ}, although dorsal ectodermal cells retain columnar shape and normal AJs (Fig. 2 J), many ventral neurogenic ectodermal cells have reduced DEcad. It appears that after division they do not regain columnar shape with small apical ends (Fig. 2, M and O, brackets). To ensure that cells properly exited mitosis, we labeled embryos with the mitotic marker antiphospho–histone H3; large regions of ventral epidermis exited mitosis without properly reassembling AJs or regaining columnar shape (Fig. 2, P and Q, arrows). AJ fragmentation occurred before loss of cortical actin (Fig. 2 R, arrows). Arm and DEcad levels are also somewhat reduced at this stage (Fig. 3, 4–8 h; DEcad 87%, Arm 83%, and αcat 102% of wild type; mean of three experiments). Morphogenesis is compromised; the epidermis separates from the amnioserosa (Fig. 2 S, arrow), and segmental grooves never retract (Fig. 2 S, arrowheads). Ultimately, ventral cells are lost (Fig. 2 T, brackets), likely explaining the retention of dorsal but not ventral cuticle (Fig. 1 G). Thus, Cno is dispensable for AJ assembly and maintenance in many tissues but regulates AJ maintenance in some morphogenetically active cells.

Cno loss disrupts mesoderm invagination

Although AJs are established normally in Cno's absence, morphogenesis is affected from the start. Gastrulation initiates after cellularization. The ventral-most cells form mesoderm and undergo coordinated apical constriction triggered by a pathway

involving the ligand Fog, the G protein concertina, RhoGEF2, and Rho (Pilot and Lecuit, 2005). In response, mesodermal cells accumulate apical actin and myosin, apically constrict (Fig. 4, A and B), and internalize as a tube (Fig. 4 C). If AJs are disrupted, mesoderm invagination is compromised (Dawes-Hoang et al., 2005), and thus, coordinating AJs and actin is critical to couple actomyosin constriction to cell shape change.

cno^{MZ} morphogenetic defects begin at gastrulation. Wild-type mesoderm, marked by the transcription factor Twist, is completely internalized during gastrulation (Fig. 4, D and E). In contrast, *cno*^{MZ} mutants do not completely internalize mesoderm; many cells remain on the embryo surface and begin to divide in this aberrant location (Fig. 4, G and H). The degree of defect in mesoderm invagination varied from complete failure to defects only at the anterior and posterior ends (unpublished data).

We next examined mechanisms by which this occurs. First, Cno, unlike Arm, is not essential for AJ assembly (Fig. 2, A–E'), even in invaginating mesoderm (Fig. 2, G vs. H). Second, Cno is not required for mesoderm specification, as *cno*^{MZ} mesoderm expresses Twist, the transcription factor conferring mesodermal fate (Fig. 4, G and H). A third hypothesis is that in Cno's absence, mesodermal cells fail to initiate apical constriction, as do *RhoGEF2* mutants (Barrett et al., 1997), or fail to constrict in a coordinated way, as do *fog* or *concertina* mutants (Sweeton et al., 1991). However, *cno*^{MZ} mutant cells initiate constriction and do so fairly synchronously (Fig. 4, F vs. I; occasional cells in both wild type and mutant constrict more slowly than their neighbors). However, *cno*^{MZ} cells arrest partway through apical constriction. Live analysis using moesin-GFP (moe-GFP) to highlight F-actin confirmed this. Wild-type mesodermal cells

constrict rapidly and fairly synchronously (Fig. 5 A and Video 1). To quantify this, we measured change in cell cross-sectional areas of eight randomly chosen cells, confirming rapid, synchronous constriction in wild type, with occasional cells lagging behind (Fig. 5 D). *cno*^{MZ} mutants (distinguished from paternally rescued embryos using a marked balancer chromosome) initiated apical constriction in a timely manner but then had a variable phenotype (like the variability in mesoderm invagination). In less severe mutants, constriction went at the same rate as in wild type (Fig. 5, B and E; and Video 2) but halted prematurely; thus, as mesodermal cells initiated division (Fig. 5 B, arrow), they reemerged from the furrow. In more severe embryos (Fig. 5, C and F; and Video 3), constriction was slower than in wild type, and more cells lagged behind; this delay allowed mesodermal cells to divide before being internalized. These data suggest that Cno acts by a novel mechanism to ensure completion of apical constriction.

To identify this mechanism, we looked in detail at cytoskeletal rearrangements. The first step is apical recruitment of actin and myosin (Fig. 6, B and H, arrows) in which they assemble into a contractile network (Fig. 6, A–A"; and not depicted); actin is also enriched in a ring at AJs (Fox and Peifer, 2007). In *cno*^{MZ}, actin and myosin are recruited to the apical cortex (Fig. 4 L, arrowhead; and Fig. 6 D, arrow). Wild-type constricting cells elongate along the apical–basal axis, and this occurs normally in *cno*^{MZ} mutants (Fig. 4 L).

In wild type, actomyosin constriction begins as soon as myosin arrives apically and is coupled to cell shape change, with AJs moving inward as constriction proceeds (Fig. 6, A–A"). One hypothesis is that Cno regulates the extent of actomyosin constriction, so it does not go to completion in *cno*^{MZ} mutants. However, this is not the

case; instead, actomyosin constriction initiated correctly (Fig. 4 I) but became uncoupled from cell shape change. In wild type, actomyosin contraction is coupled to reduction in diameter of the cell's apical end (Fig. 6, A–B, E, and H). In *cno*^{MZ}, myosin (Fig. 6, C–C'', D, and F–F'') and actin (Fig.6 I) both coalesced into "balls" at the cell apex, which were not contiguous with AJs (Fig. 6, E vs. F–F''). To explore dynamic cytoskeletal rearrangements, we used moe-GFP to visualize F-actin (Video 4) and zipper-GFP (myosin heavy chain) to visualize myosin (Video 6). In *cno*^{MZ}, balls of both F-actin (Fig. 6 J; Fig. S2, A vs. B; and Video 5) and myosin (Fig. 6 G; Fig. S2, C vs. D; and Video 7) coalesced as invagination proceeded. These data support a model (Fig. 6 L) in which *cno*^{MZ} cells apically constrict without fully effective linkage between AJs and the actomyosin network, the contractile network detaches from AJs before full cell constriction, and mesodermal cells are not efficiently internalized.

In contrast, other gastrulation events are more normal. Posterior midgut cells also apically constrict (Sweeton et al., 1991), leading to internalization (Fig. S1 K). *cno*^{MZ} mutants successfully internalize the gut (Fig. S1 L), although the midgut epithelium may be less organized (Fig. S1, M). Lateral ectodermal cells intercalate during germband elongation, narrowing the ectoderm in the dorsal–ventral axis and elongating it in the anterior–posterior axis. *cno*^{MZ} mutants extend their germbands, and intercalation proceeds normally (some *cno*^{MZ} mutants do not extend as far as wild type, but this may be a secondary consequence of ventral furrow failure; Fig. S1, N and O). Intercalation is thought to be driven by opposing planar polarization of myosin and AJ proteins (Fig. S1, P–P"; Bertet et al., 2004; Zallen and Wieschaus, 2004; Blankenship et al., 2006). Ectodermal cells in *cno*^{MZ} mutants planar polarize myosin and AJ proteins (Fig. S1, Q–

Q"); in fact, planar polarization is even more pronounced than in wild type (Fig. S1, P–P" vs. Q–Q"), and mutants retain accentuated planar polarity through the end of germband extension (Fig. S1, R vs. S).

αCat localizes to actomyosin balls in cno^{MZ}

We next looked in detail at the apparent separation of AJs and the apical actomyosin web, examining whether AJ proteins accumulated in actomyosin balls in *cno^{MZ}* mutants. We first examined DEcad, a transmembrane protein. The actomyosin balls were apical to AJs (we visualized actomyosin balls with antiphosphotyrosine, as DEcad and phalloidin are not well preserved by the same fixation; Fig. 7, C–C" [sections of the same embryo at AJs] and D–D" [more apical]). DEcad was largely retained in AJs after detachment (Fig. 7, A–A", arrows) and only weakly localized in actomyosin balls (Fig. 7, A–B", arrowheads). We sometimes noted strands of DEcad joining balls to AJs (Fig. 7, B–B", arrows); these were reminiscent of less dramatic deformations of the lateral membrane observed during normal apical constriction (Martin et al., 2009) and may represent points of remaining attachment between AJs and the balls. Ed also did not strongly accumulate in actomyosin balls (unpublished data). In contrast, αcat accumulated at easily detected levels in actomyosin balls (Fig. 7, C–E", arrows) as well as remaining in AJs (Fig. 7, C–C", arrowheads). This is consistent with the existence of two pools of αcat, one in AJs and one bound to actin (Drees et al., 2005).

Canoe is enriched at tricellular AJs along with a subset of actin

Cno localizes to AJs in embryos and imaginal discs (Takahashi et al., 1998). However, apical junctions are already complex at their assembly. Bazooka (Baz; fly PAR-3) and DEcad localize apically from cellularization onset (Harris and Peifer, 2004),

whereas aPKC, Par6, and Crumbs are recruited to an even more apical position during gastrulation (Tepass, 1996; Hutterer et al., 2004; Harris and Peifer, 2005). AJs initially assemble as spot AJs that do not precisely colocalize with actin and smooth out to form belt AJs during gastrulation.

To place Cno in the apical junctional protein network, we examined its localization and explored how it localizes apically. Cno has similarities and differences in localization with AJ proteins. Apical junctions assemble as cells form from the syncytium. As actomyosin furrows ingress, DEcad localizes to basal junctions just behind invaginating actomyosin (Thomas and Williams, 1999; Hunter and Wieschaus, 2000) and also begins to localize to apical junctions, whereas Baz is apical throughout (Harris and Peifer, 2004). Cno also remains apical, colocalizing with DEcad at apical junctions (Fig. 8, H–H", arrows) but not basal junctions (Fig. 8, H–H", arrowheads). In fact, like AJ proteins and Baz (McCartney et al., 2001; Harris and Peifer, 2004), Cno is already cortical before cellularization, localizing at apical ends of syncytial furrows (Fig. 8 G, arrow). As embryos gastrulate, DEcad and Baz localize more tightly to apical AJs (Harris and Peifer, 2004), as does Cno (Fig. 8, I–I"). Thus, Cno is part of the apical junctional complex from the start.

To get a detailed view of Cno localization, we looked at cells en face. AJs initially form as spot AJs around the apical cortex (Tepass and Hartenstein, 1994). Cno colocalizes at spot AJs apically, with some enrichment at tricellular junctions (Fig. 8, A–A", arrowheads); however, when we imaged 2 μm more basally, Cno, unlike AJ proteins, is strikingly enriched at tricellular junctions (Fig. 8, B–B", arrowheads). Intriguingly, a subset of actin is also enriched at tricellular junctions (visualized with antiactin antibody,

this is also apparent using moe-GFP; Fig. 8, E [arrowheads] and E" [inset]). As gastrulation begins, spot AJs mature into less punctate belt AJs (Harris and Peifer, 2004). Like AJ proteins and Baz, Cno also becomes more evenly distributed but remains enriched at tricellular junctions, as does actin (actin visualized with phalloidin; Fig. 8, C–D" and F–F", arrowheads). Thus, Cno is in apical junctions from the start but does not strictly colocalize with AJ proteins and localizes more closely with a subset of cortical actin.

Cno can bind DEcad but is not a core AJ component

Cno–afadin has known direct interactions with AJ proteins, including nectins/Ed (Takahashi et al., 1999; Wei et al., 2005), αcat (Tachibana et al., 2000; Pokutta et al., 2002), and the tight/AJ protein ZO-1/Pyd (Takahashi et al., 1998; Yokoyama et al., 2001). This suggests that Cno may have multiple, partially redundant interactions with AJs. Cno–afadin interacts with nectins via its PDZ domain (Takahashi et al., 1999; Wei et al., 2005). Ed (ending in the sequence EIIV) and Nectin1 (ending in EWYV) have class II PDZ-binding sites. Interestingly, DEcad also has a putative C-terminal type II PDZ-binding site (ending in the sequence GWRI; matching the consensus XøXø, where ø is any hydrophobic amino acid; Hung and Sheng, 2002) that is strongly conserved in all Diptera, which diverged ~250 million years ago (Zdobnov et al., 2002). Thus, we tested whether Cno's PDZ domain can bind the DEcad tail. Purified Cno PDZ domain does not bind GST alone but does bind GST fused at its C terminus to the last seven amino acids of DEcad (Fig. 9 A). These data are consistent with DEcad as a Cno-binding partner. Given this and Cno's localization to AJs, we explored whether Cno is a core component of the cadherin–catenin complex. DEcad, Arm, and αcat coimmunoprecipitate as a stable

complex from embryonic extracts (Fig. 9 B). In contrast, Cno is not detected in these immunoprecipitations (Fig. 9 B), suggesting that it is not in the core complex.

Cno apical recruitment requires Factin but not AJs or Echinoid

This raises questions about mechanisms by which Cno is recruited to and maintained at AJs. We first considered the hypothesis that cadherin–catenin complexes recruit Cno because Cno–afadin can bind both αcat (Pokutta et al., 2002) and DEcad (Fig. 9 A). To test this, we made arm^{MZ} mutants, in which both DEcad and αcat are lost from the cortex (Fig. 9, D–D"; Cox et al., 1996; Dawes-Hoang et al., 2005), disrupting AJs. Surprisingly, Cno localizes normally in arm^{MZ} mutants (Fig. 9, C' vs. D'). This suggests that Cno has other means of reaching the cortex.

We next tested the hypothesis that Cno is recruited by Ed. Cno is mislocalized in *ed* mutant wing disc cells, suggesting that Ed helps localize Cno to AJs (Wei et al., 2005). Ed localizes to spot AJs and transitions to belt AJs (Fig. 8, A, C, D, and I, insets). Cno localized normally in ed^{MZ} mutants (Fig. 9, E' vs. F'), which is consistent with the observation that ed^{MZ} mutants do not have morphogenetic defects until dorsal closure (Laplante and Nilson, 2006; Lin et al., 2007). Thus, although Cno binds Ed, Cno has other ways to localize to AJs in embryos.

Baz, which also localizes to apical junctions independently of AJs, is positioned apically by cytoskeletal cues, including binding an apical actin-based scaffold (Harris and Peifer, 2004, 2005). Afadin is an F-actin–binding protein (Mandai et al., 1997). Thus, we examined whether Cno could directly bind F-actin like afadin. We fused GST to the C-terminal 491 aa of Cno, which shares sequence conservation with afadin's F-actin–binding site, and performed actin sedimentation assays to determine whether Cno directly

associates with F-actin. GST alone was a negative control, and GST-αcat (aa 671–906) was a positive control (Pokutta et al., 2002). Little GST pelleted with F-actin, as most remains in the supernatant (11% pelleted; mean of six experiments; Fig. 10 A). GST-αcat pelleted with F-actin (84% pelleted; mean of three experiments; Fig. 10 A). GST-Cno (aa 1,560–2,051) also pelleted with F-actin (41% pelleted; mean of four experiments; Fig. 10 A) to a degree similar to afadin (Lorger and Moelling, 2006), suggesting that Cno can directly bind F-actin.

Cno's ability to bind actin and its colocalization with a subpool of actin at tricellular junctions suggested the hypothesis that Cno is recruited apically by an actin-based scaffold. To test this, we examined Cno localization after depolymerizing actin with cytochalasin. When actin is depolymerized at the end of cellularization, DEcad remains cortical but distributes all along the apical–basal axis (Fig. 10, B" vs. C"; Harris and Peifer, 2005). Strikingly, Cno is lost from the cortex and accumulates in the cytoplasm or nucleus (residual cortical Cno was present in cells where some cortical actin remained; Fig. 10, C–C" and E–E'" [arrows]). We saw similar effects in extended germband embryos (Fig. S3). These data suggest that Cno is recruited/retained at the cortex at least in part by interacting with the cortical actin cytoskeleton.

Rap1 is essential for mesoderm invagination and Cno cortical recruitment

Both afadin and Cno bind the small GTPase Rap1, and this is thought to activate Cno during dorsal closure (Boettner et al., 2000, 2003). Thus, we examined whether Rap1 also works with Cno during mesoderm invagination by generating $Rap1^{MZ}$ mutants using the null allele $Rap1^{CD3}$ (deleting the entire coding region; Asha et al., 1999). Previous work suggested that Rap1 plays a role in gastrulation, as midline cells, which

meet at the ventral midline after gastrulation, did not do so in *Rap1*^{MZ} (Asha et al., 1999). We extended this analysis. Loss of MZ Rap1 disrupts ventral cuticle (Fig. 1 J), and Twist-positive mesoderm remained on the surface after gastrulation (Fig. 4 J) as in *cno*^{MZ}. In some *Rap1*^{MZ} mutants, the germband became twisted during gastrulation (Fig. 4 K), as is seen in mutants like *fog* that disrupt invagination of both mesoderm and the posterior midgut (Sweeton et al., 1991).

To further examine parallels between *Rap1*^{MZ} and *cno*^{MZ} mutants, we examined localization of AJ and cytoskeletal proteins. Initial AJ assembly was normal in *Rap1*^{MZ} (Fig. S4, A vs. B) as in *cno*^{MZ} (Fig. 2, A–D'). However, as in *cno*^{MZ}, coupling between actomyosin constriction and cell shape change was disrupted in *Rap1*^{MZ}. Balls of actin (Fig. 6 O) and myosin (Fig. 6, M and N) appeared at the apical surface of mesodermal cells, and cell constriction halted prematurely, with myosin balls not contiguous with AJs (Fig. 6 N). These data are consistent with Cno and Rap1 acting together in this process.

Cno binds Rap1, and epistasis analysis suggests that Rap1 acts upstream of Cno in dorsal closure (Boettner et al., 2003). Thus, we explored whether Rap1 regulates Cno recruitment to AJs. We examined Cno localization during cellularization and early gastrulation in *Rap1*^{MZ} mutants. Cno recruitment to the cortex was substantially reduced at cellularization and early gastrulation (Fig. 9, G–J'). This suggests that Rap1 binding plays an important role in Cno cortical recruitment.

We also explored Rap1 localization using GFP-Rap1 driven by its endogenous promoter (Knox and Brown, 2002) to see whether its localization was consistent with a role in recruiting Cno to AJs. During cellularization, GFP-Rap1 accumulated in the cytoplasm in a large structure just above nuclei (Fig. S4 C, arrowheads) and all along the

lateral cell cortex from apical junctions (Fig. S4 C, arrows) to the basal end (Fig. S4 C, inset). GFP-Rap1 remained cortically enriched during gastrulation (Fig. S4, E and H). Interestingly, in apically constricting cells of the posterior midgut, although GFP-Rap1 is found all along lateral membranes (Fig. S4, G and G', arrows), it accumulates at elevated levels in a region overlapping the AJs (Fig. S4, G and G', arrowheads). We next examined whether Cno is required for GFP-Rap1 cortical localization. We saw no differences in GFP-Rap1 localization in wild type or cno^{MZ} (Fig. S4, D, F, and H–I'), which is consistent with Rap1 acting upstream of Cno in the pathway.

Discussion

AJs mediate cell adhesion and anchor and regulate the underlying actin cytoskeleton. We have a working model for how cadherin–catenin complexes regulate these events, but less is known about the parallel system of nectins and the linker Cno–afadin. Studies in mammalian cells and embryos largely focus on a model in which the nectin–afadin complex is critical for cell adhesion, working in parallel with cadherin–catenins (see Introduction). In contrast, studies of *Drosophila* Cno suggest that it is a scaffold for signal transduction (see Introduction). We completely removed MZ Cno, allowing us to assess the consequences of complete loss of function from the onset of embryogenesis and to explore Cno's mechanism of action.

Cno is not essential for AJ assembly or maturation

Work in cultured mammalian cells using nectin misexpression or dominant-negative approaches led to the model that nectin–afadin complexes play a key role in cell adhesion, recruiting cadherins to nascent AJs (Tachibana et al., 2000; Honda et al., 2003). However, multiple nectins made genetic tests of this hypothesis problematic. Afadin

knockout in mice resulted in defects at and after gastrulation and subsequent lethality (Ikeda et al., 1999; Zhadanov et al., 1999). However, defects occurred much later than those caused by loss of core AJ proteins (Larue et al., 1994; Torres et al., 1997). Thus, the mouse data suggested that loss of zygotic afadin does not disrupt adhesion to the same degree as loss of cadherin–catenin; however, as these embryos retained maternal afadin, an essential role for afadin in adhesion and epithelial integrity remained possible.

We tested whether Cno is essential for AJ assembly or maintenance by completely removing MZ Cno from the onset of fly embryogenesis. The results were striking. Initial assembly of cadherin–catenin-based AJs, establishment of epithelial cell polarity, and organization of apical actin were all normal in Cno-deficient embryos. Furthermore, the first step in AJ maturation, coalescence of spot AJs into belt AJs underlain by actin, was completed on schedule, unlike what was observed in afadin knockdown MDCK cells (Sato et al., 2006). These results are in strong contrast to loss of Arm, which disrupts all these events (Cox et al., 1996; Müller and Wieschaus, 1996). Thus, Cno is not essential for AJ assembly or initial maturation. Furthermore, many tissues maintained normal AJs and architecture through late embryogenesis, suggesting that Cno is not essential for AJ maintenance per se or essential to maintain actin–AJ connections in nonmorphogenetically active tissues, as these are essential for AJ integrity (Quinlan and Hyatt, 1999). Differences between our work and that in cultured mammalian cells could reflect differences in assembly and regulation of AJs in insects and mammals. However, they suggest further exploration of whether afadin is essential for AJ assembly in mammals is warranted; e.g., generating afadin-null epithelial cells or maternally mutant mice.

Loss of Cno does affect maintenance of tissue architecture in a subset of cells. Many cells in the neurogenic ectoderm lost columnar shape, and membrane DEcad was reduced. This coincided with two morphogenetic events: a series of cell divisions and invagination of a subset of cells to form the central nervous system. Both involve significant AJ remodeling, and thus, the ventral epidermis is particularly susceptible to reducing DEcad levels (Tepass et al., 1996; Uemura et al., 1996). The neuroepithelium is also the tissue most susceptible to afadin loss in mice (Ikeda et al., 1999; Zhadanov et al., 1999), perhaps because of similarly dynamic cell behavior. It will be interesting to explore Cno's role in this morphogenetically active tissue in more detail, using genetic approaches to block cell division or neuroblast invagination; the latter alleviates effects of reducing DEcad (Tepass et al., 1996). It will also be interesting to explore mechanisms by which Cno acts; e.g., it may regulate cadherin trafficking as suggested in mammalian cells (Hoshino et al., 2005) or it may help cells reassume a columnar shape by regulating connections between cadherin–catenin and actin.

A role for Cno in regulating AJ:actin linkage

Cross talk between AJs and actin is critical in many contexts from maintaining stable adhesion to mediating morphogenesis (Gates and Peifer, 2005). The classical view of AJs postulated direct connection between cadherin–catenin complexes and actin mediated by αcat. However, recent work undermined this idea (Drees et al., 2005; Yamada et al., 2005), raising the question of how actin is connected to AJs and causing some to question whether such a connection even occurs. One morphogenetic event that compellingly suggests that AJs are connected to actin is apical constriction, during which constriction of the apical actomyosin web is coupled to shape change (Fig. S5 A, top).

Disrupting AJs uncouples these events (Dawes-Hoang et al., 2005), supporting the need for a connection, but the nature of the link was unclear.

The phenotype of *cno* mutants is consistent with Cno playing a critical role in this connection. In its absence, AJs assemble normally, actin and myosin accumulate apically, and apical constriction initiates. However, cell constriction halts before completion, whereas cytoskeletal constriction continues, uncoupling these events (Fig. S5 A, bottom). Our data are consistent with several models for Cno in this process. The first step in all is Cno recruitment to the cortex. To our surprise, this is not dependent on either the cadherin–catenin complex or the nectin Ed, although we cannot rule out a redundant role for them. Instead, the GTPase Rap1 is critical. One speculative possibility is that Rap1 binding the RA domains opens up a closed conformation, as is seen, for example, in formins (Fig. S5, B–D). Thus, Rap1 recruitment of Cno to the cortex could also activate it, allowing it to interact with other partners. At least one partner is F-actin. Consistent with this, Cno, like afadin, can bind F-actin, and the actin cytoskeleton plays a critical role in cortical Cno localization.

Once Cno is recruited apically by Rap1 and actin, it could then help stabilize links between actomyosin and AJs in several ways. It might be a direct link, binding actin and interacting by multiple redundant and low affinity interactions with several AJ proteins (Fig. S5 E). Cno–afadin has well-documented direct interactions with nectins, αcat, and ZO-1, and we documented a direct interaction of its PDZ domain with DEcad. Alternately, Cno may regulate interactions more indirectly. It is intriguing that αcat acts later during germband elongation in linking a stable population of F-actin at spot AJs with the larger cortical actin network (Cavey et al., 2008). Our observation that αcat is

strongly enriched in actin balls that detach from AJs in Cno's absence, while also remaining at AJs, is consistent with αcat acting on both sides of the linkage. Cno may regulate interactions between junctional and actin-bound pools of αcat either directly or acting as a scaffold to recruit another regulator (Fig. S5 F). It will be important to test these models; the new *Drosophila* αcat mutants (unpublished data; U. Tepass, personal communication) will help, as will two-color simultaneous imaging of F-actin and AJs. It will also be important to further analyze Cno's actin-binding domain by site-directed mutagenesis. Other models for Cno function remain possible. Dictyostelium Rap1 regulates myosin disassembly during cell motility (Jeon et al., 2007), and activated myosin can activate Rap1 (Arora et al., 2008). For example, Cno–Rap1 might regulate actomyosin contractility, and in its absence, apical actomyosin might become hypercontractile. We did not observe any acceleration of cell constriction as might be expected from the simplest versions of this model (Fig. 5, D–F). However, Cno–Rap1 regulation of myosin remains an open possibility.

Regardless of the mechanism, Cno's enrichment at tricellular junctions along with a subpopulation of actin suggests the possibility that these structures might have a special role in AJ–actin connections. Intriguingly, mouse tricellulin plays a special role at tricellular junctions in maintaining tight junctions (Ikenouchi et al., 2005). However, our analysis and that of Martin et al. (2009) suggest that all spot AJs maintain connection to the apical actin web during normal constriction and disconnection in *cno* mutants.
It will be interesting to explore how forces are generated in the apical cortex, how contractility is regulated, and how and where the contractile network is coupled to AJs. Constriction in the *Drosophila* ventral furrow is rhythmic, suggesting a racheting

mechanism (Martin et al., 2009). This resembles what is seen in the one-cell *Caenorhabditis elegans* embryo (Munro et al., 2004). Another striking thing about the ventral furrow is that cells do not constrict isometrically but instead constrict more quickly in the dorsal–ventral dimension than in the anterior–posterior dimension (Fig. 4 F and Fig. 5 A). This bias seems less pronounced in cno^{MZ} mutants (Fig. 4 I and Fig. 5 C), perhaps suggesting a requirement for cortex–AJ connections to maintain asymmetric cell constriction.

Mammalian afadin plays a role in epithelial wound healing; in its absence, cells migrate into wounds more rapidly (Lorger and Moelling, 2006). Although afadin knockdown did not affect stable AJs, it reduced AJ association with the cytoskeleton after wounding, reducing adhesion and increasing directionality of cell migration. This function required afadin's actin-binding domain, providing a second context in which Cno–afadin may help link AJs and actin.

However, Cno is not critical for all actin–AJ connections. Cadherin-based adhesion itself, which does not require Cno, involves actin–AJ interactions (Quinlan and Hyatt, 1999). Likewise, conversion of spot AJs to belt AJs, which involves connections to actin (Maddugoda et al., 2007; Cavey et al., 2008), does not require Cno. Loss of Cno also did not halt germband extension, which involves reciprocal planar polarization of myosin and AJs. However, Cno may play a restraining role in this process, as planar polarity is enhanced in cno^{MZ} mutants. This is interesting, as actin depolymerization also enhanced AJ planar polarity (Harris and Peifer, 2007), suggesting that AJ–actin connections restrain planar polarity. Perhaps in Cno's absence, subtle uncoupling of AJs from actin occurs. Thus, we hypothesize that Cno is one aspect of regulation of AJ–actin

linkage. However, this linkage will be complex, with different proteins mediating interactions in different circumstances. The mammal-specific protein Eplin regulates maturation/remodeling of AJ–actin connections during AJ assembly (Abe and Takeichi, 2008). Likewise, αcat regulates lateral mobility of AJ complexes (Cavey et al., 2008) and myosin VI acting with vinculin, and Cno–afadin-binding partners in the ZO-1 family also regulate maturation of belt junctions (Ikenouchi et al., 2007; Maddugoda et al., 2007). Perhaps different proteins evolved to respond to distinct forces exerted on AJs, differing either in magnitude or acceleration. Our challenge is to identify all proteins regulating AJ–actin connections and to determine their mechanisms of action.

Acknowledgements

We thank the Bloomington *Drosophila* Stock Center, DHSB, D. Kierhart, E.Wieschaus, L. Nilson, S. Roth, C. Field, G. Rogers, A. Fanning, and S. Pokutta, and W. Weis for reagents, and especially thank K. Takahashi for the generous gift of Cno antibody. We thank members of the Gaul lab including J. Fak, P. Harjes, M. Heke, D. Leaman, and B. Boettner for help in generating FRT82 cno^{R2}, E. Jezuit and D. Meardon for technical assistance, A. Fanning for many informative discussions, and B. Goldstein, G. Shemer, D. Roberts, and J. Sawyer for critiques. This work was supported by NIH RO1GM47857. J.K.S. was supported by 5 T32 HD046369 and an AHA predoctoral fellowship. The screen for *cno* alleles was supported by RPG-00-237-01-CSM from the American Cancer Society (U.G.)

Materials and Methods

Fly Stocks

Mutations are described at flybase.bio.indiana.edu. Wild type was *yellow white* or *Histone-GFP*. All experiments were done at 25°C unless noted. cno^{R2} was generated by EMS on an isogenic FRT82B line. cno^{R2} was sequenced by PCR amplifying fragments of the *cno* coding sequence and sequencing them at the UNC-CH Genome Analysis Facility. Cuticle preparations were made as in Wieschaus and Nüsslein-Volhard (1986). Stocks to make *cno* germline clones were from the Bloomington Stock Center. *cno* germline clones were made by heat shocking 48-72h old $hsFLP^{1}$; FRT82Bcno^{R2}/FRT82Bovo^{D1-18} larvae 3hrs at 37°C. arm^{043A01} and ed^{F72} germline clones were generated similarly.

Immunofluorescence and image aquisition

The following fixations were used: myosin/Arm/Cno/Ed, heat-methanol (Müller and Wieschaus, 1996); phalloidin/Dcad2, 10min, 10% formaldehyde; phalloidin, 5min, 37% formaldehyde. All others were fixed as in Grevengoed et al. (2001). Embryos were methanol-devitillinized, or hand-devitillinized for phalloidin. Embryo cross-sections were performed as in (Dawes-Hoang et al., 2005). For drug treatments, dechorinated embryos were washed twice with 0.9% NaCl and incubated for 30min in 1:1 octane/0.9% NaCl with 10μg/mL cytochalasin D (Sigma, dissolved in DMSO). Control embryos were treated with DMSO carrier alone. Embryos were fixed immediately after drug treatment (Harris and Peifer, 2005). All embryos were blocked/stained in PBS/1% goat serum/0.1% Triton X-100 and mounted in Aqua-Polymount (Polysciences). Suppl. Table 1 lists antibodies and probes used. All images and movies were acquired at room

temperature. Fixed samples were imaged with LSM510 or Pascal confocal microscopes, using a Zeiss 40X NA 1.3 Plan-Neofluar oil immersion objective, and LSM software. Live imaging was performed using the Perkin-Elmer Ultra VIEW spinning disc confocal, ORCA-ER digital camera, a Nikon 40X NA 1.3 Plan-Fluor oil immersion objective, and Metamorph software. Adobe Photoshop CS2 was used to adjust input levels so the main range of signals spanned the entire output grayscale and to adjust brightness and contrast.

Vector construction, Protein Expression and Protein Purification

GST–α-catenin (671-906) was from the Weis lab (Pokutta et al., 2002). The Cno-Cterm (aa1560-2051) fragment was amplified by PCR and cloned into pGEX (Amersham). The Cno-PDZ (aa833-929) fragment was amplified by PCR and closed into pET28 (Novagen). GST-Ecad (GST-DDQGWRI) was amplified by PCR and cloned into pET28. GST fusion constructs in the pGEX vector were expressed in *E.coli* BL21-Gold (DE3) cells (Stratagene). Bacteria were grown in LB+ media with 100μg/mL ampicillin at 37°C to OD_{600} between 0.8-1.0, induced with 1mM isopropyl-g-D-thiogalactopyranoside and grown 3 hours at 37°C. Pelleted cells were resuspended in 20mM Tris pH 8.0, 200mM NaCl, 1mM EGTA, 1% Triton-X, 0.1mM PMSF + a protease inhibitor cocktail (Roche), and lysed using a microfluidizer. The lysate was cleared by centrifugation and incubated with glutathione-agarose (GE-Healthcare) O/N at 4ºC. GST fusion proteins were purified over 20mL Bio-rad columns and where either kept on beads for subsequent manipulations or eluted with 20mM Tris pH 8.0, 200mM NaCl, 10mM Glutathione (Sigma). Constructs in the pET-28 vector (H_6-CnoPDZ and H_6-GST-Ecad) were expressed in *E.coli* BL21-Gold (DE3) cells (Stratagene). Bacteria were grown in LB+ media with 20μg/mL kanamycin at 37°C to OD_{600} between 0.8-1.0,

induced with 1mM isopropyl-g-D-thiogalactopyranoside and grown 3 hours at 37°C. Pelleted cells were resuspended in 25mM Tris pH 8.0, 300mM NaCl, 10mM imidazole, 1% β-mercaptoethanol, 0.1mM PMSF and lysed using a microfluidizer. The lysate was cleared by centrifugation and incubated with Ni^{2+}-NTA agarose (Qiagen) 3 hours at 4ºC. The columns were washed with 20 column volumes of lysis buffer and bound protein step eluted using 3 column volumes of lysis buffer supplemented with 285 mM imidazole.

Actin Sedimentation Assay

Rabbit skeletal muscle actin (Cytoskeleton, Inc.) was stored in 5mM Tris, pH 8.0, 0.2mM $CaCl_2$, 0.5 mM DTT, and 0.2 mM ATP at 0.4 mg/ml. Either 1μM or 5μM actin was used. Aliquots of 156.25uL were polymerized with 3.2uL 50X polymerization buffer (2.5M KCl, 100mM $MgCl_2$, 50mM ATP, protease inhibitor cocktail (Roche)) for 1hr at RT. GST fusion proteins were precleared by centrifugation for 7min at 436,000 x g at 4ºC (TLA-100 rotor, Beckman 100 tubes). Precleared GST fusion protein (final concentrations of 5μM or 2 μM) was added to polymerized F-actin and incubated 30min at RT. Proteins bound to F-actin were separated from unbound protein by centrifugation 7min at 436,000 x g at 4ºC. Sample buffer was added to supernatant and pellet fractions, boiled, and loaded on a 10% polyacrylamide gel. Gels were stained with Coomassie Brilliant Blue.

GST pull downs

50μl of Glutathione beads were saturated with GST or GST-Ecad then washed using wash buffer (25 mM Tris pH 8.0, 300 mM NaCl, 0.1% β-mercaptoethanol). GST and GST-Ecad-bound beads were incubated in batch with 1 ml of purified CnoPDZ,

nutating at 4ºC for 30 minutes. Resin was pelleted and supernatant containing non-bound CnoPDZ was removed. Beads were washed twice in batch using 1 ml wash buffer. Proteins were eluted from the beads using 100µl of wash buffer supplemented with 50mM Glutathione. 10µl of the eluate was loaded on a 20% polyacrylamide gel as was 10µl of the CnoPDZ load. Gels were stained with Coomassie Brilliant Blue.

Protein Preparation and Immunoprecipitations

Protein samples were prepared by grinding dechorionated embryos on ice in Laemmli buffer with a plastic pestle and then boiled for 5min. Immunoprecipitations were performed as described in Harris and Peifer, 2005. Samples were separated by 6% SDS-Page and immunoblotted (see Suppl. Table 1). Signal was detected using ECL Plus (Amersham).

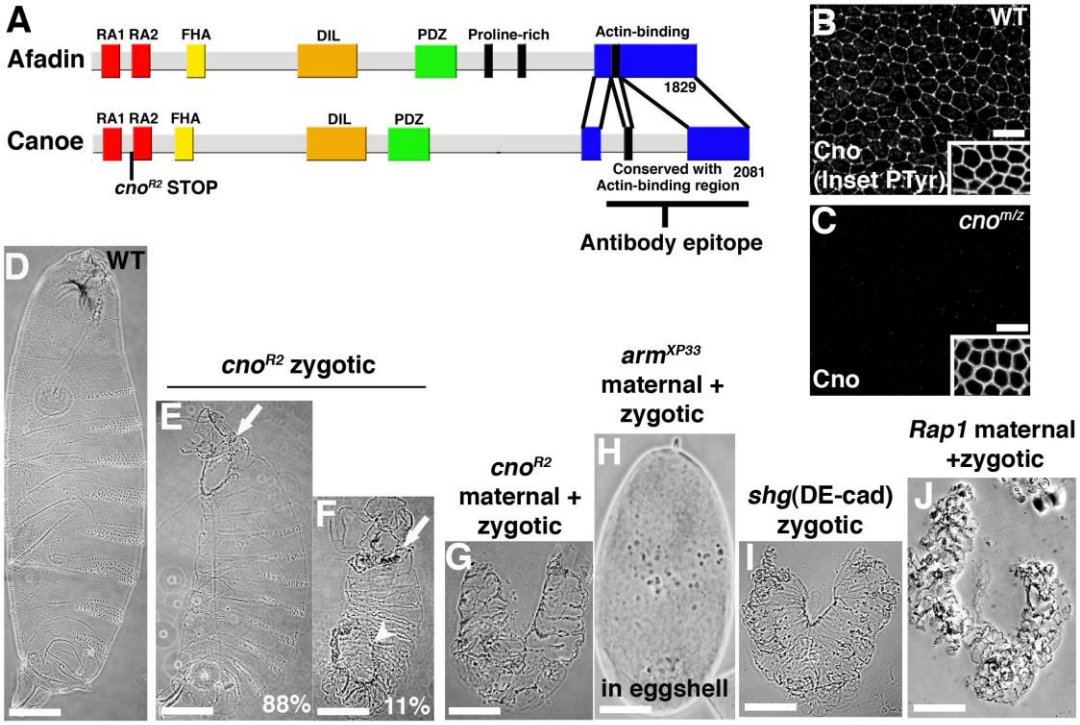

Figure 1. *cno* mutants have defects in morphogenesis.
(A) Domain structures and *cno* mutant. (B and C) Stage 7 wild-type (WT) or cno^{R2} MZ embryos stained for Cno and antiphosphotyrosine (PTyr; insets) to show cell borders imaged on same slide. (D–J) Cuticles, anterior up. Genotypes are indicated. (E and F) cno^{R2} zygotic mutants are shown. Arrows, head involution defects; arrowhead, dorsal closure defects. (G) cno^{R2} MZ is shown. Only dorsal cuticle remains. (H) arm^{XP33} MZ mutant (in eggshell) is shown, cuticle fragmented. (I) shg^{R69} zygotic mutant retains only dorsal cuticle. (J) *Rap1* MZ mutant retains only dorsal cuticle (see Results for Rap1 data). FHA, forkhead-associated domain; DIL, dilute domain. Bars: (B and C) 10 μm; (D–J) 100 μm.

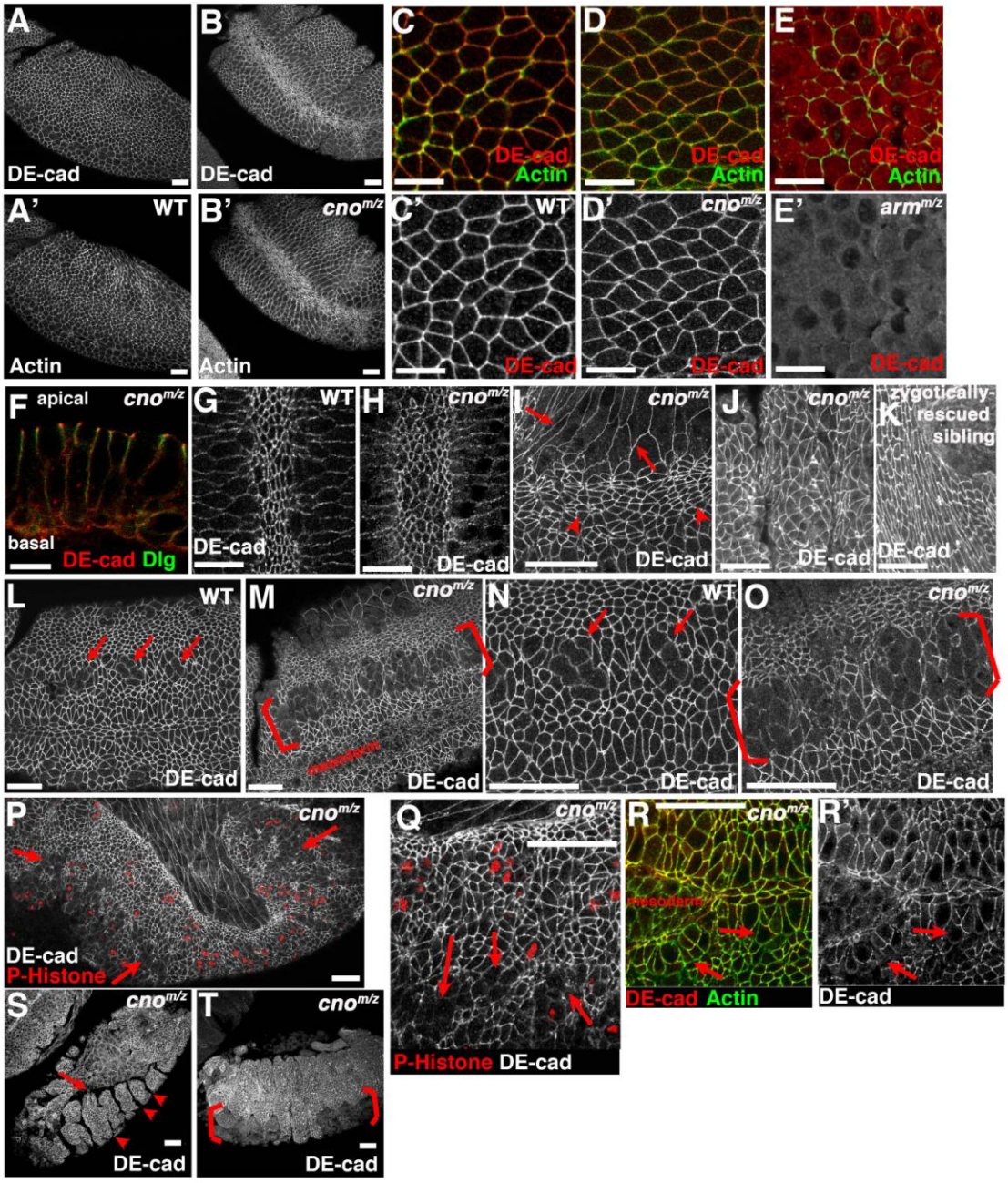

Figure 2. Cno is not essential for AJ assembly.
Embryos, antigens, and genotypes are indicated. (A–F) Stage 8 is shown. (A–B') Ventrolateral views, anterior top left. (C–C') Close ups of A and A' are shown (wild type [WT]). (D and D') Close ups of B and B' are shown (cno^{MZ}). (E and E') arm^{MZ} is shown. Cortical DEcad lost. (F) Cross section, cno^{MZ}. DEcad remains apical. (G) Wild-type ventral furrow. (H) cno^{MZ}, DEcad maintained. (I) Stage 11, cno^{MZ}. AJ is normal in amnioserosa (arrows) and dorsal epidermis (arrowheads). (J and K) Dorsal epidermis, stage 13–14. (J) cno^{MZ}, AJs intact. (K) Paternally rescued sibling. (L–O) Lateral view, stage 9–10 is shown. (L and N) Close-up views of wild-type mitotic domains (arrows) are shown. (M and O) Close-up views of cno^{MZ} are shown. Some cells have reduced DEcad (brackets). (P and Q) Stage 12, cno^{MZ}. Arrows, fragmented AJs. (R and R') Ventral midline, stage 11 cno^{MZ}. AJ fragmentation precedes loss of cortical actin (arrows). (S and T) Stage 13–14 cno^{MZ}. Amnioserosa detaches from epidermis (arrow), segmental groves never retract (arrowheads), and parts of ventral epidermis are missing (brackets). Bars: (A–B' and K–T) 30 µm; (C–J) 10 µm.

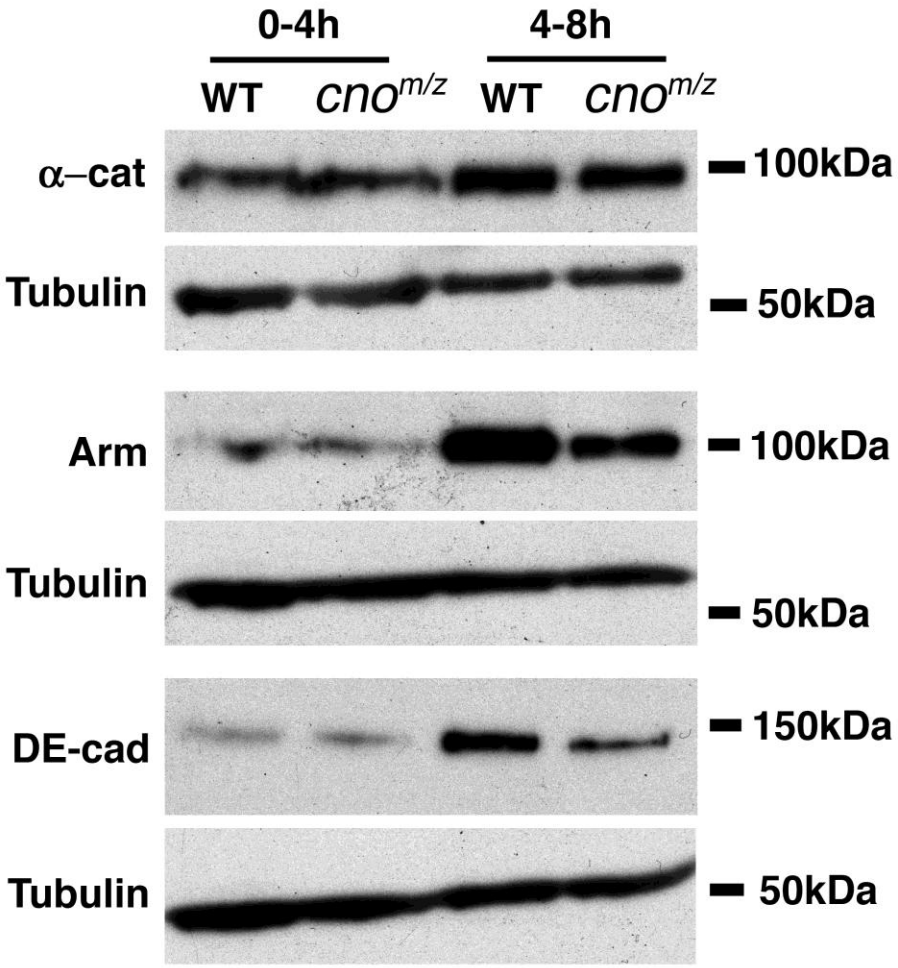

Figure 3. AJ protein levels in *cno*^{MZ}.
Immunoblots, embryo extracts, and antigens are indicated. 0–4h through mesoderm invagination and early germband extension. 4–8h extended germband, stages 8–11. Tubulin is a loading control. WT, wild type.

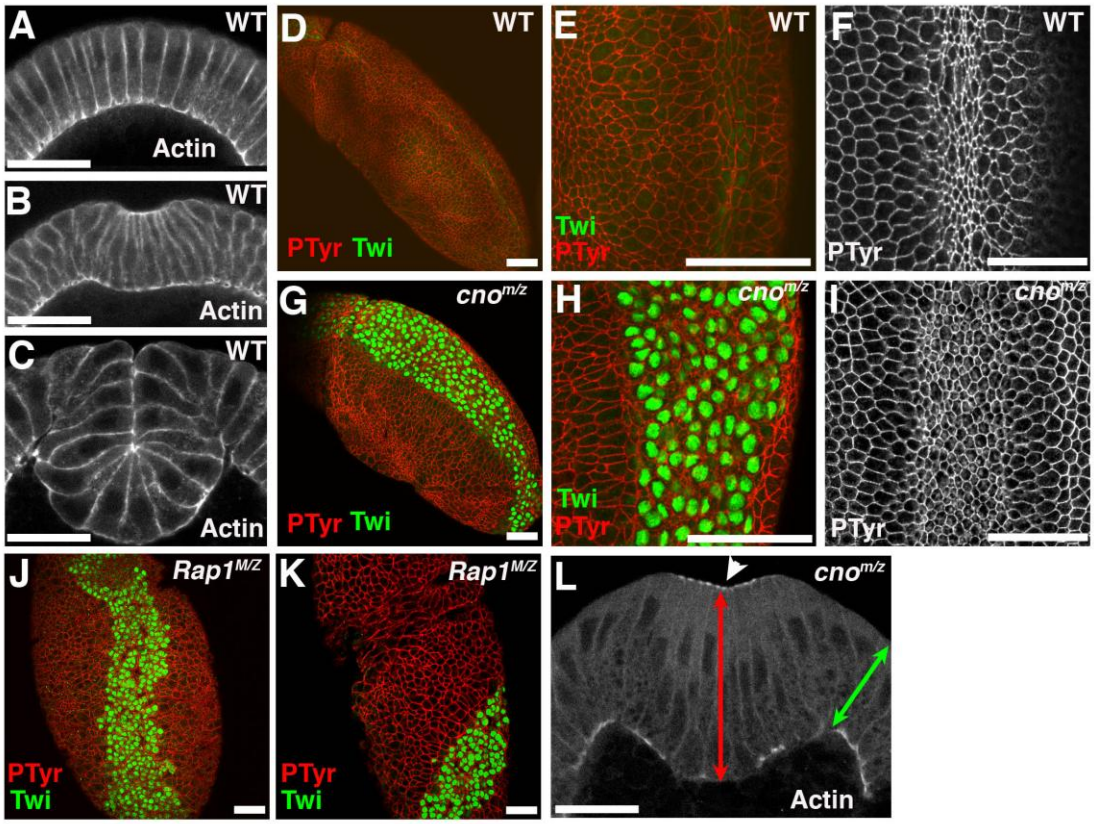

Figure 4. Cno is essential for mesoderm invagination.
Embryos, antigens, and genotypes are indicated. (A–C) Cross sections of wild-type (WT) ventral furrow. Late cellularization (A), initial furrowing (B), and mesoderm internalized (C) are shown. (D–K) Ventral views, anterior up. (D and E) Wild type, mesoderm completely internalized. (F) Wild type during constriction. (G and H) *cno*^{MZ}, Twist (Twi)-positive cells not completely internalized. (I) *cno*^{MZ} mesoderm initiates constriction. (J and K) *Rap1*^{MZ} phenocopies *cno*^{MZ}, but some exhibit twisted gastrulation. (L) *cno*^{MZ} mesodermal cells elongate along apical–basal axis (red arrow) relative to ectodermal neighbors (green arrow). Arrowhead, actin accumulating in balls. PTyr, phosphotyrosine. Bars, 30 μm.

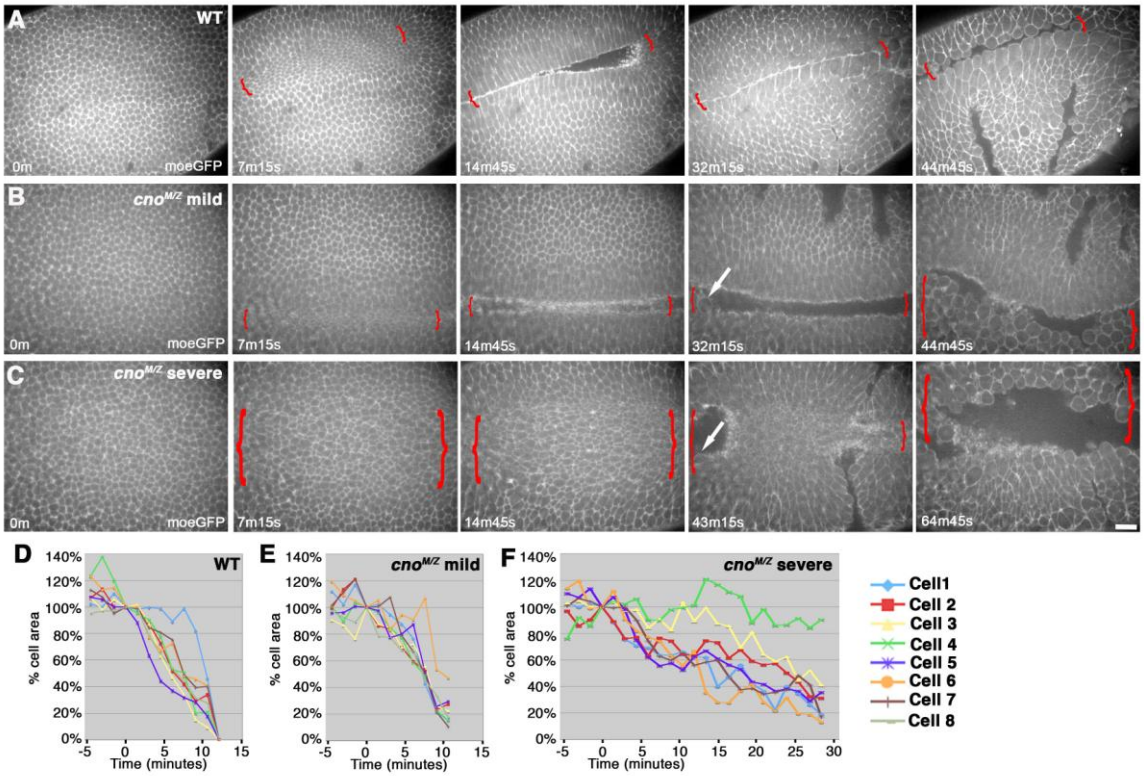

Figure 5. Mesoderm invagination in *cno*^{MZ}.
(A–C) Embryos, ventral views, anterior left, and genotypes are indicated. Moe-GFP reveals F-actin. Brackets, ventral furrow; arrows, mesoderm cells round up to divide and emerge from furrow. Still images from Videos 1 (A), 2 (B), and 3 (C) are shown. (D–F) Graphs show cell cross-sectional areas as ventral furrow invaginates. t = 0, defined as 100%. Wild-type (WT) cells constrict to essentially zero before invaginating, whereas mutant cells disappear in furrow before fully constricting. Bar, 30 μm.

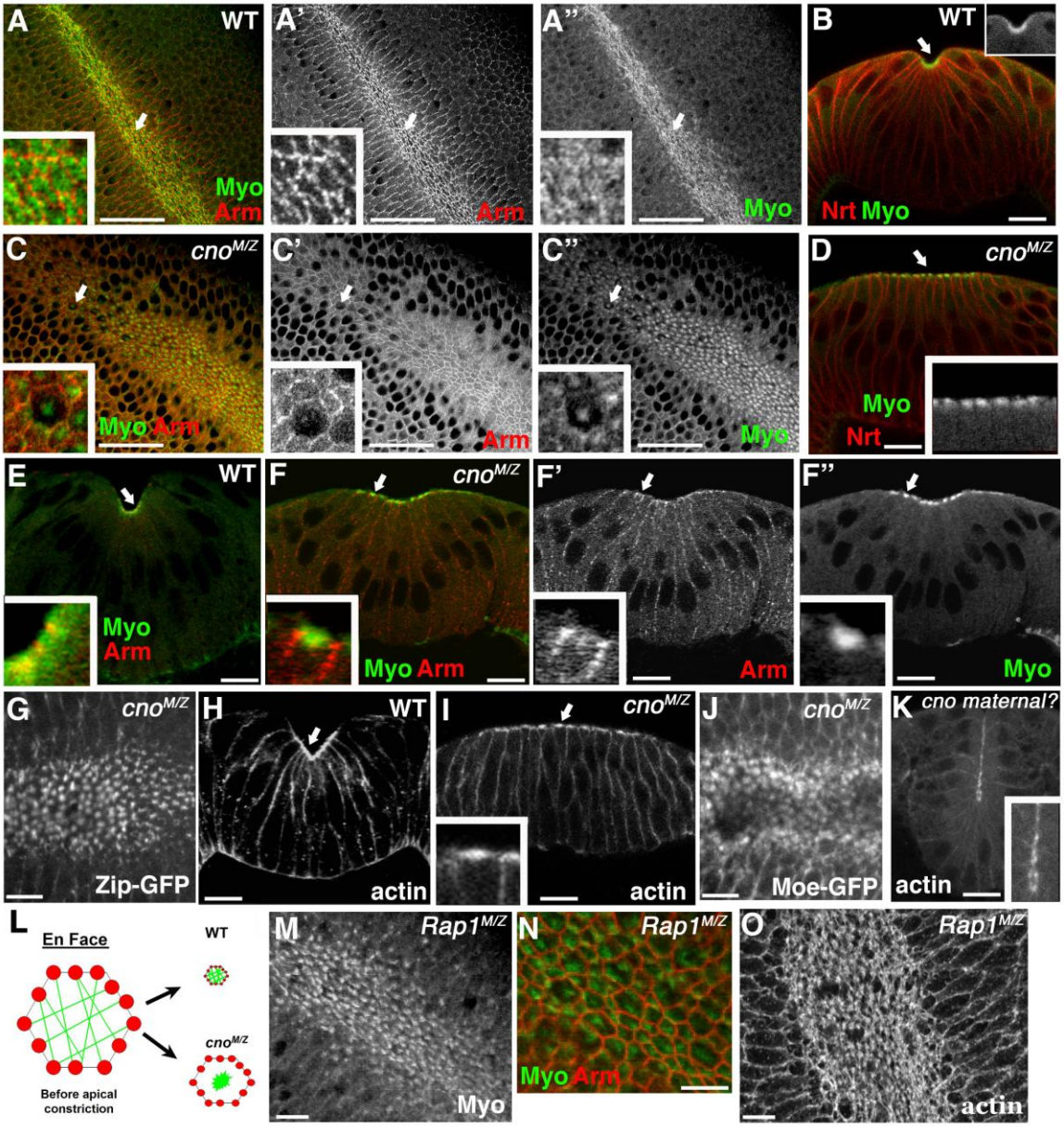

Figure 6. Cno regulates coupling of AJs to contractile network.
Embryos, stage 6–8, antigens, and genotypes are indicated. (A–A'', C–C'', G, J, and M–O) Ventral views are shown. (B, D–F', H, I, and K) Cross sections are shown. (A–A", B, and E) Wild-type (WT) ventral furrow. Myosin (Myo) covers cell apices (arrows and insets). Constriction coupled to actomyosin contraction. (C–C'', D, and F–F'') *cno*^{MZ} is shown. Myosin condensed into balls that are not contiguous with AJs (arrows and insets). Cell shape change is not completed. (G) *cno*^{MZ} is shown. Myosin balls visualized live with zipper-GFP (Zip-GFP). (H) Wild type is shown. Actin accumulates evenly at the apical surface (arrow). (I) *cno*^{MZ} is shown. Actin condenses into balls that are not contiguous with actin at AJs. Constriction arrests (arrow and inset) are shown. (J) *cno*^{MZ} is shown. F-actin balls visualized live with moe-GFP. (K) Probable *cno* maternal mutant. Balls of actin (inset) observed even in embryos initiating invagination. (L) Model of alterations in actin, myosin and constriction in *cno*^{MZ}. (M–O) *Rap1*^{MZ} is shown. (M and N) Similar balls of Myo form and separate from AJs. (O) Balls of actin. Bars: (A–A" and C–C") 30 μm; (B and D–O) 10μm.

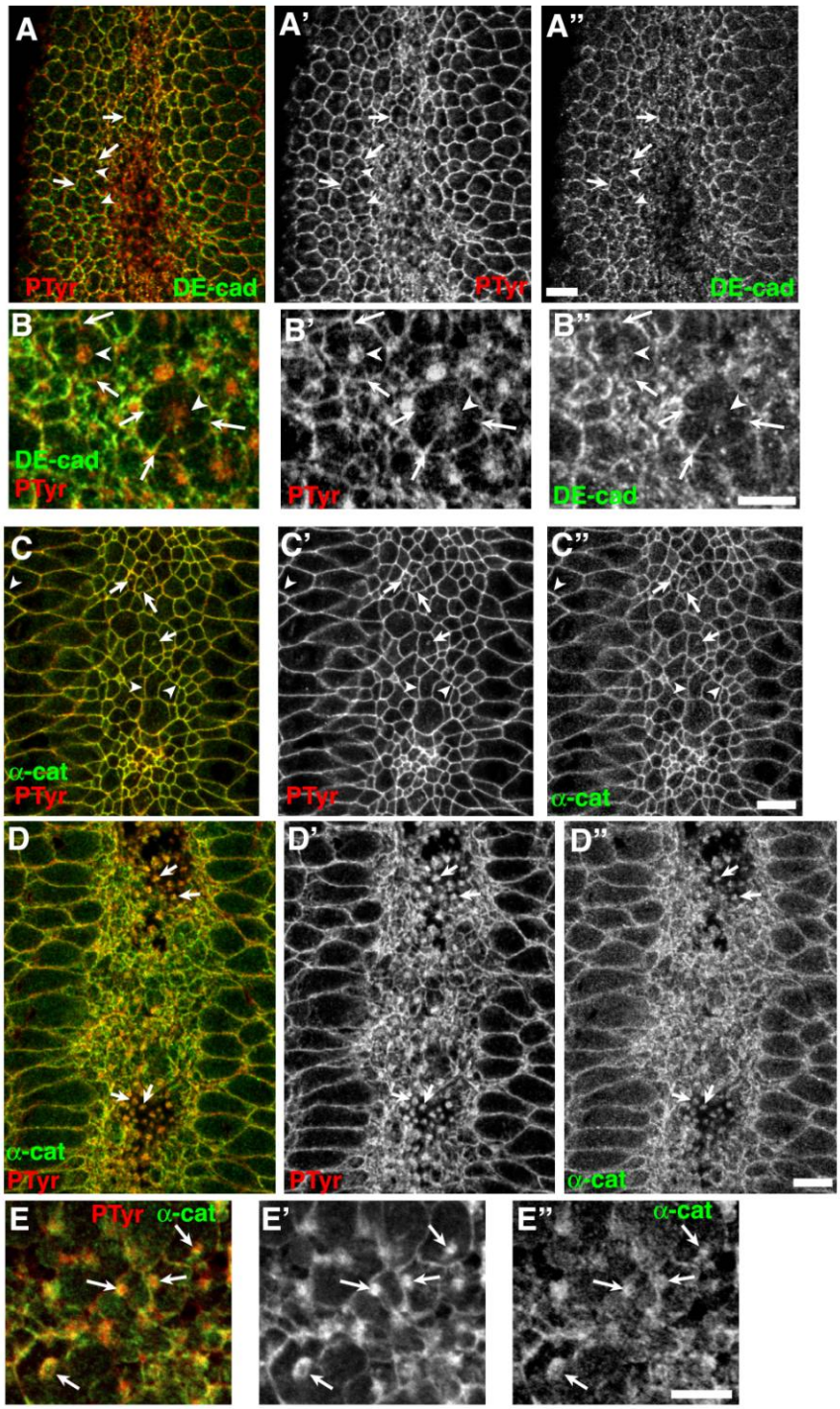

Figure 7. Pools of αcat at AJs and actomyosin balls.
Ventral views, gastrulating *cno*^{MZ}, antigens are indicated. (A–B") DEcad localizes to AJs (arrows) but is only very weakly found in actomyosin balls (arrowheads). Strands of DEcad connect AJs to balls. (C–E") Apical (C–C") and more basolateral (D–D") views of the same embryo. E–E" show close-up views. Pools of αcat at AJs (C–C", arrowheads) and actomyosin balls (C–E", arrows). PTyr, phosphotyrosine. Bars, 10μm.

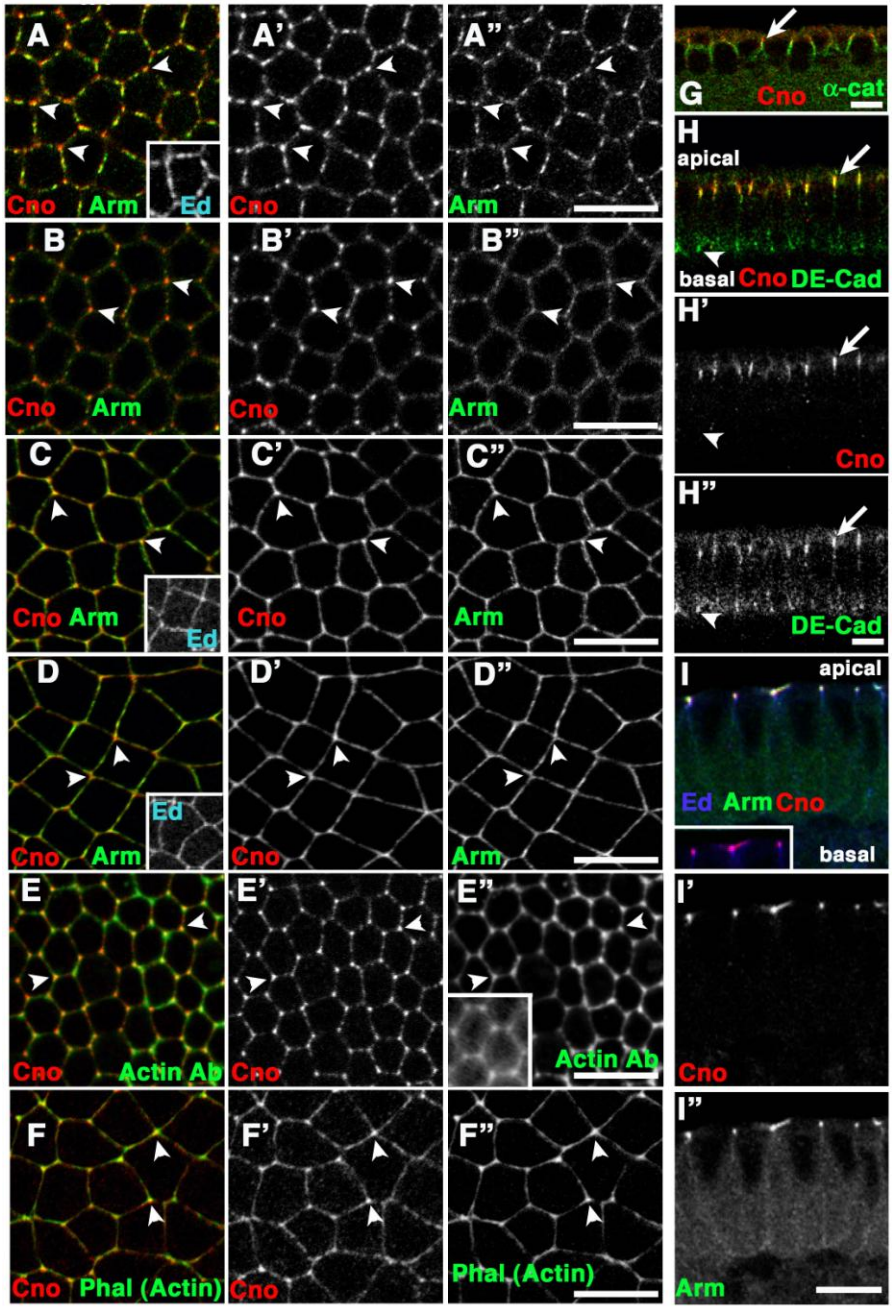

Figure 8. Cno is enriched at tricellular junctions with a subpool of actin.
Wild type, antigens are indicated. (A–F") Surface views are shown. (G–I") Cross sections are shown. (A–B") Cellularization is shown. (A–A") Apically, Cno colocalizes with Arm and Ed (inset) in spot AJs, with enrichment at tricellular junctions (arrowheads). (B–B") 2 μm more basal, Cno is strongly enriched at tricellular junctions relative to Arm (arrowheads). (C–D") Mid (C–C") to late (D–D") gastrulation. Cno, Arm, and Ed (insets) form belt AJs. Cno remains enriched at tricellular junctions (arrowheads). (E–F") Cno localizes with a subpool of actin at tricellular junctions (arrowheads) during cellularization (E–E") and gastrulation (F–F"; E" [inset], actin visualized with moe-GFP). (G) Cno is already apical in the syncytial embryo (arrow). (H–H") Cno colocalizes with DEcad in apical AJs (arrows) but not basal junctions (arrowheads). (I–I") Gastrulation. Cno tightly localized at AJs with Arm and Ed. The inset shows Cno and Ed channels alone. Bars, 10μm.

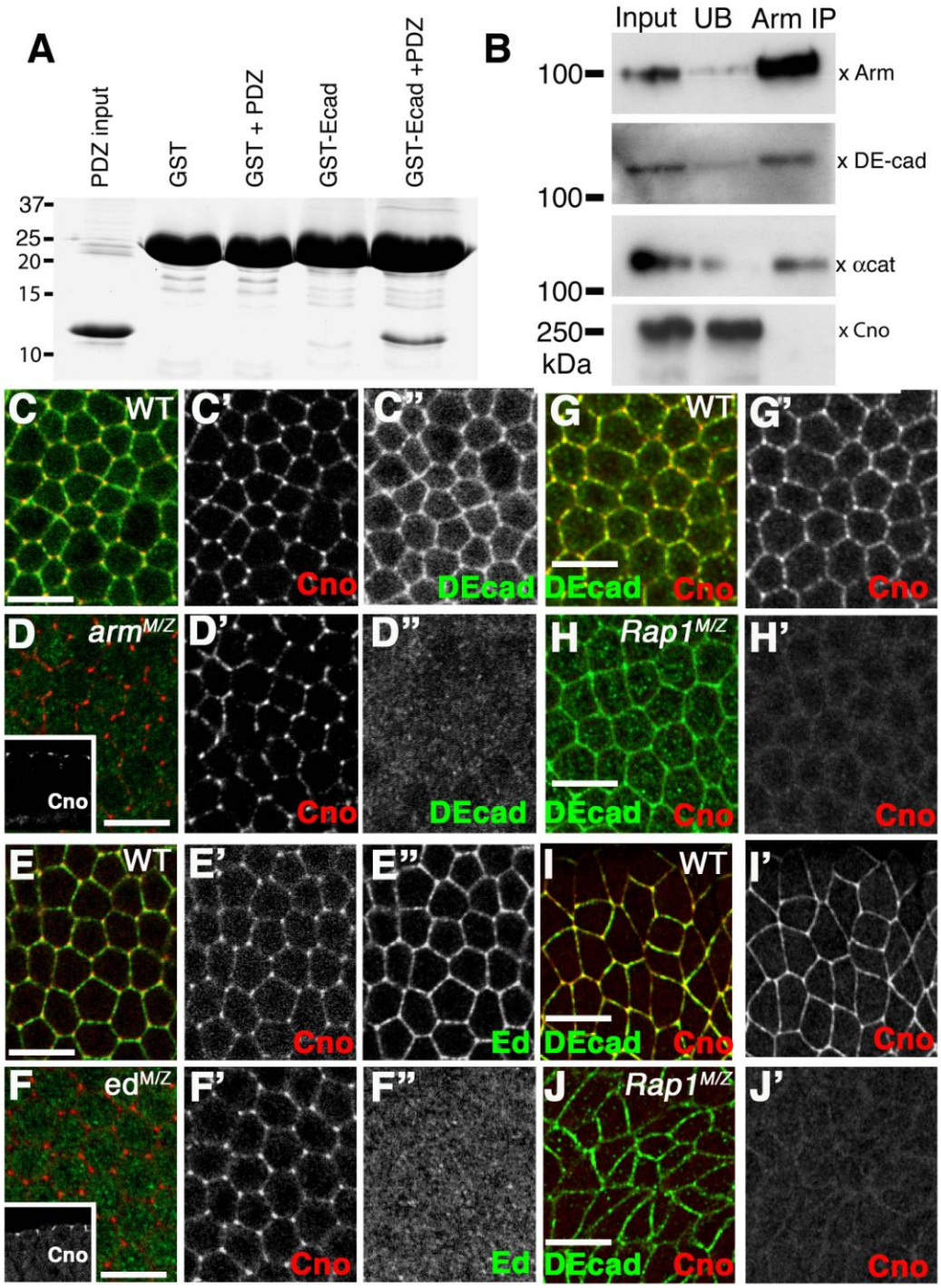

Figure 9. Rap1 but not AJs or Ed are required for apical Cno recruitment.
(A) Purified Cno PDZ domain incubated with GST or GST fused to C-terminal seven amino acids of DEcad. Input, 1% of load; bound, 10% of bound fraction. (B) Embryonic extracts immunoprecipitated with anti-Arm. Input, unbound (UN), and immunoprecipitation (IP) fractions immunoblotted with the indicated antibodies. (C–J') Antigens and genotypes are indicated. Apical surface is shown except for insets in D and F, which show cross sections. (C–H') Late cellularization. (I–J') Early gastrulation. (C–F") Removing AJs (C–D"; *arm*^{043A01}) or Ed (E–F"; *ed*^{F72}) does not affect Cno localization. (G–J') Removing Rap1 reduces cortical Cno. WT, wild type. Bars, 10 µm.

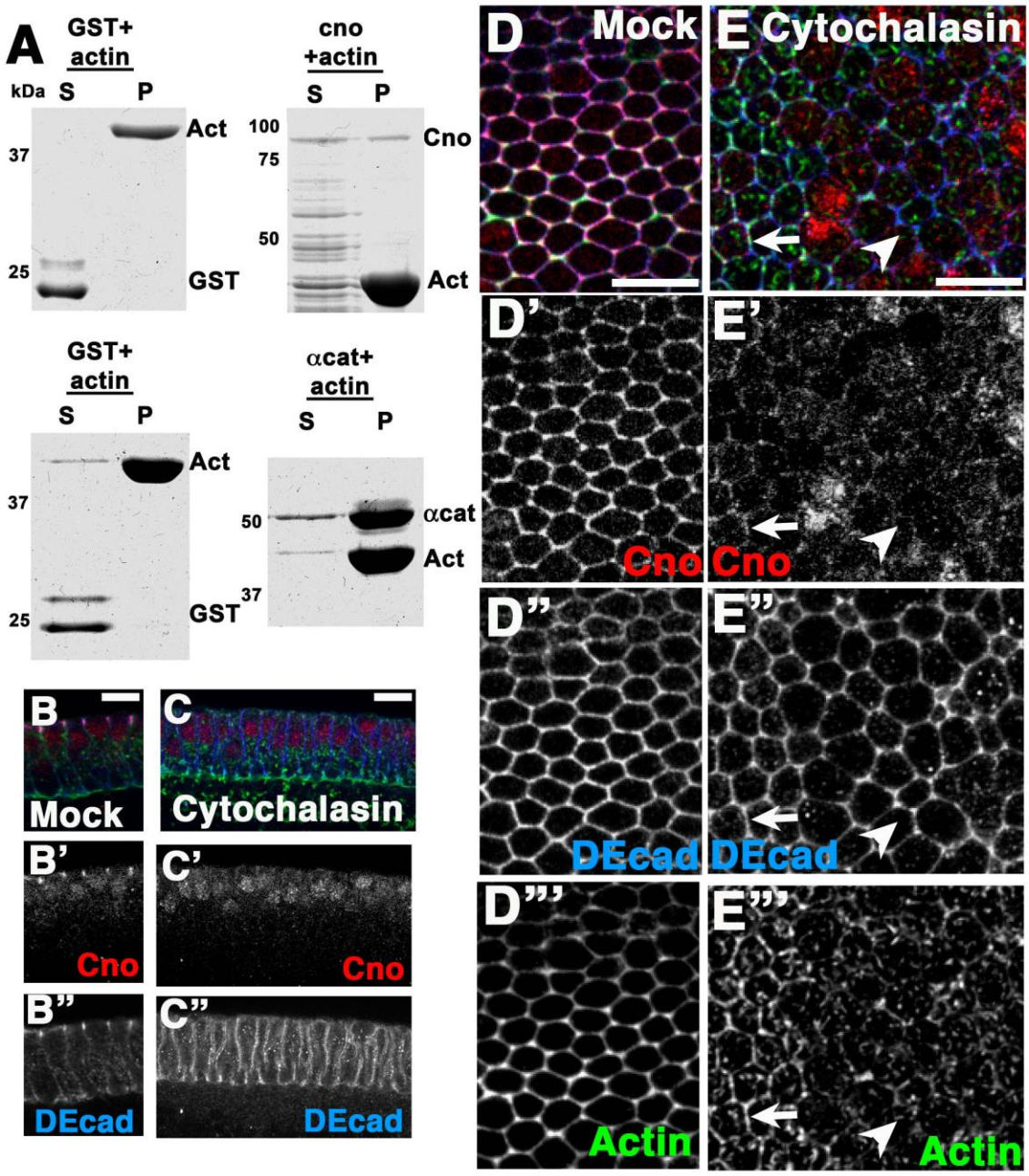

Figure 10. F-actin is required for Cno cortical localization.
(A) Actin (Act) cosedimentation assays of GST-CnoCT, GST-αcat, and GST as a negative control are shown. S, supernatant; P, high speed pellet. (B–B" and D–D"') DMSO-treated controls. (B–B") DEcad at apical and basal junctions. Cno only at apical junctions. (C–C" and E–E"') Cytochalasin treated. (C–C") After depolymerization, DEcad all along lateral cortex. Cno cytoplasmic and nuclear. (D–D"') Normal DEcad, Cno, and actin localization. (E–E"') Actin depolymerized, some residual cortical actin in cells at left (arrows). DEcad remains cortical. Cno lost from cortex (arrowheads) except where residual cortical actin remains. Bars, 10μm.

Supplementary Materials

These materials can be found in this section and/or online at:

http://jcb.rupress.org/cgi/content/full/jcb.200904001/DC1

Supplemental Table 1 includes genetic and antibody reagents used in this paper. Fig. S1 Cno is not required for the transition from spot to belt adherens junctions, posterior midgut invagination, and is not essential for intercalation but restrains planar polarity during germband extension. Fig. S2 The actomyosin cystoskeleton becomes uncoupled from cell shape change in *cno*^{MZ} mutants. Fig. S3 Actin is required to retain Cno at the cortex after gastrulation. Fig. S4 GFP-Rap1 localization overlaps AJs and does not require Cno function. Fig. S5 Models for Cno function. Video 1 shows WT ventral furrow formation, MoeGFP. Video 2 shows a mild *cno*^{MZ} mutant ventral furrow phenotype, MoeGFP. Video 3 shows a severe *cno*^{MZ} mutant ventral furrow phenotype, MoeGFP. Video 4 shows WT ventral furrow formation, MoeGFP. Video 5 shows a *cno*^{MZ} mutant ventral furrow phenotype highlighting the actin balls, MoeGFP. Video 6 shows WT ventral furrow formation, ZipGFP. Video 7 shows a *cno*^{MZ} mutant ventral furrow phenotype highlighting the myosin balls, ZipGFP.

Table S1: Fly stocks, Antibodies, and Probes

Fly stocks			**Source**
Moesin-GFP			D. Kierhart (Duke University, NC, USA)
Zip-GFP (trap #CC01626)			The Carnegie Protein Trap Library (Buszczak et al., 2007)
HisGFPIII			R. Saint, (University of Adelaide, South Australia, AUSTRALIA)
arm^{043A01}FRT101/FM7			E. Wieschaus (Princeton, NJ, USA)
ed^{F72}FRT40A/CyotwiGFP			L. Nilson (McGill University, Quebec, Canada)
Antibodies/Probes	*Dilution*		**Source**
	IF	*Western*	
anti-DE-DCAD2	1:100	N/A	DSHB
anti-DE-CAD1	N/A	1:200	M. Takeichi (Kyoto University, Japan)
anti-ArmN27A1	1:100	1:50	DSHB
anti-alpha-catenin	1:100	1:200	DSHB
Phopho-Tyrosine	1:1000		Upstate Biotechnology
MAB150 1R (Actin)	1:1000		Chemicon
anti-Cno	1:1000	1:1000	K. Takahashi (Waseda University, Japan)
anti-Twist	1:2000	N/A	S. Roth (University of Köln, Germany)
anti-Zipper ((Myosin II heavy chain)	1:1000	N/A	C. Field (Harvard, MA, USA) D. Kiehart (Duke University, NC, USA)
anti-Echinoid	1:1000	N/A	L. Nilson (McGill University, Quebec, Canada)
anti-Polycheatoid	1:1000	1:2000	A. Fanning (UNC-CH, NC, USA)
Alexa-phalloidin	1:500		Molecular Probes
anti-alpha-tubulin		1:2000	Sigma
Secondary antibodies: Alexas 488, 568, and 647	1:500	N/A	Molecular Probes
HRP Secondary Antibodies:	N/A		Thermo Scientific
Mouse/Rat		1:10,000	
Rabbit		1:100,000	

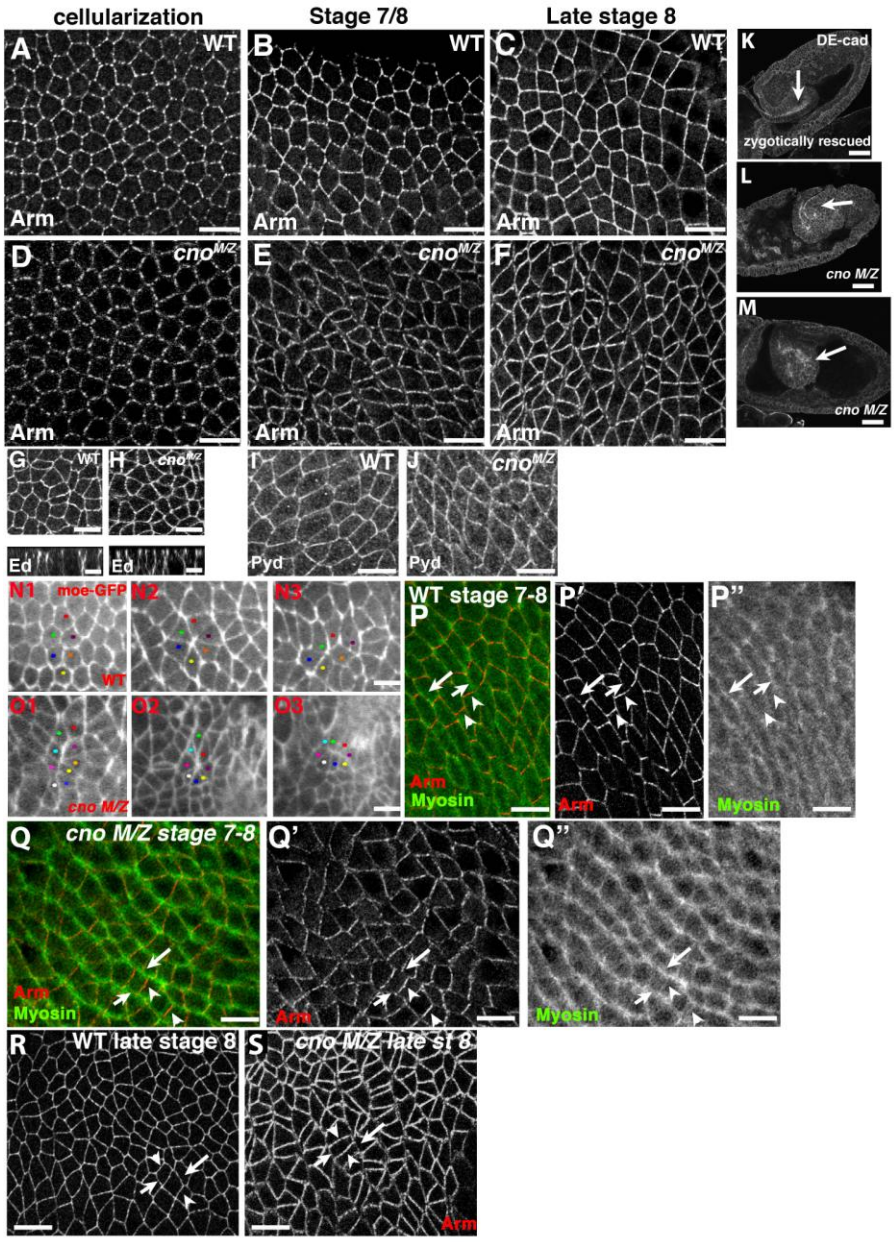

Figure S1. Cno is not required for the transition from spot to belt AJs, posterior midgut invagination, and is not essential for intercalation but restrains planar polarity during germband extension. Embryos, antigens, and genotypes are indicated. Apical surface sections are shown, except in bottom panels of G and H, which are cross sections. (A–F) Spot to belt AJ transition stages are indicated. (G–J) The Cno-binding partners Ed (G–H) and Pyd (I and J) still localize to AJs in *cno*^{MZ} mutants. (K–M) Embryos, cross sections, stage 8–9, DEcad, and genotypes are indicated. Arrows point to posterior midgut. (K) Zygotically rescued sibling with normal midgut invagination. (L and M) *cno*^{MZ} mutants. Midgut invagination is initiated (L), but invaginated midgut appears disorganized (M). (N–S) Embryos, antigens, and genotypes are indicated. (N1–O3) Each sequence shows still images from videos of live stage 8 wild-type (N) or *cno*^{MZ} embryos, visualizing moe-GFP to outline cells. Intercalating cells are color coded. (P–Q") Stage 7–8 wild-type (P–P") or *cno*^{MZ} mutant (Q–Q") cells. Normal planar polarity of myosin (enriched at anterior–posterior boundaries; arrows) and Arm (enriched at dorsal–ventral boundaries; arrowheads) is accentuated in *cno*^{MZ}. (R and S) Late stage 8 wild type (R) or *cno*^{MZ} (S). AJ planar polarity remains strong in *cno*^{MZ}. Cells form rows. Bars: (A–J and N1–S) 10 µm; (K–M) 30µm.

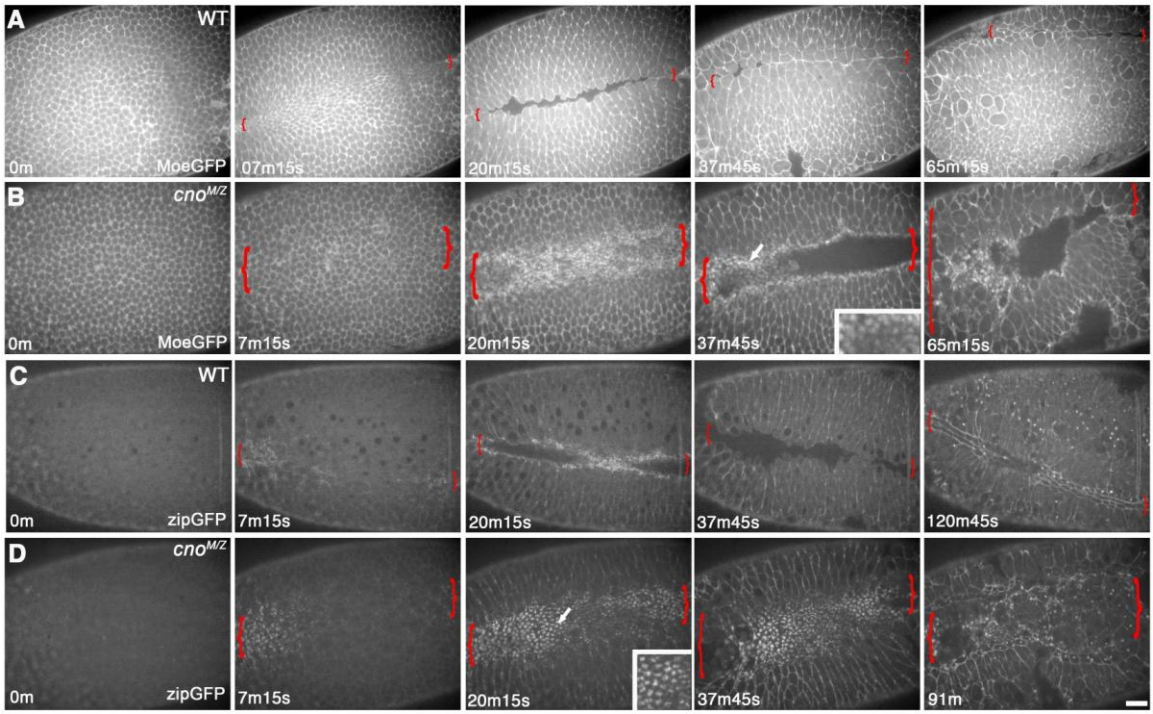

Figure S2. The actomyosin cytoskeleton becomes uncoupled from cell shape change in *cno*^{MZ} mutants.
(A–D) Still images from live imaging of gastrulating embryos, ventral view, anterior to the left, and genotypes are indicated. Brackets mark ventral furrow as it progresses. Arrows and insets show balls of either actin (B) or myosin (D). Still images from Videos 4 (A), 5 (B), 6 (C), and 7 (D) are shown. WT, wild type. Bar, 30μm.

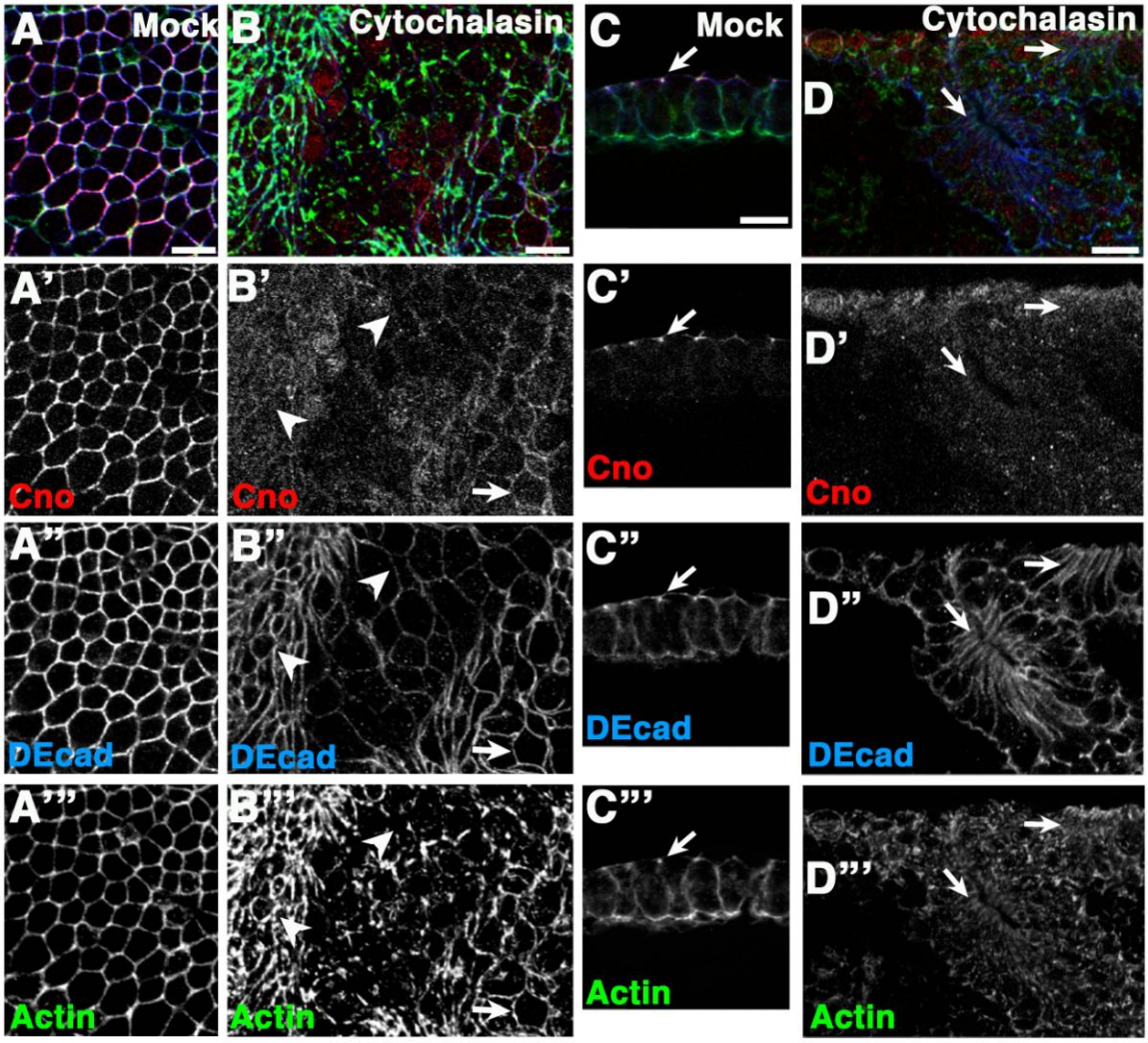

Figure S3. Actin is required to retain Cno at the cortex after gastrulation.
Stage 9 embryos, treatments and antigens indicated. (A–A”’ and C–C”’) DMSO treated control embryos. (B–B”’ and D–D”’) Cytochalasin-treated embryos. (A–A”’) Surface view. Normal DEcad, Cno, and actin localization. (B–B”’) Surface view after cytochalasin treatment. Some residual cortical actin is seen in columnar ectodermal cells (arrowheads) and in amnioserosa (arrows). DEcad remains cortical. Cno is largely lost from the cortex, although some remains at cortex in amnioserosa. (C–C”’) Cross section. DEcad, Cno, and actin at AJs (arrows). (D–D”’) Cross section through furrow after cytochalasin treatment. DEcad is now all along lateral cortex, and Cno becomes largely cytoplasmic (arrows). Bars, 10 μm.

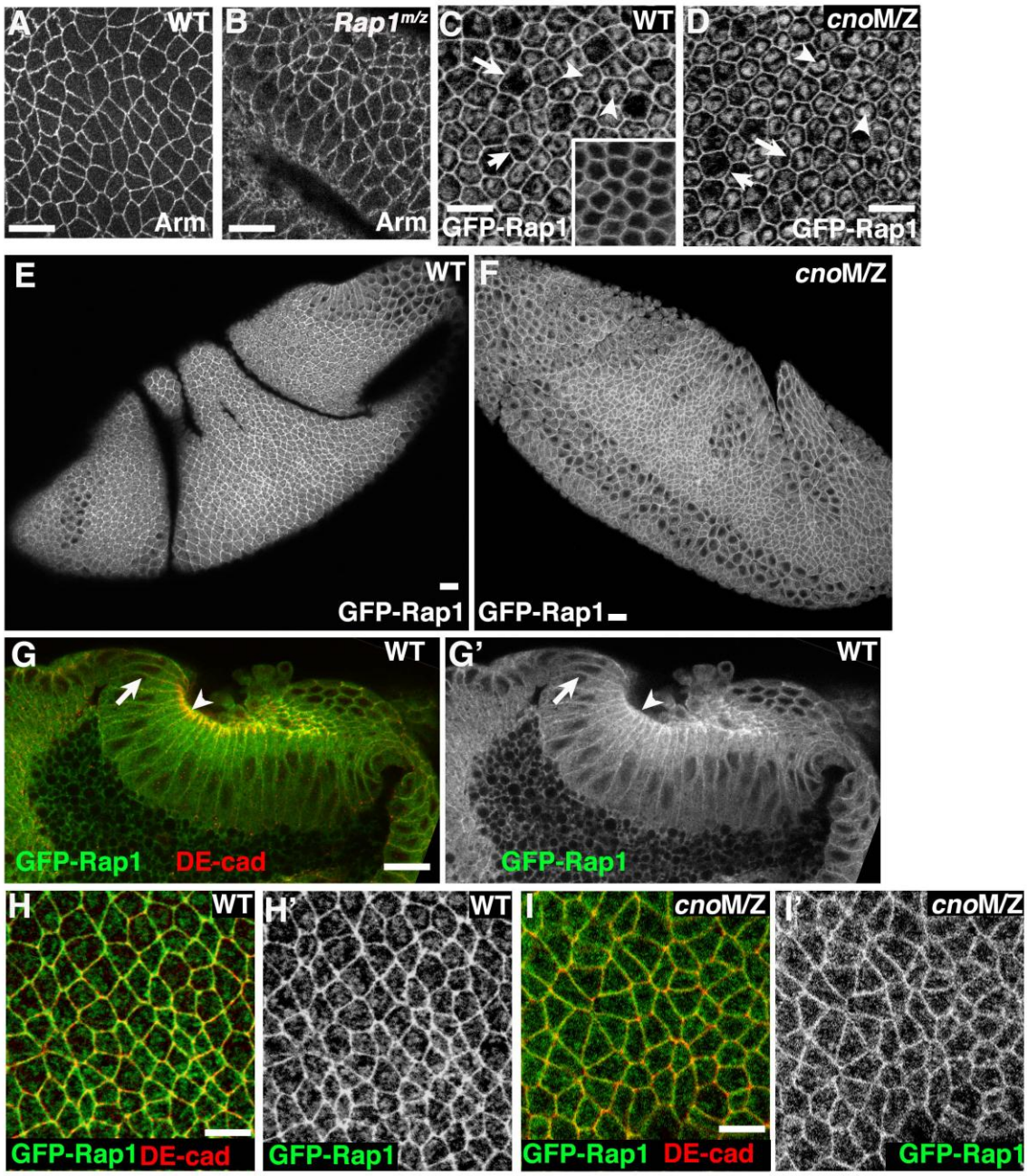

Figure S4. GFP-Rap1 localization overlaps AJs and does not require Cno function.
GFP-Rap1 localization in wild-type (WT; A, C, E, F, H, and H') and *cno*^{MZ} mutants (B, D, G, G', I, and I'). (A and B) Late cellularization. (C–G) Midgastrulation. (C and D) Arrows, cortical GFP-Rap1; arrowheads, localization to apical punctate structure. (C, inset) Basal section of cells shown in C. (G and G') Cross section through posterior midgut. Arrows, GFP-Rap1 on lateral membranes. Arrowheads, GFP-Rap1–overlapping AJs. Bars, 10μm.

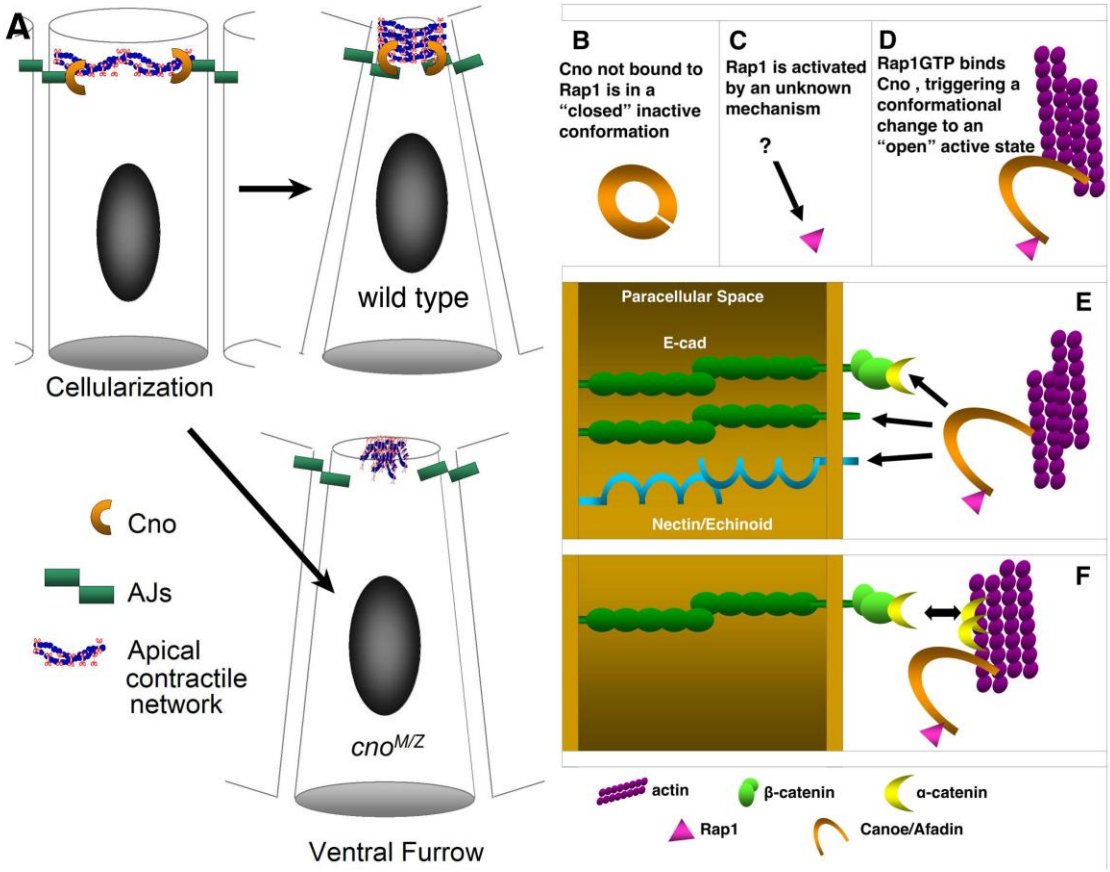

Figure S5. Models for Cno function.
(A) Apical constriction with and without Cno. (B–D) Model of Cno activation. (E and F) Potential molecular links between AJs and actin.

References

Abe, K., and M. Takeichi. 2008. EPLIN mediates linkage of the cadherin catenin complex to Factin and stabilizes the circumferential actin belt. *Proc Natl Acad Sci USA*. 105:13-9.

Arora, P.D., M.A. Conti, S. Ravid, D.B. Sacks, A. Kapus, R.S. Adelstein, A.R. Bresnick, and C.A. McCulloch. 2008. Rap1 activation in collagen phagocytosis is dependent on nonmuscle myosin II-A. *Mol Biol Cell*. 19:5032-46.

Asha, H., N.D. de Ruiter, M.G. Wang, and I.K. Hariharan. 1999. The Rap1 GTPase functions as a regulator of morphogenesis in vivo. *Embo J*. 18:605-15.

Barrett, K., M. Leptin, and J. Settleman. 1997. The Rho GTPase and a putative RhoGEF mediate a signaling pathway for the cell shape changes in Drosophila gastrulation. *Cell*. 91:905-15.

Bertet, C., L. Sulak, and T. Lecuit. 2004. Myosin-dependent junction remodelling controls planar cell intercalation and axis elongation. *Nature*. 429:667-71.

Blankenship, J.T., S.T. Backovic, J.S. Sanny, O. Weitz, and J.A. Zallen. 2006. Multicellular rosette formation links planar cell polarity to tissue morphogenesis. *Dev Cell*. 11:459-70.

Boettner, B., E.E. Govek, J. Cross, and L. Van Aelst. 2000. The junctional multidomain protein AF-6 is a binding partner of the Rap1A GTPase and associates with the actin cytoskeletal regulator profilin. *Proc Natl Acad Sci USA*. 97:9064-9.

Boettner, B., P. Harjes, S. Ishimaru, M. Heke, H.Q. Fan, Y. Qin, L. Van Aelst, and U. Gaul. 2003. The AF-6 homolog canoe acts as a Rap1 effector during dorsal closure of the Drosophila embryo. *Genetics*. 165:159-69.

Buszczak, M., S. Paterno, D. Lighthouse, J. Bachman, J. Planck, S. Owen, A.D. Skora, T.G. Nystul, B. Ohlstein, A. Allen, J.E. Wilhelm, T.D. Murphy, R.W. Levis, E. Matunis, N. Srivali, R.A. Hoskins, and A.C. Spradling. 2007. The carnegie protein trap library: a versatile tool for Drosophila developmental studies. *Genetics*. 175:1505-31.

Carmena, A., S. Speicher, and M. Baylies. 2006. The PDZ protein Canoe/AF-6 links Ras-MAPK, Notch and Wingless/Wnt signaling pathways by directly interacting with Ras, Notch and Dishevelled. *PLoS ONE*. 1:e66.

Cavey, M., M. Rauzi, P.F. Lenne, and T. Lecuit. 2008. A two-tiered mechanism for stabilization and immobilization of E-cadherin. *Nature*. 453:751-6.

Chou, T.B., E. Noll, and N. Perrimon. 1993. Autosomal P[ovoD1] dominant female-sterile insertions in Drosophila and their use in generating germ-line chimeras. *Development*. 119:1359-69.

Cox, R.T., C. Kirkpatrick, and M. Peifer. 1996. Armadillo is required for adherens junction assembly, cell polarity, and morphogenesis during Drosophila embryogenesis. *J Cell Biol*. 134:133-48.

Dawes-Hoang, R.E., K.M. Parmar, A.E. Christiansen, C.B. Phelps, A.H. Brand, and E.F. Wieschaus. 2005. folded gastrulation, cell shape change and the control of myosin localization. *Development*. 132:4165-78.

Drees, F., S. Pokutta, S. Yamada, W.J. Nelson, and W.I. Weis. 2005. Alpha-catenin is a molecular switch that binds E-cadherin-beta-catenin and regulates actin-filament assembly. *Cell*. 123:903-15.

Fox, D.T., and M. Peifer. 2007. Abelson kinase (Abl) and RhoGEF2 regulate actin organization during cell constriction in Drosophila. *Development*. 134:567-78.

Fukuhara, A., K. Irie, A. Yamada, T. Katata, T. Honda, K. Shimizu, H. Nakanishi, and Y. Takai. 2002. Role of nectin in organization of tight junctions in epithelial cells. *Genes Cells*. 7:1059-72.

Gates, J., and M. Peifer. 2005. Can 1000 reviews be wrong? Actin, alpha-Catenin, and adherens junctions. *Cell*. 123:769-72.

Gatfield, D., L. Unterholzner, F.D. Ciccarelli, P. Bork, and E. Izaurralde. 2003. Nonsense-mediated mRNA decay in Drosophila: at the intersection of the yeast and mammalian pathways. *Embo J.* 22:3960-70.

Grevengoed, E.E., J.J. Loureiro, T.L. Jesse, and M. Peifer. 2001. Abelson kinase regulates epithelial morphogenesis in Drosophila. *J Cell Biol*. 155:1185-98.

Halbleib, J.M., and W.J. Nelson. 2006. Cadherins in development: cell adhesion, sorting, and tissue morphogenesis. *Genes Dev*. 20:3199-214.

Harris, T.J., and M. Peifer. 2004. Adherens junction-dependent and -independent steps in the establishment of epithelial cell polarity in Drosophila. *J Cell Biol*. 167:135-47.

Harris, T.J., and M. Peifer. 2005. The positioning and segregation of apical cues during epithelial polarity establishment in Drosophila. *J Cell Biol*. 170:813-23.

Harris, T.J., and M. Peifer. 2007. aPKC controls microtubule organization to balance adherens junction symmetry and planar polarity during development. *Dev Cell*. 12:727-38.

Honda, T., K. Shimizu, T. Kawakatsu, M. Yasumi, T. Shingai, A. Fukuhara, K. Ozaki-Kuroda, K. Irie, H. Nakanishi, and Y. Takai. 2003. Antagonistic and agonistic effects of an extracellular fragment of nectin on formation of E-cadherin-based cell-cell adhesion. *Genes Cells*. 8:51-63.

Hoshino, T., T. Sakisaka, T. Baba, T. Yamada, T. Kimura, and Y. Takai. 2005. Regulation of E-cadherin endocytosis by nectin through afadin, Rap1, and p120ctn. *J Biol Chem*. 280:24095-103.

Hung, A.Y., and M. Sheng. 2002. PDZ domains: structural modules for protein complex assembly. *J Biol Chem*. 277:5699-702.

Hunter, C., and E. Wieschaus. 2000. Regulated expression of nullo is required for the formation of distinct apical and basal adherens junctions in the Drosophila blastoderm. *J Cell Biol*. 150:391-401.

Hutterer, A., J. Betschinger, M. Petronczki, and J.A. Knoblich. 2004. Sequential roles of Cdc42, Par-6, aPKC, and Lgl in the establishment of epithelial polarity during Drosophila embryogenesis. *Dev Cell*. 6:845-54.

Ikeda, W., H. Nakanishi, J. Miyoshi, K. Mandai, H. Ishizaki, M. Tanaka, A. Togawa, K. Takahashi, H. Nishioka, H. Yoshida, A. Mizoguchi, S. Nishikawa, and Y. Takai. 1999. Afadin: A key molecule essential for structural organization of cell-cell junctions of polarized epithelia during embryogenesis. *J Cell Biol*. 146:1117-32.

Ikenouchi, J., M. Furuse, K. Furuse, H. Sasaki, S. Tsukita, and S. Tsukita. 2005. Tricellulin constitutes a novel barrier at tricellular contacts of epithelial cells. *J Cell Biol*. 171:939-45.

Ikenouchi, J., K. Umeda, S. Tsukita, M. Furuse, and S. Tsukita. 2007. Requirement of ZO-1 for the formation of belt-like adherens junctions during epithelial cell polarization. *J Cell Biol*. 176:779-86.

Jeon, T.J., D.J. Lee, S. Merlot, G. Weeks, and R.A. Firtel. 2007. Rap1 controls cell adhesion and cell motility through the regulation of myosin II. *J Cell Biol*. 176:1021-33.

Jürgens, G., E. Wieschaus, and C. Nüsslein-Volhard. 1984. Mutations affecting the pattern of the larval cuticle in Drosophila melanogaster. II. Zygotic loci on the third chromosome. . *Roux's Arch. Dev. Biol.* 193:283-295.

Knox, A.L., and N.H. Brown. 2002. Rap1 GTPase regulation of adherens junction positioning and cell adhesion. *Science*. 295:1285-8.

Kofron, M., A. Spagnuolo, M. Klymkowsky, C. Wylie, and J. Heasman. 1997. The roles of maternal alpha-catenin and plakoglobin in the early Xenopus embryo.

Development. 124:1553-60.

Komura, H., H. Ogita, W. Ikeda, A. Mizoguchi, J. Miyoshi, and Y. Takai. 2008. Establishment of cell polarity by afadin during the formation of embryoid bodies. *Genes Cells*. 13:79-90.

Kooistra, M.R., N. Dube, and J.L. Bos. 2007. Rap1: a key regulator in cell-cell junction formation. *J Cell Sci*. 120:17-22.

Laplante, C., and L.A. Nilson. 2006. Differential expression of the adhesion molecule Echinoid drives epithelial morphogenesis in Drosophila. *Development*. 133:3255-64.

Larue, L., M. Ohsugi, J. Hirchenhain, and R. Kemler. 1994. E-cadherin null mutant embryos fail to form a trophectoderm epithelium. *Proc Natl Acad Sci USA*. 91:8263-7.

Lin, H.P., H.M. Chen, S.Y. Wei, L.Y. Chen, L.H. Chang, Y.J. Sun, S.Y. Huang, and J.C. Hsu. 2007. Cell adhesion molecule Echinoid associates with unconventional myosin VI/Jaguar motor to regulate cell morphology during dorsal closure in Drosophila. *Dev Biol*. 311:423-33.

Linnemann, T., M. Geyer, B.K. Jaitner, C. Block, H.R. Kalbitzer, A. Wittinghofer, and C. Herrmann. 1999. Thermodynamic and kinetic characterization of the interaction between the Ras binding domain of AF6 and members of the Ras subfamily. *J Biol Chem*. 274:13556-62.

Lorger, M., and K. Moelling. 2006. Regulation of epithelial wound closure and intercellular adhesion by interaction of AF6 with actin cytoskeleton. *J Cell Sci*. 119:3385-98.

Maddugoda, M.P., M.S. Crampton, A.M. Shewan, and A.S. Yap. 2007. Myosin VI and vinculin cooperate during the morphogenesis of cadherin cell cell contacts in mammalian epithelial cells. *J Cell Biol*. 178:529-40.

Mandai, K., H. Nakanishi, A. Satoh, H. Obaishi, M. Wada, H. Nishioka, M. Itoh, A. Mizoguchi, T. Aoki, T. Fujimoto, Y. Matsuda, S. Tsukita, and Y. Takai. 1997. Afadin: A novel actin filament-binding protein with one PDZ domain localized at cadherin-based cell-to-cell adherens junction. *J Cell Biol*. 139:517-28.

Martin, A.C., M. Kaschube, and E.F. Wieschaus. 2009. Pulsed contractions of an actin-myosin network drive apical constriction. *Nature*. 457:495-9.

Matsuo, T., K. Takahashi, E. Suzuki, and D. Yamamoto. 1999. The Canoe protein is necessary in adherens junctions for development of ommatidial architecture in the Drosophila compound eye. *Cell Tissue Res*. 298:397-404.

McCartney, B.M., D.G. McEwen, E. Grevengoed, P. Maddox, A. Bejsovec, and M. Peifer. 2001. *Drosophila* APC2 and Armadillo participate in tethering mitotic spindles to cortical actin. *Nat Cell Biol*. 3:933-938.

Miyamoto, H., I. Nihonmatsu, S. Kondo, R. Ueda, S. Togashi, K. Hirata, Y. Ikegami, and D. Yamamoto. 1995. canoe encodes a novel protein containing a GLGF/DHR motif and functions with Notch and scabrous in common developmental pathways in Drosophila. *Genes Dev*. 9:612-25.

Muhlemann, O., A.B. Eberle, L. Stalder, and R. Zamudio Orozco. 2008. Recognition and elimination of nonsense mRNA. *Biochim Biophys Acta*. 1779:538-49.

Müller, H.-A.J., and E. Wieschaus. 1996. *armadillo*, *bazooka*, and *stardust* are critical for formation of the zonula adherens and maintenance of the polarized blastoderm epithelium in *Drosophila*. *J Cell Biol*. 134:149-165.

Munro, E., Nance, J., and J.R. Priess JR. 2004. Cortical flows powered by asymmetrical contraction transport PAR proteins to establish and maintain anterior-posterior polarity in the early C. elegans embryo. *Dev Cell* 7:413-24.

Pilot F, and T. Lecui. (2005). Compartmentalized morphogenesis in epithelia: from cell to tissue shape. Dev Dyn. 232:685-94.

Pokutta, S., F. Drees, Y. Takai, W.J. Nelson, and W.I. Weis. 2002. Biochemical and structural definition of the l-afadin- and actin-binding sites of alpha-catenin. *J Biol Chem*. 277:18868-74.

Quinlan, M.P., and J.L. Hyatt. 1999. Establishment of the circumferential actin filament network is a prerequisite for localization of the cadherin-catenin complex in epithelial cells. *Cell Growth Differ*. 10:839-54.

Sakisaka, T., W. Ikeda, H. Ogita, N. Fujita, and Y. Takai. 2007. The roles of nectins in cell adhesions: cooperation with other cell adhesion molecules and growth factor receptors. *Curr Opin Cell Biol*. 19:593-602.

Sato, T., N. Fujita, A. Yamada, T. Ooshio, R. Okamoto, K. Irie, and Y. Takai. 2006. Regulation of the assembly and adhesion activity of E-cadherin by nectin and afadin for the formation of adherens junctions in Madin-Darby canine kidney cells. *J Biol Chem*. 281:5288-99.

Speicher, S., A. Fischer, J. Knoblich, and A. Carmena. 2008. The PDZ protein Canoe regulates the asymmetric division of Drosophila neuroblasts and muscle progenitors. *Curr Biol*. 18:831-7.

Sweeton, D., S. Parks, M. Costa, and E. Wieschaus. 1991. Gastrulation in Drosophila: the formation of the ventral furrow and posterior midgut invaginations. *Development*. 112:775-89.

Tachibana, K., H. Nakanishi, K. Mandai, K. Ozaki, W. Ikeda, Y. Yamamoto, A. Nagafuchi, S. Tsukita, and Y. Takai. 2000. Two cell adhesion molecules, nectin and cadherin, interact through their cytoplasmic domain-associated proteins. *J Cell Biol*. 150:1161-76.

Takahashi, K., T. Matsuo, T. Katsube, R. Ueda, and D. Yamamoto. 1998. Direct binding between two PDZ domain proteins Canoe and ZO-1 and their roles in regulation of the jun N-terminal kinase pathway in Drosophila morphogenesis. *Mech Dev*. 78:97-111.

Takahashi, K., H. Nakanishi, M. Miyahara, K. Mandai, K. Satoh, A. Satoh, H. Nishioka, J. Aoki, A. Nomoto, A. Mizoguchi, and Y. Takai. 1999. Nectin/PRR: an immunoglobulin-like cell adhesion molecule recruited to cadherin-based adherens junctions through interaction with Afadin, a PDZ domain-containing protein. *J Cell Biol*. 145:539-49.

Tepass, U. 1996. Crumbs, a component of the apical membrane, is required for zonula adherens formation in primary epithelia of *Drosophila*. *Dev Biol* 177:217-225.

Tepass, U., E. Gruszynski-DeFeo, T.A. Haag, L. Omatyar, T. Torok, and V. Hartenstein. 1996. shotgun encodes Drosophila E-cadherin and is preferentially required during cell rearrangement in the neurectoderm and other morphogenetically active epithelia. *Genes Dev*. 10:672-85.

Tepass, U., and V. Hartenstein. 1994. The development of cellular junctions in the Drosophila embryo. *Dev Biol*. 161:563-96.

Thomas, G.H., and J.A. Williams. 1999. Dynamic rearrangement of the spectrin membrane skeleton during the generation of epithelial polarity in Drosophila. *Journal of Cell Science*. 112:2843-52.

Torres, M., A. Stoykova, O. Huber, K. Chowdhury, P. Bonaldo, A. Mansouri, S. Butz, R. Kemler, and P. Gruss. 1997. An alpha-E-catenin gene trap mutation defines its function in preimplantation development. *Proc Natl Acad Sci U S A*. 94:901-6.

Uemura, T., H. Oda, R. Kraut, S. Hayashi, Y. Kotaoka, and M. Takeichi. 1996. Zygotic Drosophila E-cadherin expression is required for processes of dynamic epithelial cell rearrangement in the Drosophila embryo. *Genes Dev*. 10:659-71.

Wei, S.Y., L.M. Escudero, F. Yu, L.H. Chang, L.Y. Chen, Y.H. Ho, C.M. Lin, C.S. Chou, W. Chia, J. Modolell, and J.C. Hsu. 2005. Echinoid is a component of adherens junctions that cooperates with DEcadherin to mediate cell adhesion. *Dev*

Cell. 8:493-504.

Wieschaus, E., and C. Nüsslein-Volhard. 1986. Looking at embryos. *In Drosophila*, A Practical Approach. D.B. Roberts, editor. IRL Press, Oxford, England. 199-228.

Yamada, S., S. Pokutta, F. Drees, W.I. Weis, and W.J. Nelson. 2005. Deconstructing the cadherin-catenin-actin complex. *Cell*. 123:889-901.

Yokoyama, S., K. Tachibana, H. Nakanishi, Y. Yamamoto, K. Irie, K. Mandai, A. Nagafuchi, M. Monden, and Y. Takai. 2001. alpha-catenin-independent recruitment of ZO-1 to nectin-based cell-cell adhesion sites through afadin. *Mol Biol Cell.* 12:1595-609.

Zallen, J.A., and E. Wieschaus. 2004. Patterned gene expression directs bipolar planar polarity in Drosophila. *Dev Cell*. 6:343-55.

Zdobnov, E.M., C. von Mering, I. Letunic, D. Torrents, M. Suyama, R.R. Copley, G.K. Christophides, D. Thomasova, R.A. Holt, G.M. Subramanian, H.M. Mueller, G. Dimopoulos, J.H. Law, M.A. Wells, E. Birney, R. Charlab, A.L. Halpern, E. Kokoza, C.L. Kraft, Z. Lai, S. Lewis, C. Louis, C. Barillas-Mury, D. Nusskern, G.M. Rubin, S.L. Salzberg, G.G. Sutton, P. Topalis, R. Wides, P. Wincker, M. Yandell, F.H. Collins, J. Ribeiro, W.M. Gelbart, F.C. Kafatos, and P. Bork. 2002. Comparative genome and proteome analysis of Anopheles gambiae and Drosophila melanogaster. *Science*. 298:149-59.

Zhadanov, A.B., D.W. Provance, Jr., C.A. Speer, J.D. Coffin, D. Goss, J.A. Blixt, C.M. Reichert, and J.A. Mercer. 1999. Absence of the tight junctional protein AF-6 disrupts epithelial cell-cell junctions and cell polarity during mouse development. *Curr Biol*. 9:880-8.

CHAPTER 3

CANOE REGULATES AJ-ACTOMYOSIN LINKAGES DURING EPITHELIAL ELONGATION

Preface

In the third chapter, I have included my unpublished work on Cno's role in morphogenesis after ventral furrow formation (described in Chapter 2). In our previous work, we found Cno is required to regulate the linkage between AJs and the apical actomyosin cytoskeleton during ventral furrow formation. In addition, we hypothesized that Cno plays this role in other dynamic morphogenetic processes. In this study, we examined Cno's role in other morphogenetically active tissues. Specifically, we had noted a loss of ventral epidermis and wanted to understand how this phenotype arises. The ventral epidermis is exquisitely sensitive to loss of adhesion due to its dynamic nature; cells in this tissue must rearrange, divide, and delaminate. I carefully examined cno^{MZ} mutants during germband extension (described in Chapter 1), when the ventral epidermis is most dynamic.

Introduction

Morphogenesis is an amazing process, which takes relatively simple cell and tissue shapes and forming more complex ones. One current challenge in developmental biology is to understand how morphogenesis is regulated. Cell-cell adhesion and cell shape change are two important aspects of morphogenesis, and coordination of the two is essential. Cells must change shape, divide, and move, all while maintaining their adhesion. Cell-cell adhesion and cell shape change are coordinated by adherens junctions (AJs) and an apical actomyosin cytoskeleton, but it is still unclear how AJs and the cytoskeleton are connected. This connection was thought to be direct via catenins, but biochemical evidence indicates otherwise (Drees et al., 2005; Gates and Peifer, 2005; Yamada et al., 2005). To try to understand more about this connection, we began to investigate the role of an AJ protein, Canoe (Cno/Afadin). Cno is an excellent candidate because it localizes to AJs and can bind directly to F-actin. Previously, we found Cno plays a role in regulating the linkage between AJs and the actomyosin network during the process of mesoderm internalization (ventral furrow formation) in *Drosophila* (Sawyer et al., 2009a). This work led us to the hypothesis that Cno is required in dynamic morphogenetic processes.

Another dynamic tissue in *Drosophila* is the ventral ectoderm. This tissue arises just after gastrulation; as the body axis extends during a convergence-extension process called germband elongation (Zallen and Blankenship, 2008). As this process initiates, cells planar polarize junctional proteins along dorsal-ventral (DV) borders and cytoskeletal proteins along their anterior-posterior (AP) borders. This planar polarity allows non-muscle Myosin II (Myosin) to accumulate on AP borders, and its constriction

is thought to shrink these borders, driving intercalation and elongation of the ventral ectoderm (Blankenship et al., 2006; Zallen and Wieschaus, 2004). Indeed, embryos lacking Myosin zygotically fail in GBE (Bertet et al., 2004). As GBE proceeds, cells within mitotic domains begin to divide and neuroblasts delaminate from the plane of the epithelium (Campos-Ortega, 1993). All these processes make the ventral ectoderm exquisitely sensitive to changes in adhesion and/or the cytoskeleton. In our previous work, we noted that Cno function is largely dispensable for adhesion in the dorsal ectoderm, but ventral ectoderm is lost (Sawyer et al., 2009a).

We thus wanted to determine what role Cno plays in the ventral ectoderm. Previously, we noted that planar polarity of certain proteins appeared enhanced in cno^{MZ} mutants (Sawyer et al., 2009a). We have now examined this in detail. We found that planar polarity of junctional proteins, but not cytoskeletal proteins, is enhanced in cno^{MZ} mutants. While the planar polarity of cytoskeletal proteins is not enhanced, their localization is altered so that they are no longer tightly associated with apical junctions along AP borders. These defects in planar polarity and aberrant cytoskeletal protein localization lead to abnormal cell morphology, which in turn leads to slower elongation of the germband. The planar polarity defects seen in cno^{MZ} mutants cannot be replicated by global loss of adhesion, but are closely replicated by global disruption of actin. This suggests that Cno specifically regulates connections between junctions and the actomyosin network along AP borders, where we found it is enhanced. As morphogenesis proceeds, and cells begin to divide and delaminate, epithelial integrity is lost in the ventral ectoderm in cno^{MZ} mutants. Taken together, these data suggest Cno

acts during dynamic morphogenetic process at specific cellular locations to regulate the linkage between junctions and the actomyosin network.

Results

GBE is slowed in cno^{MZ} mutants

In our earlier work, we found that cells in *cno^{MZ}* mutants can form and resolve rosettes and thus intercalate. However, we noted that some *cno^{MZ}* mutants did not elongate as far as WT embryos, possibly as a secondary consequence from a failure in internalizing the mesoderm efficiently (Sawyer et al., 2009a). To further determine how GBE was affected, we calculated the rate of elongation in living WT and *cno^{MZ}* mutants, by comparing total length of the embryo (measured from the cephalic furrow to the posterior end) to the length of the germband (measured from the tip of germband to the posterior end; Fig. 1A'). Time point zero was defined as the point when the cephalic furrow became visible. Percent elongation was first assessed at 10min, and then at 10min intervals until 80min, when GBE should be complete. After 80min in WT, the germband elongates to 84.06%±0.98% of the total length (Fig. 1A', N=8 embryos). In *cno^{MZ}* mutants, the germband elongates to only 62.24%±1.47% of the total length (Fig. 1B', N=6 embryos). In the first 20min of GBE, WT and *cno^{MZ}* mutants extend at similar rates; but after 30min *cno^{MZ}* mutants slow elongation significantly (Fig. 1C). Despite this slowed elongation, the midgut is still internalized (Sawyer et al., 2009a). We think it likely that both failure of internalizing the mesoderm and enhanced planar polarity contribute to slower GBE. While rosettes can form and resolve in *cno^{MZ}* mutants (Sawyer et al., 2009a), they may do so more slowly due to defects in the ventral ectoderm.

Planar polarity of junctional proteins, but not cytoskeletal proteins, is enhanced in cno^{MZ} mutants

During GBE, junctional proteins (Armadillo(Arm)/β-catenin, E-cadherin(DEcad), and Bazooka(Baz)) become enriched on DV borders, while the cytoskeletal components F-actin and Myosin become enriched on AP borders (Blankenship et al., 2006; Zallen and Blankenship, 2008; Zallen and Wieschaus, 2004). This differential enrichment is thought to help drive GBE. In our previous studies, we noted in passing that Arm and Myosin planar polarity appeared to be enhanced in cno^{MZ} mutants (Sawyer et al., 2009a). To examine this phenotype in more detail, we carefully examined the planar polarity of various junctional and cytoskeletal proteins in wild type (WT) and cno^{MZ} mutant embryos immediately following gastrulation onset, during stage 7 and early stage 8 (Fig. 2A). To do so, we measured the mean fluorescence intensities on all cell borders in a chosen area (cells between the cephalic furrow and posterior midgut invagination on the lateral side) and used ImageJ to select and compare boundaries most clearly aligned along the AP and DV axes (see Materials and Methods for details). To compare WT to cno^{MZ} mutants, we compared the ratio of AP/DV borders, to remove variation between experiments due to differential staining.

As a control, we first examined the basolateral protein Neurotactin (Nrt). Nrt is not planar polarized in WT or cno^{MZ} mutants (Table 2, Fig.2C-C'), with DV/AP ratios close to 1.0 for both WT and cno^{MZ} mutants (DV/AP ratios, WT=0.94±0.03 vs. cno^{MZ}=1.01±0.03, p=0.157, N=5 embryos). Next, we examined the AJ components Arm and DEcad. Arm is subtly planar polarized on DV borders in WT (Table 2; Fig. 2E). In cno^{MZ} mutants, this polarity was slightly, but significantly, enhanced (Fig. 2E'; DV/AP

ratios, WT=1.08±0.09 vs. *cno*^{MZ} =1.56±0.14, p=0.021, N=5 embryos). In contrast to previous studies, we could not detect significant planar polarization of DEcad in WT (Blankenship et al., 2006; Harris and Peifer, 2007). This is likely due to differences in fixation conditions and/or how the measurements were obtained. However, in *cno*^{MZ} mutants, DEcad became obviously planar polarized (Fig. 2D'; DV/AP ratios, WT=0.98±0.06 vs. *cno*^{MZ}=1.23±0.05, p=0.015, N=5 embryos), suggesting DEcad is likely planar polarized on DV borders in WT, although this enhancement may be quite subtle.

This led us to examine the apical polarity proteins Baz and aPKC. Baz is initially colocalized with Arm and DEcad in nascent spot AJs (Harris and Peifer, 2005). Baz was previously found to be enhanced with AJ proteins on DV borders (Blankenship et al., 2006; Zallen and Wieschaus, 2004). Strikingly, the planar polarity of Baz is strongly enhanced in *cno*^{MZ} mutants (Fig. 2F'; DV/AP ratios, WT=1.91±0.22 vs. *cno*^{MZ}=8.81±1.48, p=0.002, N=5 embryos). We also examined another apical polarity protein, atypical protein kinase C (aPKC). aPKC is localized apically to Baz and AJs during late cellularization and early gastrulation (Harris and Peifer, 2005). We found that aPKC is also enriched on DV borders in WT (Table 2; Fig. 2G). aPKC planar polarity is also strongly enhanced in *cno*^{MZ} mutants (Fig. 2G'; DV/AP ratios, WT=1.26±0.14 vs. *cno*^{MZ}=5.19±0.89, p=0.002, N=5 embryos).

Our previous work revealed that Cno plays an important role in regulating linkage between AJs and the apical actomyosin network in the ventral furrow. We hypothezed that defects in this linkage might lead to defects in planar polarity of cytoskeletal components. Myosin and F-actin are both enhanced on AP borders in WT (Blankenship

et al., 2006) and Myosin planar polarity is thought to play an important role in GBE (Bertet et al., 2004). Surprisingly, we did not find enhancement of the planar polarity of either Myosin (Fig. 2H-H'; AP/DV ratios, WT=2.61±0.33 vs. cno^{MZ}=2.93±0.71, p=0.688, N=5 embryos) or F-actin (Fig. 2J-J'; AP/DV ratios, WT=1.61±0.10 vs. cno^{MZ}=1.67±0.26, p=0.853, N=5 embryos) in cno^{MZ} mutants. However, while planar polarity of cytoskeletal proteins is not enhanced in cno^{MZ} mutants, there are clear differences in their localization, which will be discussed in more detail in a subsequent section.

Cno is planar polarized, but localizes with cytoskeletal proteins, not AJ proteins

We thus wondered where Cno acts during planar polarity establishment. Cno localizes to AJs at the onset of gastrulation, but rather than strictly associating with AJ proteins, it is enhanced at tricellular junctions with a subset of actin (Sawyer et al., 2009a). We explored whether Cno is planar polarized. Interestingly, Cno is enhanced on AP borders (Fig. 2B; Table 2), along with Myosin and F-actin. Together, these data suggest that Cno plays a role in restraining planar polarity in the ventral lateral ectoderm. Even more interesting, loss of Cno specifically affects the planar polarity of junctional proteins and not cytoskeletal proteins, despite colocalization with the latter. Further, loss of Cno has more dramatic effects on the apical polarity markers, Baz and aPKC. This suggests that in the ventral ectoderm Cno plays an important role in regulating the linkage between junctions and the apical actomyosin network specifically along AP borders.

aPKC and Baz are less apically restricted in cno^{MZ} mutants

To determine the role Cno plays in restraining planar polarity, we examined the consequences of its loss in more detail. Aside from the modest enhancement on DV

borders, Arm and DEcad localization in WT and *cno*^{MZ} mutants were similar, and Arm and DEcad remained detectable on all cell borders (Fig. 2D-E'). However, this is not the case for apical polarity markers, Baz and aPKC. Baz localization is largely lost from AP borders. Additionally, Baz does not extend along the entire DV border and is more punctate than in WT (Fig. 4A"' vs. 4D"'). Like Baz, aPKC is largely lost from AP borders, but in contrast it does not become punctate on DV borders (Fig. 4A" vs. Fig. 4D"). Instead, it is concentrated in a short strong band that does not extend along the entire DV border. This gives the impression that gaps exist between cells, but in fact the basolateral membrane marker Nrt shows cells are still closely apposed (Fig. 4D').

Baz is a key initiator of apical-basal polarity, and becomes apically enriched along with DEcad at cellularization (Harris and Peifer, 2004; Harris and Peifer, 2005). Baz localization is established apically in spot junctions during cellularization in *cno*^{MZ} mutants (Fig. 3B''' enface, yellow arrowheads). However, some Baz is also mislocalized along the lateral membrane and some accumulates at basal junctions, where in WT it is strictly apical (Fig. 3B''' Xsection vs. 3A''' Xsection, yellow arrows). Even more intriguing, in *cno*^{MZ} mutants the basal Baz puncta become planar polarized very early, during the onset of ventral furrow formation (data not shown). This is quite surprising, as *cno*^{MZ} mutants localize AJ proteins normally along their apical-basal axis (Sawyer et al., 2009a). As gastrulation begins, Baz remains largely apically localized in *cno*^{MZ} mutants, but often Baz puncta are often seen 2μm more basal (Fig. 4E"', yellow arrowheads); this basal localization is rare in WT (Fig. 4B"', yellow arrowhead). The pool of Baz retained apically in *cno*^{MZ} mutants appears to be sufficient to establish proper apical-basal polarity. This also suggests that Cno plays a role in retaining Baz apically.

aPKC had previously been shown to localize apically to Baz and AJs during cellularization and early gastrulation and requires Baz for its apical localization (Harris and Peifer, 2005). We thus wanted to examine the localization of aPKC. Our preliminary evidence indicates that aPKC begins to localize at celluarization into apical puncta that overlap with Baz in WT (Fig. 3A", A''' enface, yellow arrowheads). In cno^{MZ} mutants, aPKC is still maintained apically in puncta that overlap with Baz (Fig. 3B", B'''' enface, yellow arrowheads), and does not seem to be mislocalized along the lateral membrane or in basal junctions as dramatically as Baz (Fig. 3B", B''' Xsection, yellow arrows). However, we may have missed mislocalization, since aPKC accumulated at lower levels than Baz during cellularization. In the future, it will be important to examine the localization of Baz and aPKC during cellularization more closely, using deconvolution software to get better resolution. As gastrulation begins, aPKC in cno^{MZ} mutants also remains largely apically localized, but is found in puntca with Baz 2μm more basal (Fig. 4E"). By examining optical cross sections, WT aPKC and Baz are restricted apically, while in cno^{MZ} mutants aPKC and Baz puncta extend more basally (Fig. 4C-C"' vs. 4F'-F"'). Previous work demonstrated that during cellularization Baz can become mislocalized along the basolateral membrane when overexpressed (Harris and Peifer, 2005). In cno^{MZ} mutants, it may be that Baz and aPKC lost from the AP borders are re-localized to DV borders, over-saturating the apical scaffold, causing excess Baz and aPKC to extend their localization more basally. Indeed, most of the basal puncta are found on DV borders (Fig. 4E', E"'). This suggests that Cno may be important for retaining Baz and aPKC apically, and perhaps specifically on AP borders.

In cno^{MZ} mutants Myosin loses its tight association with apical junctions

While Myosin planar polarity is not enhanced in *cno*^{MZ} mutants, we wanted to determine if there were other changes in its localization. In WT, there is an apical Myosin network covering the apical surface of each cell (Fig. 5A, A" white arrow). However, most Myosin is tightly associated with apical junctions on AP borders, so tightly that Myosin in opposing cells appears as one boundary (Fig. 5A, A" white arrowheads). In WT, Baz spans the entire DV border, extending right up to the Myosin on AP borders, where Baz localization becomes less prominent (Fig. 5A',C). As cells rearrange and rosettes form, Myosin becomes highly concentrated at the vertex into which AP borders have contracted (Fig. 5G, white arrowheads, I). We also observed Myosin dynamics live using GFP tagged Zipper (Myosin heavy chain; (Buszczak et al., 2007). Myosin-GFP is also tightly associated between cells in these images (Fig. 5E, yellow arrowhead), while a pulsing dynamic Myosin network is present along the cells' apical surfaces (Fig. 5E', yellow arrowheads). This behavior is especially apparent as rosettes form; pulses of Myosin appear to move across the top of cells and coalesce along shrinking AP borders. This behavior is reminiscent of the ratchet-like pulses seen in ventral furrow cells as they apically constrict to internalize the mesoderm (Martin et al., 2009).

We thus examined how Myosin localization changed in *cno*^{MZ} mutants. In *cno*^{MZ} mutants, Myosin remained planar polarized along AP borders. However, we observed two distinct Myosin lines that were not tightly associated with the apical junctions. Instead, it appears as if the Myosin in opposing cells does not meet, leaving apparent gaps in Myosin localization (Fig. 5B, B" white arrowheads). These gaps were also

apparent with Myosin-GFP (Fig. 5F, F' yellow arrowheads). However, Nrt, a basolateral maker, can be seen in between the two Myosin boundaries demonstrating that cells have not separated (Fig. 5B"',H"). This is especially striking in rosettes, where Myosin does not become highly concentrated at vertices where AP borders are shrinking (Fig. 5H, H' white arrowhead). Instead, it appears as if the Myosin cannot reach the vertex and instead stops short (Fig. 5J). Interestingly, neither Baz nor aPKC extend past these Myosin boundaries, explaining the gaps in their localization on the ends of DV borders (Fig. 5B', D, data not shown). In addition, there appears to be less Myosin on the apical surface of cells (Fig. 5B, white arrow, F'). F-actin exhibited similar alterations in its localization in *cno*^{MZ} mutants (Fig. 2J'), although it is not as striking, likely due to the large pool of cortically associated actin at AJs and along the basolateral membrane in these cells, making the more dynamic pool of actin difficult to observe.

Thus in *cno*^{MZ} mutants, Myosin is unable to tightly associate along AP borders, especially at vertices of forming rosettes; this aberrant localization appears to restrict the ability of Baz to extend along the DV border. Myosin's aberrant localization may also restrict the ability of cells to rearrange efficiently. This also suggests that Cno may help link the actomyosin network tightly to AP borders.

Cells in cno^{MZ} mutants are impaired in cell flattening and are more isometric

To determine how defects in the planar polarity of junctional proteins and aberrant Myosin localization affect GBE, we examined the morphology of cells in the lateral ventral ectoderm. During cellularization and the initiation of gastrulation, cells have rounded apices (Sweeton et al., 1991). Also, cells are isometric and hexagonal, in an ordered honeycomb array (Fig. 6A; (Zallen and Zallen, 2004). As GBE begins, cells

flatten apically (Fig. 7B, yellow arrow) and become more anisometric (Fig. 6B). In fact, previous work demonstrated that the degree of anisometry correlates with the extent of GBE. Mutants that retain the honeycomb pattern fail to elongate, while mutants with partial anisometry will elongate, but not completely (Zallen and Zallen, 2004). We quantified changes in cell shapes during stage 7, when GBE begins. We measured the lengths of AP and DV borders in WT using the basolateral marker, Nrt; we then compared the lengths (measured in pixels, using ImageJ to compare and align borders along AP and DV boundaries as we did for measuring planar polarity). AP borders are significantly shorter than DV borders in WT (29.38±1.48 vs. 43.78±2.49, $p=4.33x10^{-7}$, N=143 borders from 5 embryos), with a DV/AP ratio of 1.49. This fits with the idea that Myosin shrinks cells along their AP borders to drive intercalation and elongate the germband (Blankenship et al., 2006). This also suggests that planar polarity of Myosin drives cell flattening and elongates cells along their DV axis.

We thus examined if cells in *cno*^{MZ} mutants retained these two cell shape changes. First, we examined cell flattening. Preliminary results suggest that prior to GBE onset, cells in *cno*^{MZ} mutants are isometric and many cells are apically rounded similar to WT (Fig. 6A vs. 6C, Fig. 7A vs. 7C, yellow arrows). In the future, it will be important to examine these early stages in detail. As gastrulation proceeds, many *cno*^{MZ} mutant cells remain apically rounded. In addition, deep furrows can be seen along some AP borders (Fig. 7D, yellow arrow). In *cno*^{MZ} mutants, many cells seem unable to flatten completely, or alternatively, are unable to maintain their flattened state. Either being impaired in cell flattening could explain why Myosin is unable to meet at apical junctions of AP borders, or defects in Myosin localization lead to defects in cell flattening. One idea is that

Myosin may never reach AP borders. Another idea is that Myosin may initially reach the AP borders, but is unable to establish a stable connection and therefore retracts.

We thus wanted to examine how AP and DV borders changed shape during the onset of GBE. In *cno*^{MZ} mutants, as in WT, AP borders are shorter than DV borders (25.56±1.30 vs. 30.59±1.92, p=0.03, N=171 borders from 5 embryos), consitent with the fact that some GBE and cell intercalation still occurs. However, this difference is decreased in *cno*^{MZ} mutants, so that the DV/AP ratio is 1.20, relative to 1.49 in WT. Surprisingly, *cno*^{MZ} AP borders are slightly shorter than WT AP borders (25.56±1.30 vs. 29.38±1.48, p=0.05, N=188 borders from 5 embryos), but *cno*^{MZ} DV borders are much shorter than WT DV borders (30.59±1.92 vs. 43.78±2.49, p=2.86 x10^{-5}, N=126 borders from 5 embryos). These results suggest that lateral ventral ectoderm cells in *cno*^{MZ} mutants are more isometric than WT. This fits with our finding that GBE is slowed in *cno*^{MZ} mutants, since the level of anisometry correlates with the extent of GBE.

Apical cell borders in cno^{MZ} mutants appear less convoluted

We thus wanted to examine how cell morphology was affected during GBE. As GBE proceeds, large groups of cells begin to divide. Many cells near mitotic domains have hightly convoluted cell borders (Fig. 8A-B, cells highlighted in green). These convoluted borders may be more flexible and allows cells to accommodate the dramatic changes in size of cells dividing near them. These convoluted cell borders are not apparent in *cno*^{MZ} mutants. Instead, cells have very straight borders and form straight rows (Fig. 8C-D). This change in morphology may also contribute to slow GBE. Previously, we found that rosettes can form and resolve in *cno*^{MZ} mutants (Sawyer et al.,

2009a). One possibility is that they do so more slowly in *cno*^{MZ} mutants, due to changes in cell morphology and flexibility.

Disrupting cell adhesion globally does not mimic loss of Cno

We next explored the mechanism by which Cno regulates planar polarity considering two hypotheses; the enhanced planar polarity in *cno*^{MZ} mutants could be due to defects in adhesion and/or cytoskeletal regulation. To distinguish between these possibilities, we examined embryos where adhesion was impaired or where F-actin was disrupted and determined if planar polarity was affected and if so, to what extent.

To address whether reduced adhesion could lead to an enhancement of planar polarity, we examined embryos with reduced levels of the AJ protein Arm both maternally and zygotically (*arm*^{MZ}). Since null alleles of *arm* lead to defects in oogenesis (Peifer et al., 1993), we used a truncated allele, *arm*^{043A01}; this is a strong, but not null, loss of function allele that allows completetion of oogenesis (Dawes-Hoang et al., 2005; Martin et al., 2010). While embryos can initiate mesoderm invaginvation, as morphogenesis proceeds and mitotic domains begin to divide because cells are unable to adhere to their neighbors and *arm*^{MZ} mutants fall apart quickly. In contrast, the ventral ectoderm in *cno*^{MZ} mutants maintains epithelial integrity during this stage (Fig. 9B vs. 9C). Thus the adhesion defects in *arm*^{MZ} mutants should exceed those of *cno*^{MZ} mutants.

To explore the consequences of reduced adhesion on planar polarity, we examined stage 7 *arm*^{MZ} mutant embryos, before the loss of epithelial integrity. We measured and compared mean fluorescence intensities of junctional and cytoskeletal proteins along AP and DV cell borders as we did for *cno*^{MZ} mutants. Nrt, a basolateral marker, was not planar polarized in *arm*^{MZ} mutants (Fig. 9J; DV/AP ratios,

WT=0.94±0.03 vs. arm^{MZ}=0.91±0.03, p=0.561, N=5 embryos). We did not assess the planar polarity of AJ proteins in arm^{MZ} mutants, since their levels are strongly reduced (Dawes-Hoang et al., 2005; Sawyer et al., 2009a). Instead, we examined the planar polarity of the apical polarity proteins, Baz and aPKC. Interestingly, Baz planar polarity is not enhanced in arm^{MZ} mutants (Fig. 9J; DV/AP ratios, WT=1.91±0.22 vs. arm^{MZ}=2.17±0.22, p=0.434, N=5 embryos). This is in strong contrast with what we saw in cno^{MZ} mutants (Fig. 9J; DV/AP ratios, arm^{MZ}=2.17±0.22 vs. cno^{MZ}=8.81±1.48, p=0.002, N=5 embryos). aPKC planar polarity is subtly, but significantly enhanced in arm^{MZ} mutants (Fig. 9J; DV/AP ratios, WT=1.26±0.14 vs. arm^{MZ}=1.87±0.21, p=0.038, N=5 embryos). However, this enhancement is substantially weaker than that see in cno^{MZ} mutants (Fig. 9J; DV/AP ratios, arm^{MZ}=1.87±0.21 vs. cno^{MZ}=5.19±0.89, p=0.007, N=5 embryos). We then examined the planar polarity of the cytoskeletal protein, Myosin. In arm^{MZ} mutants, Myosin planar polarity is not enhanced (Fig. 9J; DV/AP ratios, WT=2.61±0.33 vs. arm^{MZ} =1.88±0.24, p=0.107, N=5 embryos); in this they resemble cno^{MZ} mutants. These data suggest that defects in adhesion alone are insufficient to produce the changes in planar polarity we saw in cno^{MZ} mutants, at least when adhesion is globally reduced. One possibility is that in cno^{MZ} mutants, adhesion is lost in a planar polarized way along AP borders, and this asymmetry drives a more dramatic enhancement.

While planar polarity is not dramatically enhanced in arm^{MZ} mutants, we wanted to determine if there are other similarities between cno^{MZ} and arm^{MZ} mutants. Baz localization is established normally in arm^{MZ} mutants during cellularization (Harris and Peifer, 2004). This is contrast to what we saw in cno^{MZ} mutants, where Baz was also

present more basally during cellularization. aPKC overlaps apically in puncta with Baz during cellularization in arm^{MZ} mutants as in WT (Fig.9D-D"', yellow arrows). We next examined the localization of Baz and aPKC immediately after the onset of gastrulation, during stage 7. In arm^{MZ} mutants, both Baz and aPKC extend along the entire DV border (Fig. 9G-G"). Additionally, Baz and aPKC remain apically restricted, and Baz puncta are rarely seen 2μm more basal (data not shown). Both of these facts strongly contrast with cno^{MZ} mutants.

We then examined the localization of Myosin in arm^{MZ} mutants. In many places, Myosin remains tightly associated with apical junctions on AP borders (Fig. 9F, white arrowheads), in contrast with cno^{MZ} mutants (Fig. 5B"). However, where rosettes form, Myosin gaps, similar to those we observed in cno^{MZ} mutants, are readily apparent (Fig. 9F, white arrows). Intriguingly, Nrt projections are present in these gaps (Fig. 9F, white arrows). It appears as if basolateral membrane is being squeezed up in the center of these Myosin gaps in forming rosettes, which we did not see in cno^{MZ} mutants (Fig. 5H). Since AJs are strongly reduced in arm^{MZ} mutants, the basolateral protein Nrt may be able to invade the apical domain. This data suggests that reduced adhesion can lead to defects in rosette formation.

Finally, we compared changes in cell shapes. An isometry of cells in in arm^{MZ} mutants resembles WT (28.22±1.17 vs. 38.50±1.89, $p=2.40x10^{-6}$, N=180 borders from 5 embryos), with a DV/AP ratio 1.36 (vs. WT DV/AP ratio of 1.49). Indeed, when comparing WT and arm^{MZ} mutants there is no significant difference between AP (29.38±1.48 vs. 28.22±1.17, p=0.534, N=201 borders from 5 embryos) or DV borders

(43.78±2.49 vs. 38.50±1.89, p=0.089, N=122 borders from 5 embryos). This is contrast to what we saw in *cno*^{MZ} mutants, where cells were smaller and more isometric.

Global reduction of F-actin closely resembles loss of Cno

We then examined whether disrupting cytoskeletal regulation would resemble the planar polarity enhancement we saw in *cno*^{MZ} mutants. To address whether disrupting the cytoskeleton could lead to an enhancement of planar polarity, we examined embryos treated with the actin-depolymerizing drug, cytochalasin D (cytoD). Previous work demonstrated that the establishment of DEcad and Baz planar polarity are accelerated and enhanced in embryos treated with cytoD (Harris and Peifer, 2007). We examined this in more detail, using the methods we employed for assessing planar polarity in *cno*^{MZ} mutants. First, we examined the AJ protein DEcad. DEcad becomes significantly enhanced on DV borders in cytoD treated embryos (Fig. 10B,C, DV/AP Ratios, DMSO=1.10±0.05 vs. cytoD=1.48±0.08, p=0.003, N=5 embryos). In fact, this enhancement is slightly, but significantly more than we observed in *cno*^{MZ} mutants (Fig. 10C, DV/AP Ratios, cytoD=1.48±0.08 vs. *cno*^{MZ}=1.23±0.05, p=0.025, N= 5 embryos). This suggests that disrupting the cytoskeleton directly has a greater impact on AJ proteins. Treatment with cytoD disrupts cortical actin, while loss of Cno may specifically affect the more dynamic apical actin network, so this is perhaps not surprising, since having a stable cortical actin network stabilizes AJs (Quinlan and Hyatt, 1999). We next examined how the planar polarity of Baz is affected in *cno*^{MZ} mutants. Baz is strongly enhanced on DV borders after cytoD treatment compared to DMSO treated embryos (Fig. 10B,C, DV/AP Ratios, DMSO=1.60±0.08 vs. cytoD=3.21±0.15, p=1.42x10^{-5}, N=5 embryos). However, this enhancement is not as dramatic as what is

seen in *cno*^{MZ} mutants (Fig. C, DV/AP Ratios, cytoD=3.21±0.15 vs. *cno*^{MZ}=8.81±1.48, p=0.006, N= 5 embryos). This is an interesting result because in cytoD treated embryos, Cno localization is lost from the cortex (Sawyer et al., 2009a). Therefore, we might have expected the enhancement of Baz on DV borders to be similar to *cno*^{MZ} mutants. However, it may be that Cno present before cytoD treatment was sufficient to exert some restraining influence. As in *cno*^{MZ} mutants, in cytoD treated embryos Baz puncta are found frequently 2μm more basal, primarily on DV borders (data not shown). cytoD treated embryos also appear to be smaller and more isometric than DMSO treated embryos (Fig. 10A vs. 10B). In the future, we will quantitate this by assessing the lengths of cell borders using Nrt as a marker as we did for *cno*^{MZ} and *arm*^{MZ} mutants.

Taken together, these results suggest that disruption of the cytoskeleton, not loss of adhesion, more closely resembles the planar polarity enhancement seen in *cno*^{MZ} mutants. This fits with the idea that Cno facilitates connections between junctions and the cytoskeleton, specifically at AP borders.

As morphogenesis proceeds, cno^{MZ} mutants lose epithelial integrity in the ventral ectoderm

In our previous studies, we noted that later in morphogenesis portions of the ventral ectoderm are lost (Sawyer et al., 2009a). We thus examined in detail when these defects in epithelial integrity first arise. As GBE continues and cells enter mitosis in *cno*^{MZ} mutants, the enhanced planar polarity seen immediately after gastrulation onset and in the early stages of GBE, disappears (Fig. 11D). Cell division may relieve this enhancement and/or the signals for planar polarity may be temporal in nature. During stage 9, large regions of the epithelium lose accumulation of junctional proteins (Fig.

11B,D",E",F'). On the sides and in the center of these regions are islands of constricted apical ends of cells. The constricted ends are positive for AJs and apical polarity proteins (Fig. 11B,D",E",F', red arrowheads). In contrast, the dorsal ectoderm remains intact (Sawyer et al., 2009a). Originally, we thought these regions arose because cells exiting cell division were unable to resume their columnar shape (Sawyer et al., 2009a). To better understand these regions that lost junctional protein localization, we assessed the localization of the basolateral markers, Discs Large (Dlg) and Nrt to determine how cells were shaped. If cells were unable to reassume their columnar shape, we predicted cells would remain rounded. To our surprise, cells in these regions lacking junctional proteins were not round, but elongated. In fact, cells appeared to lie on their sides, stretched toward the islands of constricted apical ends (Fig. 11D, inset). These data suggest that cells in the ventral ectoderm are being pulled apart, producing epithelial tears.

If cells were in fact being pulled apart, we expected that the microtubule (MT) cytoskeleton would reflect this. In WT, centrosomes are localized above the nucleus along with the minus ends of MTs, which then extend their plus ends basally. This gives the appearance of an inverted basket of MTs in the apical ends of cells (Harris and Peifer, 2005). In arm^{MZ} mutants, cells lose adhesion and form epithelial rosettes with constricted apical ends at the center (Fig. 9C). This roughly resembles what we observed in stage 9 cno^{MZ} mutants, although the arm^{MZ} mutant phenotype is much more severe in timing and extent (compare Fig. 9B to Fig. 9C). The cells in these epithelial rosettes in arm^{MZ} mutants retain basic MT cytoskeletal polarity (Harris and Peifer, 2004). In cno^{MZ} mutants, basic MT cytoskeletal polarity is also retained. MTs in stretched cells are

polarized toward the constricted apical ends (Fig. 11E', yellow arrow). This suggests cells in the ventral ectoderm are in fact being pulled apart.

Interestingly, this epithelial integrity phenotype is primarily seen in cells near the ventral midline. In WT, these cells have an interesting morphology. They are stretched along their DV axes and quite short along their AP axes (Fig. 11A, yellow arrows). This suggests that these cells may be under more tension than other cells in the ventral ectoderm. We thus examined the cytoskeletal proteins, Myosin and F-actin. Interestingly, bands of Myosin often surround the islands of constricted apical ends (Fig. 11F, white arrows). We next examined F-actin in the ventral ectoderm. In cno^{MZ} mutants, cells in lateral ectoderm have more actin-rich projections than WT cells during this stage (Fig. 11G vs. 11H, yellow arrows). This is reminiscent of the phenotype of embryos lacking Crumbs (Crb), a protein that helps maintain the apical domain. In *crb* mutants, as cells lose adhesion they begin to project more actin-rich filopodia (Roeth et al., 2009). Interestingly, this loss of adhesion in *crb* mutants is first apparent in the ventral ectoderm. This data suggests that cells near the ventral midline may be under more tension, and this tension in cno^{MZ} mutants causes cells to pull apart. As cells pull apart, they begin to lose adhesion to with one another and extend more F-actin rich projections.

Why are cells in the ventral ectoderm under more tension? One possibility is that it is inherent to their location between the midline and mitotic domains, which makes their morphology unique. Another process that makes the ventral ectoderm unique is that neuroblasts will delaminate from this tissue and later divide. We wanted to examine the possibility that delaminating neuroblasts cause the defects in epithelial integrity seen in

cno^{MZ} mutants. We examined the localization of Miranda (Mira), a neuroblast marker. Preliminary results suggest that in *cno*^{MZ} mutants, some neuroblasts are found on the surface (Fig. 11J). This could have arisen if they did not delaminate, or started to delaminate, but returned to surface because cells in the epithelium did not seal over them. Sometimes a neuroblast can be seen in the islands of constricted cell apices (Fig. 11K-K'), suggesting that delaminating neuroblasts could cause cells in *cno*^{MZ} mutants to pull apart. We plan to examine this more closely in the future.

Discussion

Our data suggests that Cno plays important roles in regulating the linkage between AJs and the actomyosin network during GBE. We found that planar polarity of cytoskeletal proteins is not enhanced, but planar polarity of junctional proteins is enhanced in *cno*^{MZ} mutants. However, cytoskeletal proteins are no longer tightly associated along AP borders in *cno*^{MZ} mutants, where Cno localization is enhanced in WT. Global loss of adhesion does not replicate the planar polarity defects seen in *cno*^{MZ} mutants. Instead, these defects in planar polarity are closely replicated by global disruption of actin, suggesting that Cno specifically regulates connections between junctions and the actomyosin network along AP borders during GBE. As morphogenesis proceeds, and cells begin to divide and delaminate, epithelial integrity is lost in the ventral ectoderm in *cno*^{MZ} mutants, perhaps because apical tension in *cno*^{MZ} mutants is disrupted. Taken together, these data suggest Cno acts during dynamic morphogenetic process at specific cellular locations to regulate the linkage between junctions and the actomyosin network.

Loss of Cno leads to planar polarity enhancement of junctional proteins

In WT, junctional proteins are enhanced on DV borders and cytoskeletal proteins on AP borders. In *cno*^{MZ} mutants, junctional components are even more enhanced along DV borders, while the planar polarity of cytoskeletal components is unaffected. Interestingly, the planar polarity of the apical polarity markers Baz and aPKC is strongly enhanced in comparison to WT, while AJ proteins Arm and DEcad are only slightly enhanced. Even more intriguing, Baz localizes apically in *cno*^{MZ} mutants, but is also found more basally, often in a planar polarized way. Previous work showed that actin is responsible either directly or indirectly for the apical positioning of Baz (Harris and Peifer, 2005). Our work suggests that Cno may play a role in retaining Baz apically, either directly or indirectly by modifying the actin network.

Myosin loses its tight association with apical junctions in cno^{MZ} mutants

While planar polarity of the cytoskeletal proteins, Myosin and F-actin, are not enhanced in *cno*^{MZ} mutants, there are defects in their localization. Myosin is no longer tightly associated with apical junctions along AP borders. This is especially apparent where rosettes begin to form. Intriguingly, in WT, Cno is enhanced along AP borders with Myosin and F-actin. This suggests that Cno plays an important role in facilitating connections between junctions and the actomyosin network specifically along AP borders. Normally, WT junctional proteins are reduced along AP borders, while cytoskeletal proteins are enhanced. This may cause a slight reduction in adhesion along these borders, which may help to allow for the shrinkage of these borders and the eventual formation of rosettes. Normally, the enhancement of Cno along these borders may provide extra support at AJs and strengthen the connection between AJ-actomyosin linkages along AP borders, yet still allow cell borders to change shape. However, in

cno^{MZ} mutants, junctional proteins become reduced along AP borders, perhaps because there is no Cno to provide extra support. Additionally, many cells in *cno*^{MZ} mutants are more rounded in their apices than WT, either because Myosin is unable to drive or maintain cell flattening, or that defects in cell flatenining lead to abnormal Myosin localization. In the future, it will be important to examine the localization of Myosin and a junctional maker live to distinguish between these two possibilities. Importantly, cells do not separate along the basolateral membrane, suggesting that Cno's role in regulating AJ-actomyosin linkages is specific to the apical domain. Global loss of adhesion (*arm*^{MZ} mutants) does not lead to the enhancement of planar polarity that we observe in *cno*^{MZ} mutants, suggesting loss of adhesion alone is insufficient to enhance planar polarity. However, disruption of the cytoskeleton leads to enhancement of planar polarity of junctional proteins similar to that seen in *cno*^{MZ} mutants. Taken together, these data suggest that during GBE Cno plays an important role in reinforcing AJ-actomyosin linkages along AP borders.

cno*^{MZ} *mutants lose epithelial integrity in the ventral ectoderm

As morphogenesis proceeds, *cno*^{MZ} mutants begin to lose epithelial integrity specifically in the ventral ectoderm. Our data suggests that Cno plays an important role in this tissue, possibly by facilitating stronger connections between AJs and the apical actomyosin network. This seems a reasonable hypothesis, since Cno plays a similar role in mesoderm invagination (Chaper 1; (Sawyer et al., 2009a) and in GBE (this study). In mesoderm invagination, the actomyosin network separates from AJs, as cells initiate invagination. During GBE, the actomyosin network loses its tight cortical localization along AP borders, where Cno is normally enhanced. However, later in the ventral

ectoderm, as cells divide and neuroblasts delaminate, it is unclear how Cno function is important. Therefore, in the future it will be important to directly test the role of Cno in this tissue. First, it would be interesting to block cell division. With this experiment we could address two questions: (1) Does cell division contribute the eventual loss of ventral ectoderm in *cno*^{MZ} mutants? (2) Is the planar polarity enhancement seen in *cno*^{MZ} mutants retained if cell division is blocked? If the loss of ventral ectoderm in *cno*^{MZ} mutants was suppressed by blocking cell division, this would confirm our earlier hypothesis that some cells are unable to reassume their columnar shape after cell division and this could contribute to the loss of ventral ectoderm. Additionally, we could assess planar polarity enhancement of junctional proteins, which would give us clues as to whether cell division relieves planar polarity, or if it is temporally regulated. Our preliminary data suggests that neuroblast delamination may lead to the loss of ventral ectoderm in *cno*^{MZ} mutants. The loss of ventral ectoderm in *cno*^{MZ} mutants is similar to the phenotype of embryos lacking zygotic DEcad (Sawyer et al., 2009a; Tepass et al., 1996). The loss of ventral ectoderm in zygotic DEcad mutants can be suppressed by expressing an activated form of Notch, blocking the formation of neuroblasts, and therefore delamination (Tepass et al., 1996). It would be interesting to try this approach in *cno*^{MZ} mutants, to see if this would suppress the loss of ventral ectoderm. Both of these experiments would make the ventral ectoderm a less morphogenetically active tissue. If these strategies suppress, or partially suppress, the loss of ventral ectoderm, it would suggest that Cno has a role in regulating apical tension across cells, since in the absence of Cno cells in the ventral epidermis pull apart from each other. These epithelial tears are reminiscent to those found during mesoderm invagination in mutants with reduced adhesion. In this case, the idea is that apical

tension is regulated by actomyosin attachments at spot-AJs (Martin et al., 2010). It is tempting to speculate that Cno may also play a role in regulating apical tension, but through tricellular junctions, where it is enhanced with a pool of F-actin (Sawyer et al., 2009a).

Supporting AJ-actomyosin linkages during dynamic morphogenesis

This work illustrated the importance of coordinating cell adhesion and cell shape change. Cells are not static, but instead do amazing things. They change shape, move, and divide, all while maintaining epithelial integrity. We have shown that Cno is crucially important in coordinating AJ-actomyosin linkages during dynamic morphogenesis. Cno is likely not the only protein that regulates AJ-actyomyosin linkages, as Cno is not required for all processes that require these linkages. In the future, it will be exciting to uncover the suite of proteins that help to coordinate the intricate dance of morphogenesis.

Acknowledgements

We would like to thank the Bloomington stock center, DSHB, J. Zallen, E. Wieshcaus, and C. Doe for reagents. We would like to thank J. Zallen, T. Harris, and A. Martin for helpful discussions. We would like to thank V. Madden of the Microscopy Services Laboratory at UNC for assistance with SEM, and J. M. Sawyer for assistance with DIC imaging. Thanks to S. Nowotarski and J. M. Sawyer for critical reading and editing.

Materials and Methods

Fly Stocks

Mutations are described at flybase.bio.indiana.edu. Wild type was *yellow white*

or *Histone-GFP*. All experiments were done at 25°C unless otherwise noted. Stocks to make *cno* germline clones were from the Bloomington Stock Center. *cno* germline clones were made by heat shocking 48-72h old *hsFLP*^{1}; FRT82B*cno*^{R2}/FRT82B*ovo*$^{D1-18}$ larvae 3hrs at 37°C. *arm*^{043A01} germline clones were generated similarly.

Immunofluorescence

The following fixations were used: Baz/aPKC/myosin/Arm/Cno/Ed, heat-methanol (Muller and Wieschaus, 1996); phalloidin/Dcad2, 10min, 10% formaldehyde or 5min, 37% formaldehyde. All others were fixed in 4% formaldehyde for 20min. Embryos were methanol-devitillinized, or hand-devitillinized for phalloidin. For cytochalasin treatments, dechorinated embryos were washed twice with 0.9% NaCl and incubated for 30min in 1:1 octane/0.9% NaCl with 10µg/mL cytochalasin D (Sigma, dissolved in DMSO). Control embryos were treated with DMSO carrier alone. Embryos were fixed immediately after drug treatment. All embryos were blocked/stained in PBS/1% goat serum/0.1% Triton X-100 and mounted in Aqua-Polymount (Polysciences). All images and movies were acquired at room temperature.

Image acquisition

Fixed samples were imaged with LSM510 confocal microscopes, using a Zeiss 40X NA 1.3 Plan-Neofluar oil immersion objective, and LSM software. Live fluorescence imaging was performed using the Perkin-Elmer Ultra VIEW spinning disc confocal, ORCA-ER digital camera, a Nikon 40X NA 1.3 Plan-Fluor oil immersion objective, and Metamorph software. 4-D differential interference contrast (DIC) microscopy was carried out with a Diagnostic Instruments SPOT2 camera mounted on a Nikon Eclipse

800 microscope with a 20X lens. Images were acquired at 11μm optical sections every 2 min during embryogenesis and analyzed with Metamorph v.6.3r5 (Molecular Devices). Adobe Photoshop CS2 was used to adjust input levels so the main range of signals spanned the entire output grayscale and to adjust brightness and contrast.

SEM

Embryos were dechorionated with 50% bleach and fixed for 20 minutes at room temperature with a 1:1 mixture of 4% formaldehyde in PBS buffer. Embryos were methanol-devitillinized and post-fixed in 2.5% gluteraldehyde in 0.1 M Cacodylate buffer. Embryos were then taken to the Microscopy Services Laboratory at UNC for specimen preparation. Samples were imaged using a Zeiss Supra 25 Field Emissions Scope.

Quantification of immunoflurosence

Images were acquired as stacks using a Zeiss 40X NA 1.3 Plan-Neofluar oil immersion objective with zoom 2. Mean fluorescence intensities of all borders (zoom 300%) were measured using the ImageJ line tool, with a line width of 3. Stacks of 4 planes, 0.5μm apart were used to ensure the entire border was measured. These four measurements were averaged to obtain the value for the border, and this was subtracted from the background (measured the same way, but in the cytoplasm of cells) to obtain the final value for the border. Only stage 7 and early stage 8 embryos were measured. The measurements were then sorted by angles (in relation to anterior-posterior axis of the embryo). Only AP borders (angles 0-29) and DV borders (angles 75-90) were compared to obtain the AP/DV or DV/AP ratio. When comparing WT to mutant ratios, ratios from 5 embryos from at least two different experiments were averaged.

Table 1: Fly stocks, Antibodies, and Probes

Fly stocks		**Source**
ubiecadGFP,sqhCherII		J. Zallen (Sloan-Kettering, USA)
Zip-GFP (trap #CC01626)		The Carnegie Protein Trap Library (Buszczak et al., 2007)
HisGFPIII		R. Saint, (University of Adelaide, South Australia, AUSTRALIA)
cno^{R2}/TM3twiGFP		
*arm^{043A01}*FRT101/FM7		E. Wieschaus (Princeton, NJ, USA)
Antibodies/Probes	*Dilution* *IF*	**Source**
anti-DE-DCAD2	1:100	DSHB
anti-ArmN27A1	1:100	DSHB
Anti-Nrt	1:100	DHSB
anti-Cno	1:1000	J. Sawyer and N. Harris (UNC-CH, USA)
anti-Baz	1:1000	J. Zallen (Sloan-Kettering, USA)
anti-aPKC	1:1000	Santa Cruz Biotechnology
anti-Mira	1:100	C. Doe (Univ. Oregon, USA)
anti-Zipper ((Myosin II heavy chain)	1:1000	C. Field (Harvard, MA, USA) D. Kiehart (Duke University, NC, USA)
Alexa-phalloidin	1:500	Molecular Probes
anti-alpha-tubulin		Sigma
Secondary antibodies: Alexas 488, 568, and 647	1:500	Molecular Probes

Table 2: Planar Polarity in WT, *cno*^{MZ}, and *arm*^{MZ} mutants

Protein	**WT**			
	AP ± s.e.m	**DV ± s.e.m**	**N (AP+DV)**	**p**
Nrt	127.92±2.97	123.15±3.13	143	0.288
Arm	86.47±3.06	95.83±2.39	132	0.016
Dcad	71.12±2.50	69.88±2.65	173	0.697
aPKC	31.95±1.69	40.42±2.24	137	0.001
Baz	33.13±2.47	56.22±2.30	120	8.07×10^{-10}
Myo	39.21±2.42	15.45±2.28	165	1.44×10^{-11}
F-actin	74.11±3.98	46.84±3.09	180	6.70×10^{-7}
Cno	72.66±2.24	60.53±2.58	214	0.0005
Protein	***cno*^{MZ}**			
	AP ± s.e.m	**DV ± s.e.m**	**N (AP+DV)**	**p**
Nrt	88.71±2.73	89.71±2.94	171	0.808
Arm	65.00±3.94	101.92±4.48	98	1.60×10^{-8}
Dcad	93.35±3.28	115.12±4.06	180	4.73×10^{-5}
aPKC	11.69±1.89	52.74±3.40	195	2.18×10^{-22}
Baz	7.74±1.64	64.37±3.94	160	2.76×10^{-31}
Myo	42.38±1.69	17.24±1.48	176	1.24×10^{-19}
F-actin	92.78±3.07	68.83±3.81	197	1.80×10^{-5}
Cno	ND	ND	ND	ND
Protein	***arm*^{MZ}**			
	AP ± s.e.m	**DV ± s.e.m**	**N (AP+DV)**	**p**
Nrt	98.36±3.87	89.21±4.79	180	0.146
Arm	ND	ND	ND	ND
Dcad	ND	ND	ND	ND
aPKC	40.50±2.56	73.27±3.68	175	2.76×10^{-12}
Baz	41.42±2.31	88.22±4.35	191	2.18×10^{-15}
Myo	48.26±2.70	27.68±2.26	197	1.89×10^{-7}
F-actin	ND	ND	ND	ND
Cno	ND	ND	ND	ND

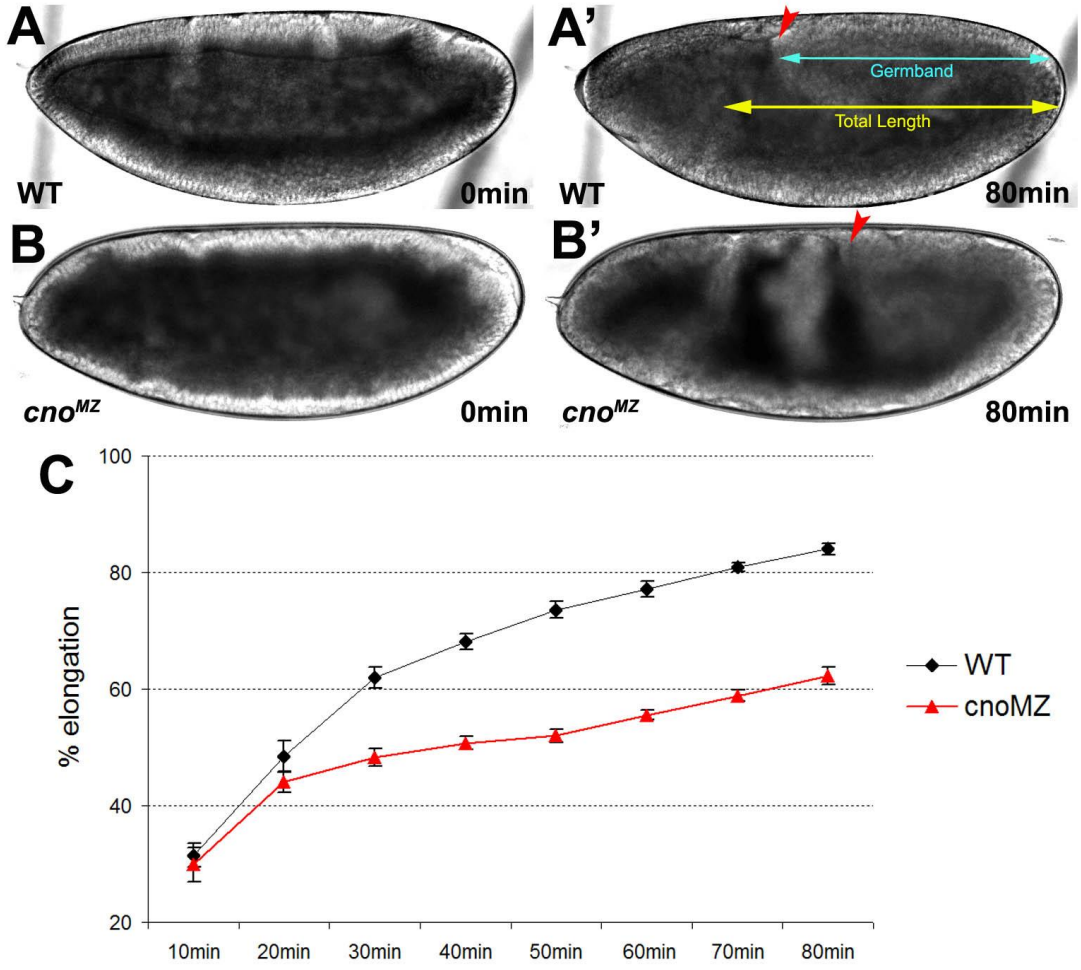

Figure 1. GBE is slowed in *cno*^{MZ} mutants.
(A-B') Embryos anterior to the left. (A) WT embryo at time 0, when the cephalic furrow appears. (A') WT embryo after 80min, when GBE is complete. Red arrow indicates the end of the germband. Yellow line represents the measurement of total length, cephalic furrow to posterior. Blue line indicates the measurement of the germband. (B) *cno*^{MZ} mutant at time 0. (B') *cno*^{MZ} mutant after 80min, GBE is slowed and does not extend as far as WT. (C) Rate of GBE. Initially, WT and *cno*^{MZ} mutants elongate at the same rate, but after 20min, *cno*^{MZ} mutants slow down significantly. WT, N=8. *cno*^{MZ} mutants, N=6. Error bars are s.e.m.

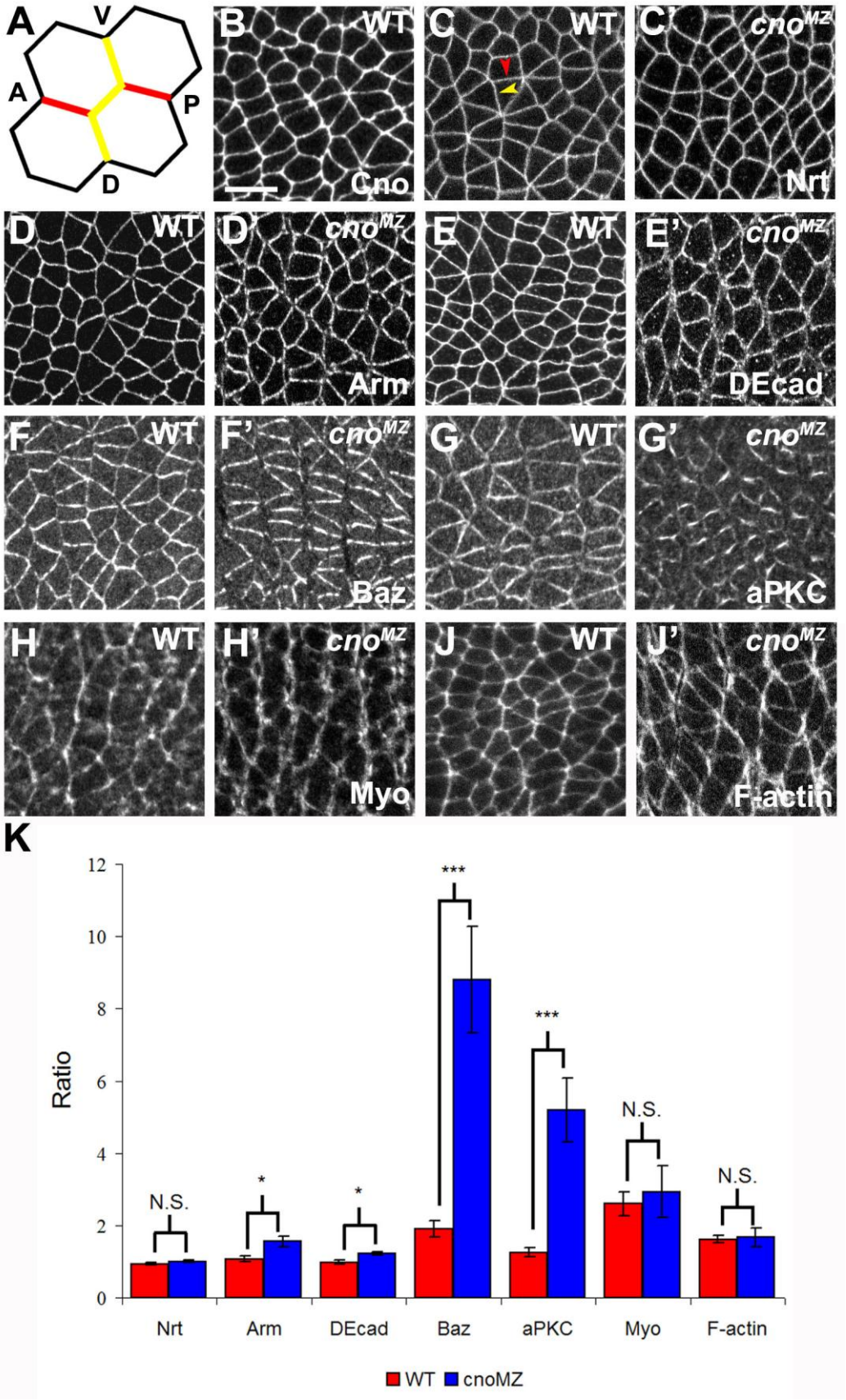
A
V
A
P
D
B WT
Cno
C WT
C' cnoMZ
Nrt
D WT
D' cnoMZ
Arm
E WT
E' cnoMZ
DEcad
F WT
F' cnoMZ
Baz
G WT
G' cnoMZ
aPKC
H WT
H' cnoMZ
Myo
J WT
J' cnoMZ
F-actin
K
Ratio
12
10
8
6
4
2
0
***
***
*
*
N.S.
N.S.
N.S.
Nrt
Arm
DEcad
Baz
aPKC
Myo
F-actin
WT
cnoMZ

Figure 2. Planar polarity of junctional, but not cytoskeletal proteins is enhanced in *cno*^{MZ} mutants. (B-H') Stage 7 embryos, anterior to the left. (B,C,D,E,F,G,H,J) WT. (C',D',E',F',G',H') *cno*^{MZ}. (A) Schematic of lateral epidermis cells at stage 7. Red lines indicate DV borders. Yellow lines indicate AP borders. (B) Cno is enhanced on AP borders in WT. (C-C') Nrt, a basolateral marker, is not planar polarized in WT or *cno*^{MZ}. Red arrowhead indicates an AP border. Yellow arrowhead indicates a DV border. (D-E') AJ proteins, Arm and DEcad, are slightly more planar polarized in *cno*^{MZ}. (F-G') Apical polarity proteins, Baz and aPKC, are strongly more planar polarized in *cno*^{MZ}. (H-J') Cytoskeletal proteins, Myo and F-actin, are not more planar polarized in *cno*^{MZ}. (K) Quantitation of planar polarity (see Material and Methods). Nrt, Arm, DEcad, Baz, aPKC are DV/AP ratios. Myo and F-actin are AP/DV ratios. Error bars indicate s.e.m. * = P<0.03. *** = P<0.003. Scale bar = 10μm.

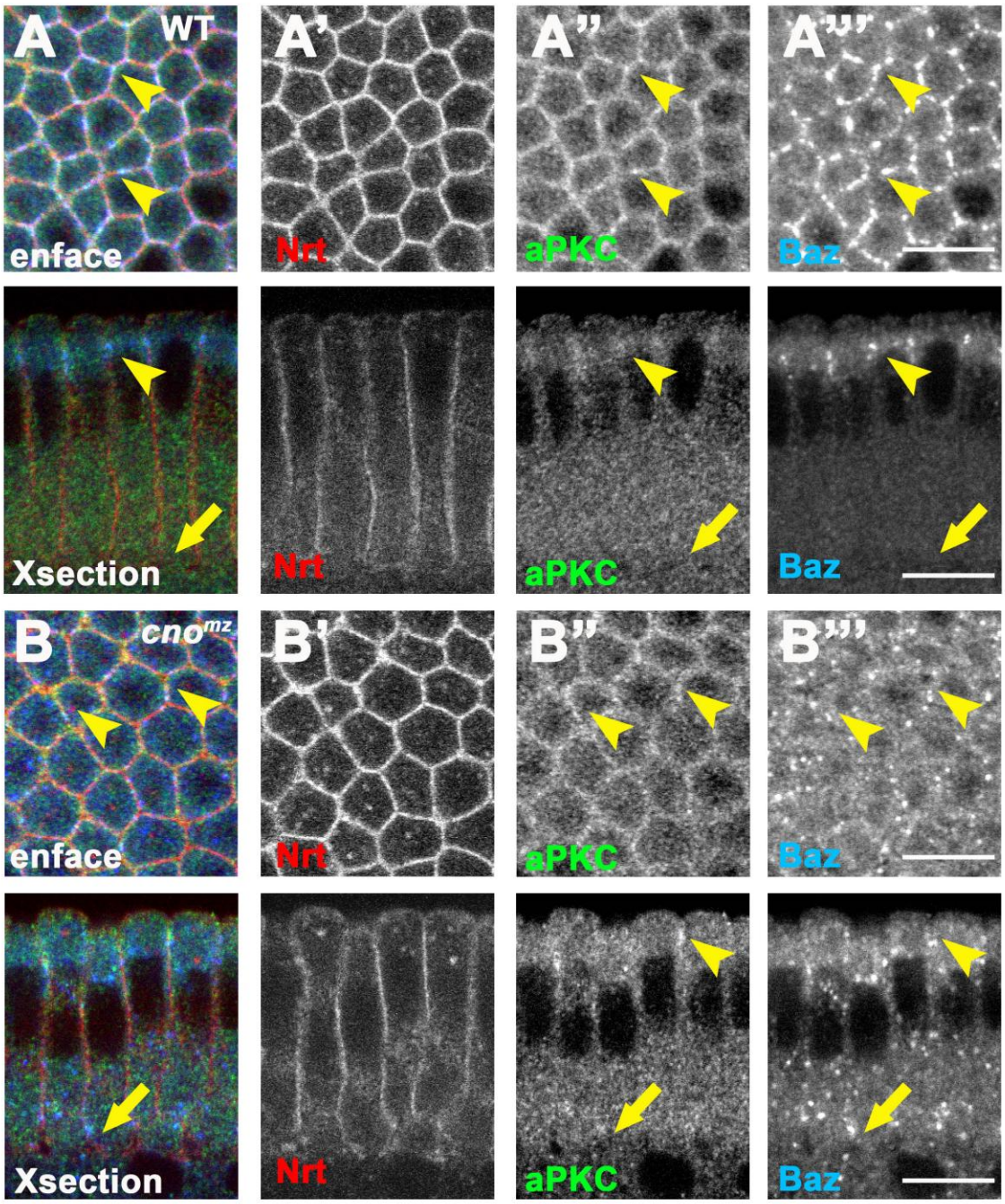

Figure 3. Baz is not restricted apically in *cno*^{MZ} during cellularization.
Late cellularizing embryos, antigens indicated. (A-A''') WT, enface and Xsections. Baz and aPKC overlap (yellow arrowheads) and are restricted apically (yellow arrows) (B-B''') *cno*^{MZ}, enface and Xsections. Baz and aPKC still overlap (yellow arrowheads), but Baz is mislocalized along the lateral membrane and is present in basal junctions (yellow arrows). Scale bars = 10μm.

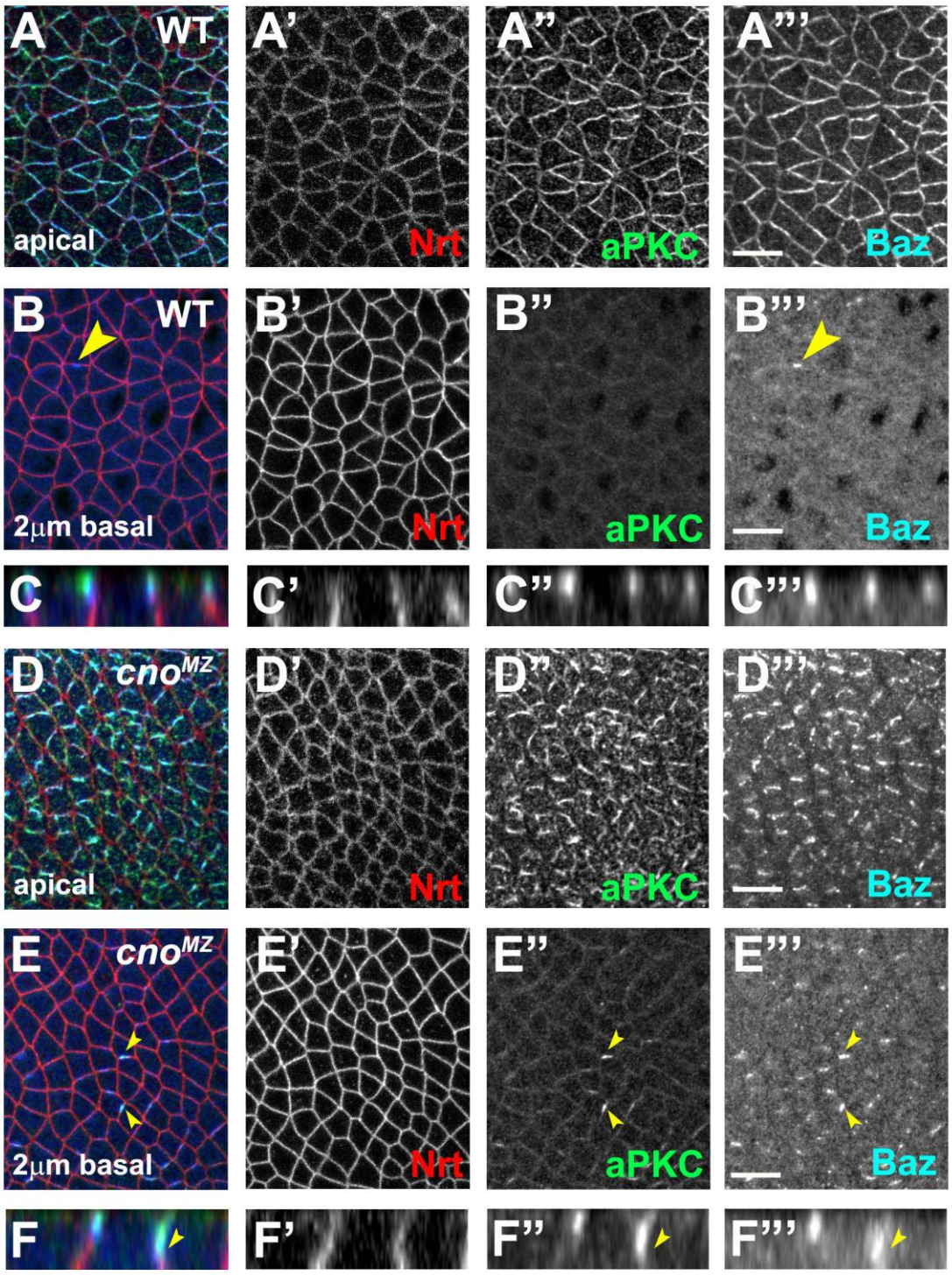

Figure 4. Baz and aPKC do not extend along the entire DV border, and are less apically restricted *cno*^{MZ} mutants.

(A-B''', D-E''') Stage 7 embryos, anterior to left, antigens indicated. (C-C''', F-F''') Cross-sections. (A-C''') WT. (A-A''') Baz and aPKC are restricted apically. (B-B''') Occasional puncta of Baz are seen 2μm more basally, yellow arrowheads. (D-F''') *cno*^{MZ} mutants. (D-D''') In the apical plane, Baz and aPKC do not extend to the ends of the DV borders. (E-E''') 2μm more basal, many Baz and aPKC puncta are seen, yellow arrowheads. Scale bars = 10μm.

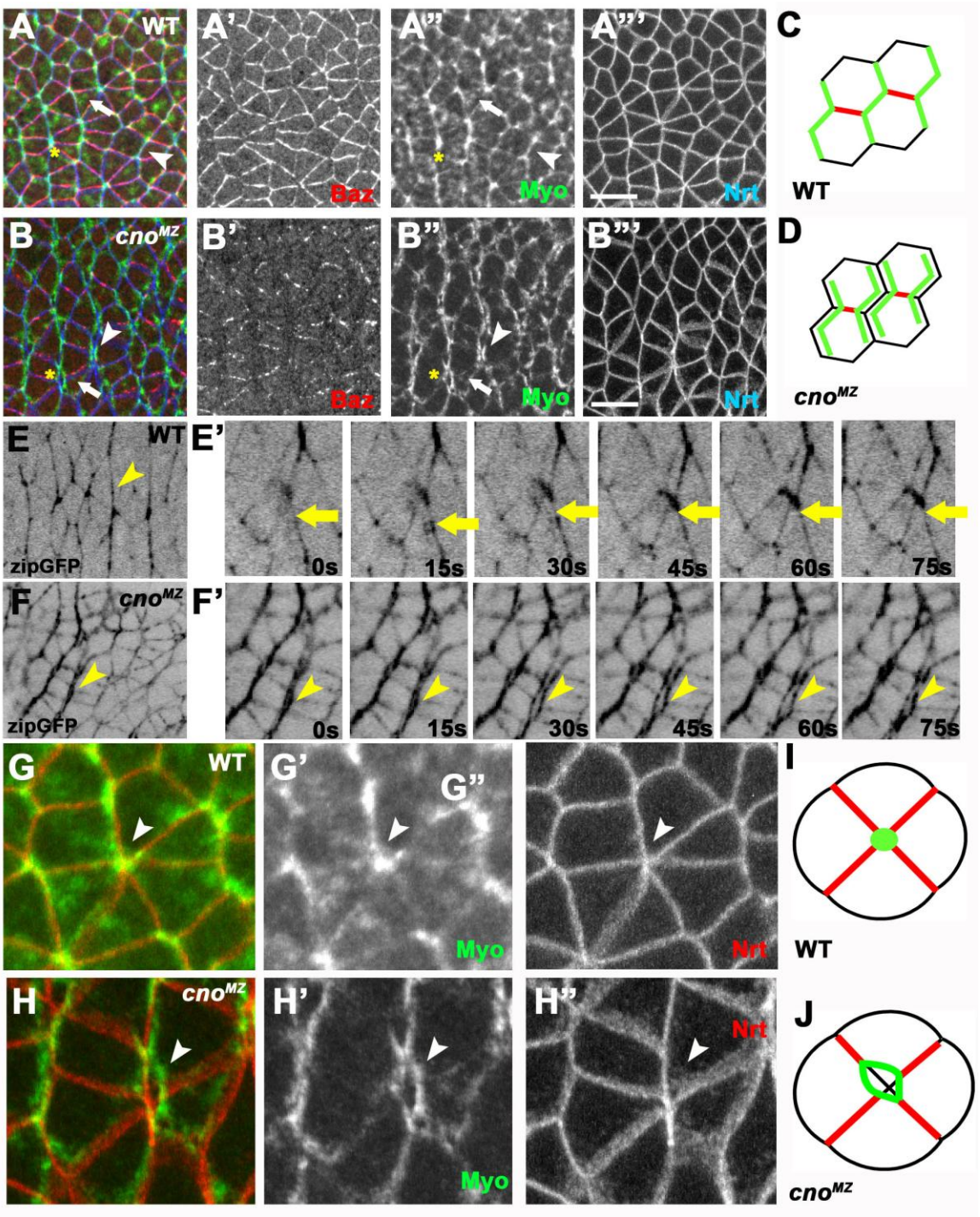
A
WT
A'
Baz
A''
Myo
A'''
Nrt
C
WT
B
cnoMZ
B'
Baz
B''
Myo
B'''
Nrt
D
cnoMZ
E
WT
zipGFP
E'
0s
15s
30s
45s
60s
75s
F
cnoMZ
zipGFP
F'
0s
15s
30s
45s
60s
75s
G
WT
G'
G''
Myo
Nrt
I
WT
H
cnoMZ
H'
Myo
H''
Nrt
J
cnoMZ

Figure 5. Myosin in *cno*^{MZ} mutants is not tightly associated with apical junctions.
(A-B”’, G-H”) Stage 7 embryos, anterior to left, antigens indicated. Maximum intensity projection of a 2μm stack. (E-F’) Stills from zipGP movies, stage 7 to stage 8 embryos. Anterior to the left. (A-A”’,C, E-E’, G-G”, I) WT. (B-B”’, D F-F’, H-H”, J) *cno*^{MZ} mutants. (A-A”’) In WT, Myo is tightly associated apical junctions, white arrowheads, and at the vertices of rosettes, yellow asterisks. Myo also assembles in an apical meshwork, white arrows. Baz extends along entire DV border. (B-B”’) In *cno*^{MZ} mutants, Myo is not tightly associated between cells along AP borders, and gaps appear, white arrows. Especially where rosettes are beginning to form, yellow asterisks. Little apical Myo is present, white arrows. Baz does not extend along entire DV border. (E) WT, zipGFP movie. Myo localization is tightly associated between cells along AP borders, yellow arrowhead. (E’) Close-up WT, time series. A dynamic apical Myo network is apparent, especially is cells forming rosettes, yellow arrows. (F) *cno*^{MZ}, zipGFP movie. Gaps are present between cells, yellow arrowhead. (F’) Close-up *cno*^{MZ}, time series. Very little apical Myo is apparent, but gaps in Myosin localization are obvious, yellow arrowheads (C,D,I,J) Cartoon representation of Myo (Green) and Baz (Red) localization in WT and *cno*^{MZ} mutants. Scale bars A-B’’’ = 10μm.

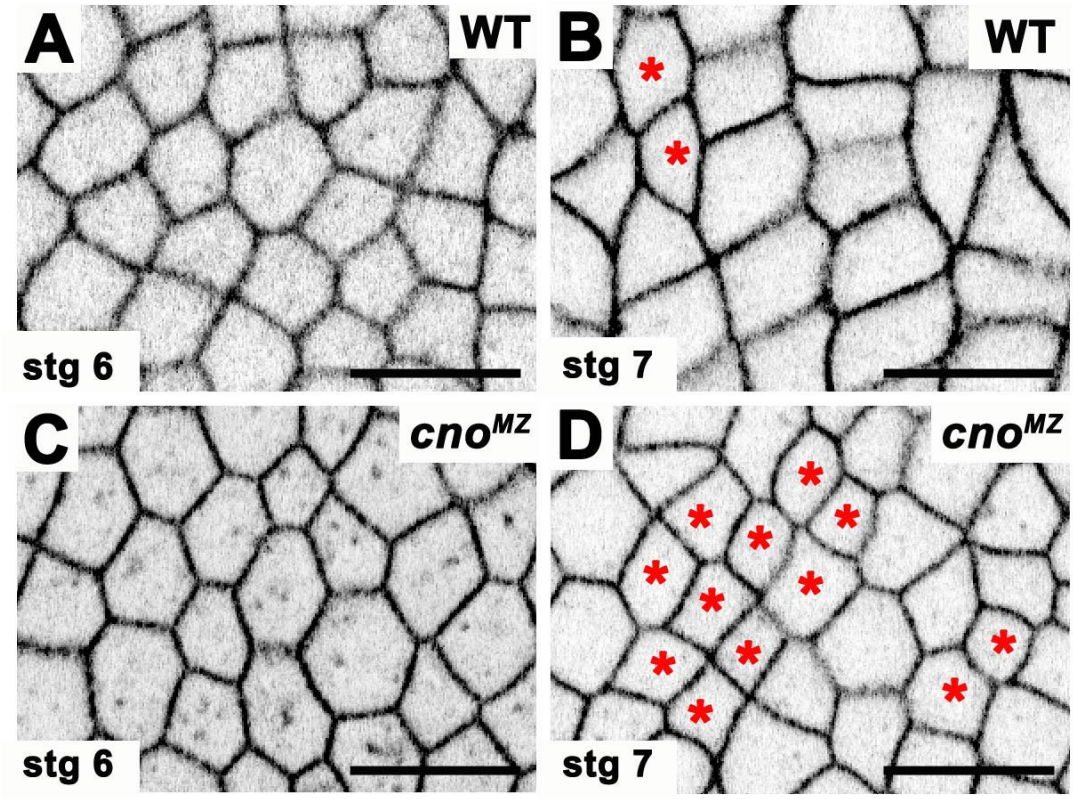

Figure 6. Cells in *cno*^{MZ} mutants are isometric at the onset of GBE.
(A-D) Stage 6 and 7 embryos, anterior to left, Nrt staining to highlight cell borders. (A) WT vs. (C) *cno*^{MZ} at stage 6. Cells are isometric in both WT and *cno*^{MZ} mutants. (B) WT vs. (D) *cno*^{MZ} at stage 7. In WT, cells become more anisometric, lengthening their DV borders in relation to their AP borders. In *cno*^{MZ}, cells remain more isometric, and are shorter along their AP and DV borders. Scale bars = 10μm.

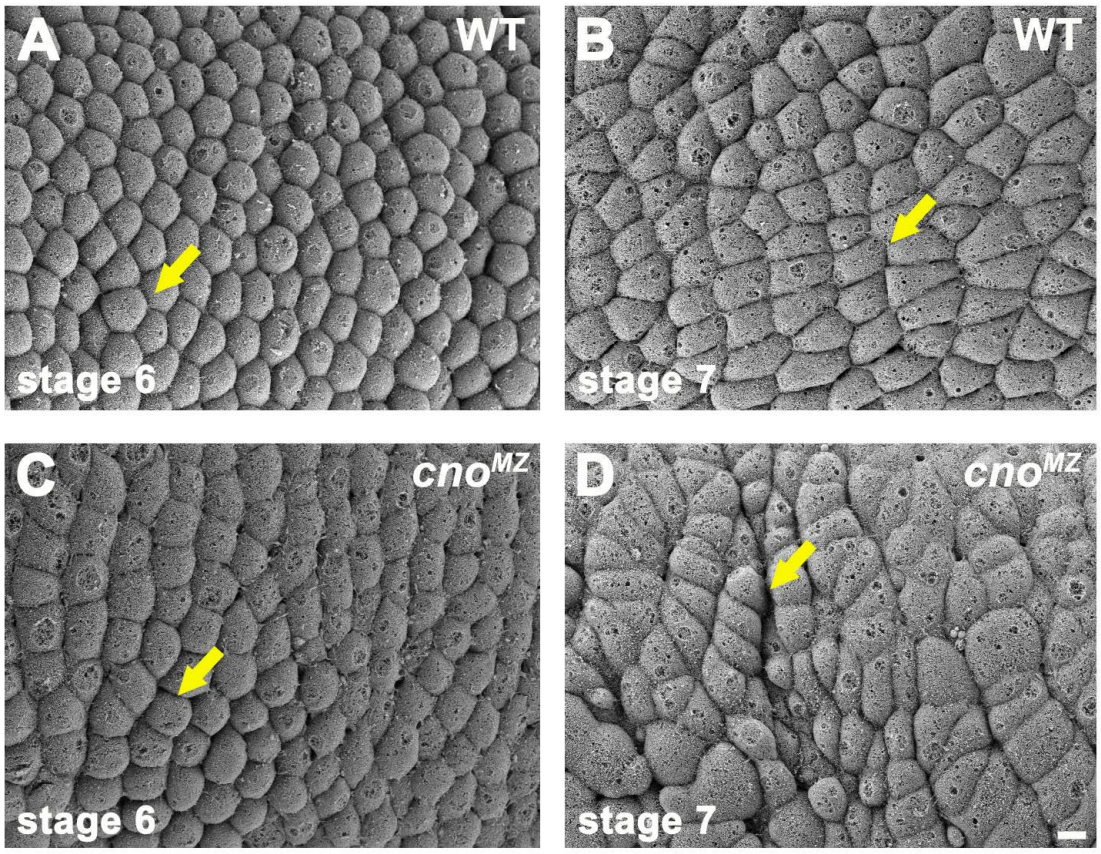

Figure 7. Cells in *cno*^{MZ} mutants are impaired in cell flattening.
(A-D) Scanning micrographs, anterior to the left. (A) WT vs. (C) *cno*^{MZ} mutants, stage 6. Most cells are rounded in WT and *cno*^{MZ} mutants, yellow arrows. (B) WT vs. (C) *cno*^{MZ} mutants, stage 7. WT cells begin to flatten their apices, yellow arrow. In *cno*^{MZ} mutants, many cells are rounded and often gaps are present between cells on AP borders, yellow arrow. Scale bar = 3μm.

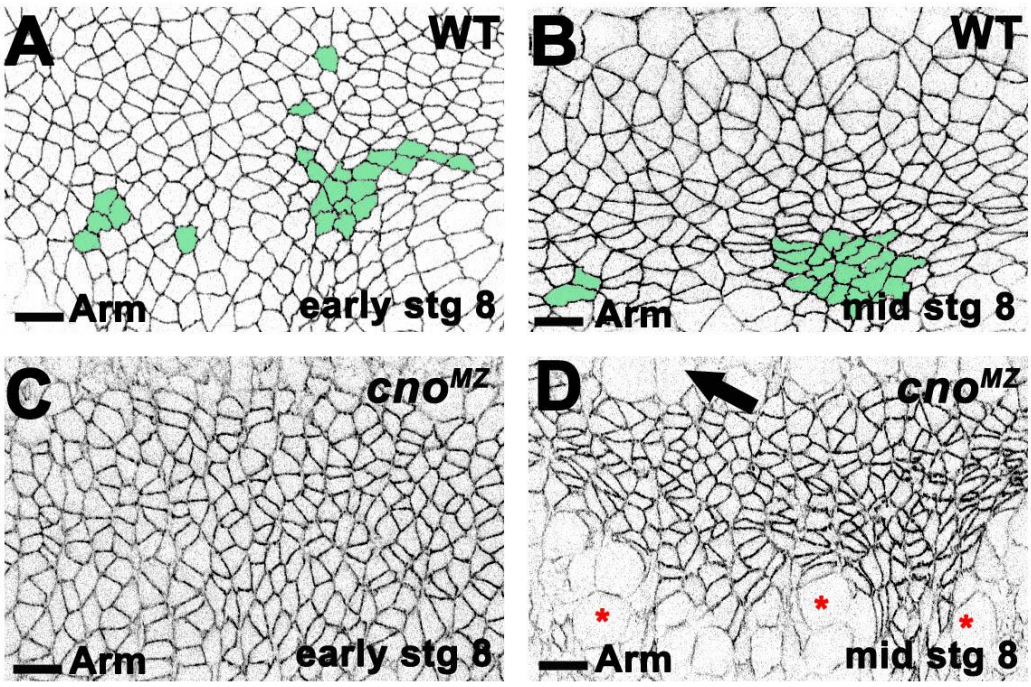

Figure 8. Apical cells borders in *cno*^{MZ} mutants are less convoluted
(A-D) Early to mid stage 8 embryos, anterior to the left, Arm staining to highlight apical cell borders. (A) WT vs. (C) *cno*^{MZ} at early stage 8. As mitotic divisions begin many cells in WT have convoluted cell borders (highlighted in green), which are not apparent in *cno*^{MZ} mutants. (B) WT vs. (D) *cno*^{MZ} at mid stage 8. The convoluted nature of WT cells continues as morphogenesis proceeds, but *cno*^{MZ} mutant cells have very straight borders. Black arrow indicates dividing ventral furrow cells. Red asterisks indicate mitotic domains. Scale bars = 10μm.

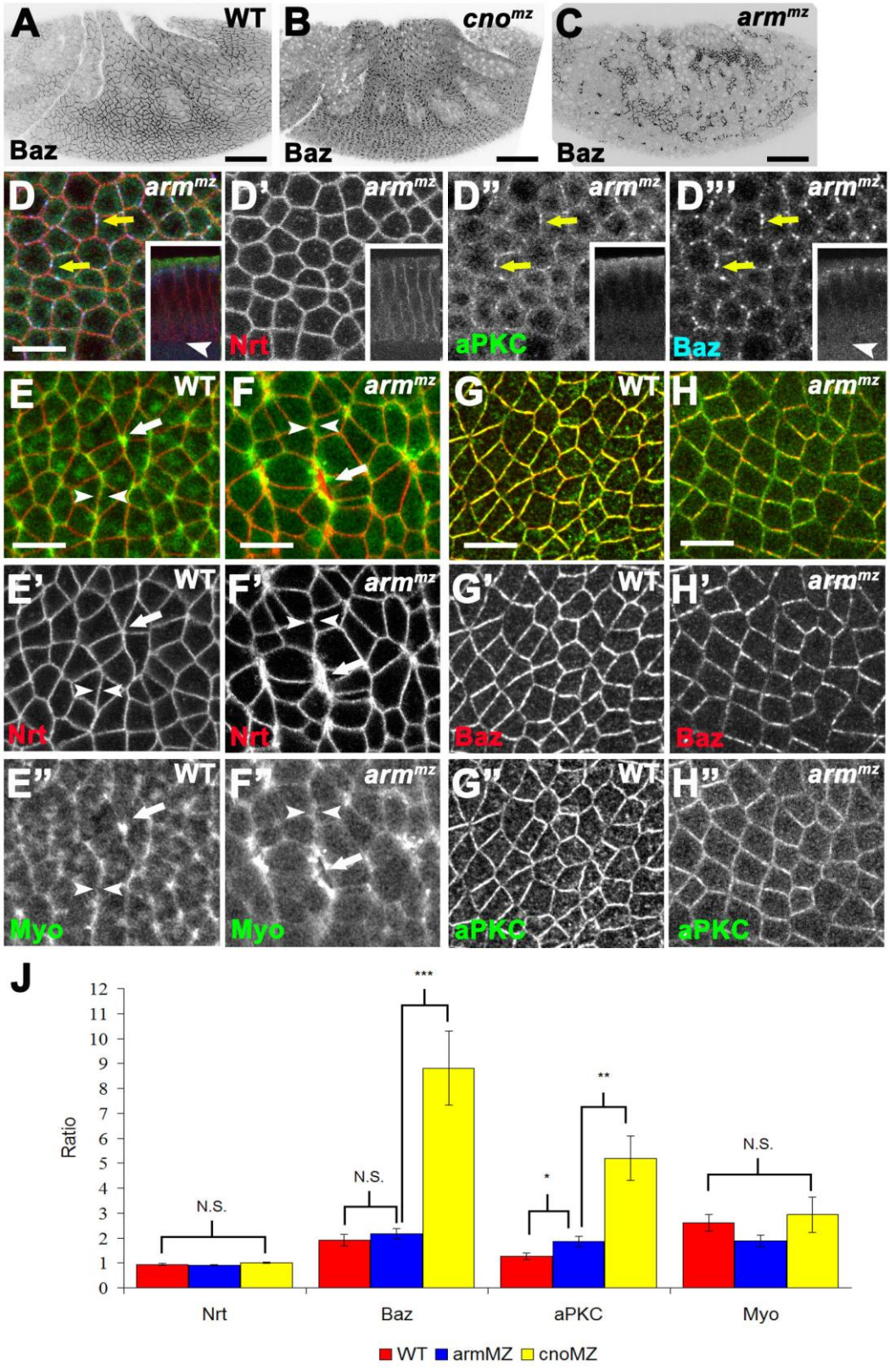
A
WT
Baz
B
cno^mz
Baz
C
arm^mz
Baz
D
arm^mz
D'
arm^mz
Nrt
D''
arm^mz
aPKC
D'''
arm^mz
Baz
E
WT
F
arm^mz
G
WT
H
arm^mz
E'
WT
Nrt
F'
arm^mz
Nrt
G'
WT
Baz
H'
arm^mz
Baz
E''
WT
Myo
F''
arm^mz
Myo
G''
WT
aPKC
H''
arm^mz
aPKC
J
Ratio
12
11
10
9
8
7
6
5
4
3
2
1
0
***
**
*
N.S.
N.S.
N.S.
N.S.
Nrt
Baz
aPKC
Myo
WT
armMZ
cnoMZ

Figure 9. Global loss of adhesion does not lead to the planar polarity enhancement seen in *cno*^{MZ} mutants

(A-C) Stage 8 embryos, anterior to the left, antigens and genotypes indicated. *arm*^{MZ} mutants lose epithelial integrity before *cno*^{MZ} mutants. Scale bars = 50μm. (D-D”’) *arm*^{MZ} mutants, anterior to the left, antigens indicated. Baz and aPKC overlap in apical puncta (yellow arrows). Inset = Xsection, Baz is not found in basal junctions (white arrow heads). (E-H”) Stage 7 embryos, anterior to the left, antigens indicated. (E-E”) WT, Myosin is tightly associated with the cortex (white arrowheads) and at vertices of rosettes (white arrows). (F-F”) *arm*^{MZ} mutants, Myosin is tightly associated with the cortex in most places (white arrowheads), but separates from cortex in forming rosettes (white arrows). (G-G”) WT, Baz and aPKC is planar polarized and is in (H-H”) *arm*^{MZ} mutants. (D-H”) Scale bars = 50μm. (J) Planar polarity in WT, *arm*^{MZ} mutants, and *cno*^{MZ} mutants. Error bars are s.e.m. * = P<0.03 ** = P<0.01 *** = P<0.003.

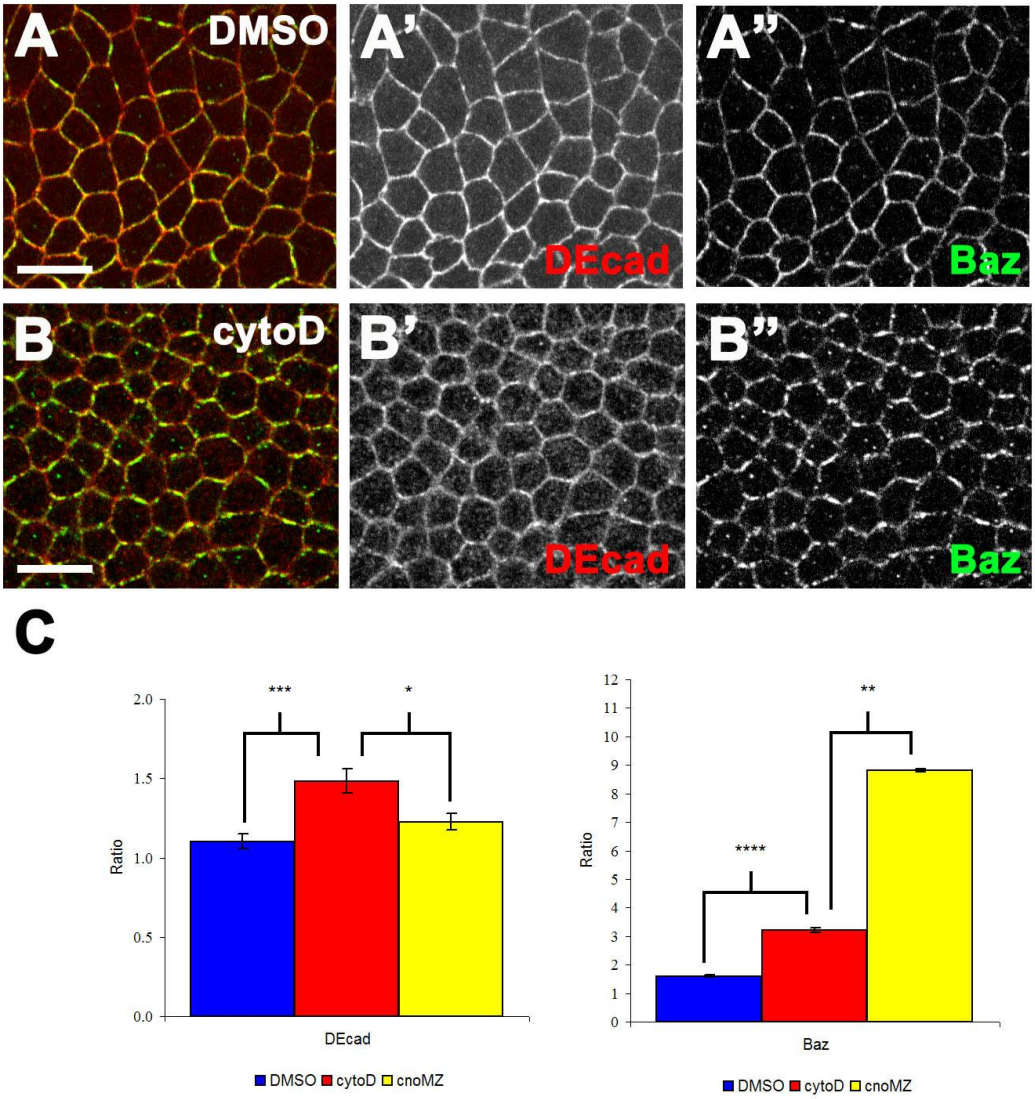

Figure 10. Global disruption of actin closely mimics the planar polarity enhancement seen in *cno*^{MZ} mutants

(A-B") Stage 7 embryos, anterior to the left, antigens and genotypes indicated. Scale bars = 10µm. (A-A") DMSO treated embryos. (B-B") cytoD treated embryos. Planar polarity of DEcad and Baz are enhanced. Cells appear more isometric. (C) Planar polarity in DMSO, cytoD, and *cno*^{MZ} mutants. Error bars are s.e.m. * = P<0.03 *** = P<0.003 **** = P<0.0001.

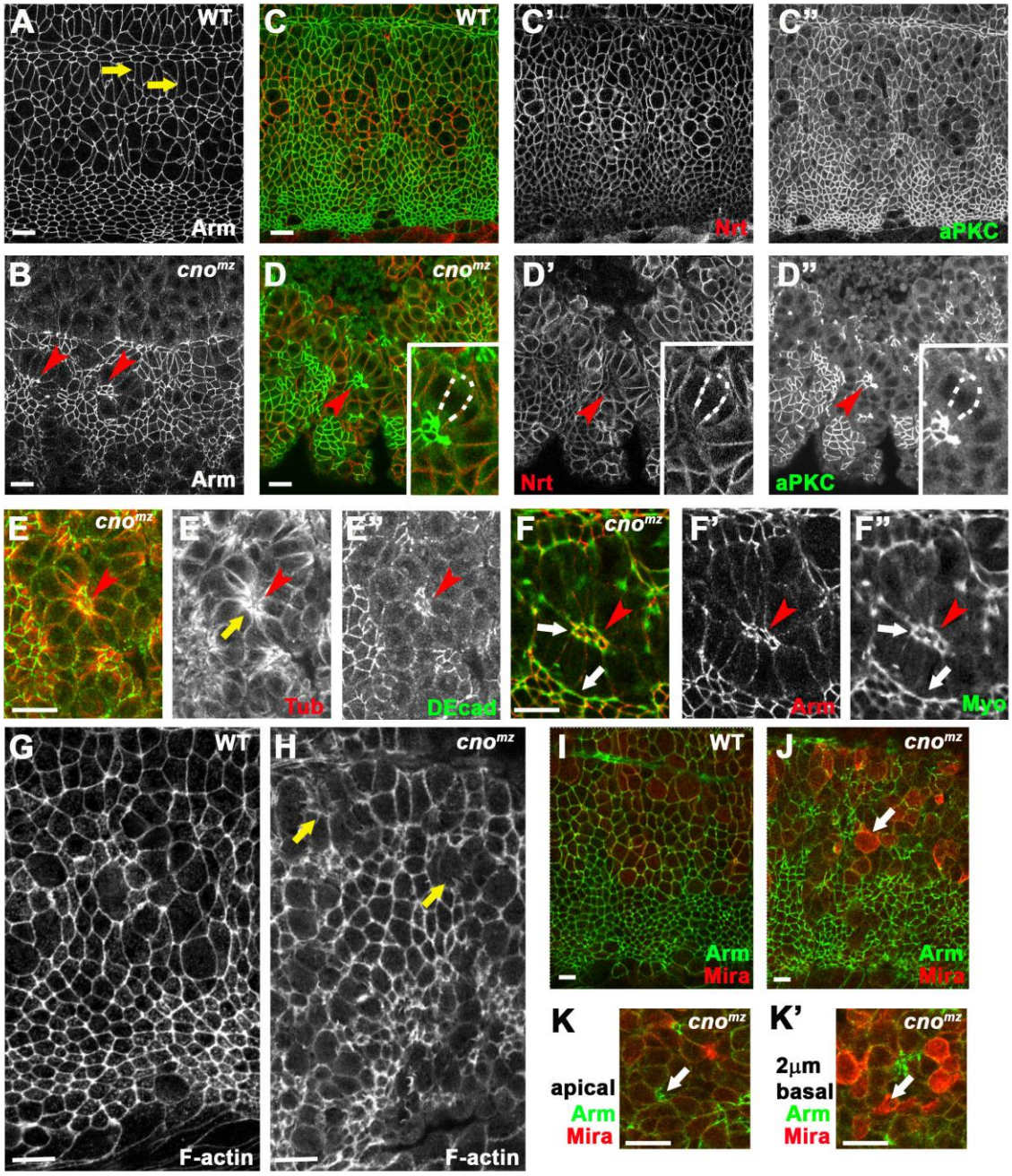

Figure 11. Defects in epithelial integrity arises in *cno*^{MZ} mutants later in morphogenesis
(A-K') Stage 9-10 embryos, anterior to the left, antigens and genotypes indicated. (A) WT, ventral ectoderm cells have unique morphology. (B) *cno*^{MZ} mutant, cells pull apart, red arrowheads point out contricted apical ends. (C-D") WT vs. *cno*^{MZ} mutants, planar polarity is lost. Constricted apical ends are also positive for aPKC, red arrowheads. Inset, outlined cell that was pulled over. (E-E") In *cno*^{MZ} mutant, the MT cytoskeleton retains basic polarity, yellow arrow indicated MTs polarized toward constricted apical ends, indicated with red arrow. (F-F") Epithelial rosettes, indicated with red arrowhead, in *cno*^{MZ} mutant are surrounded by bands of Myosin, white arrows. (I) vs. (J) *cno*^{MZ} mutant have neuroblasts on the surface, white arrow. (K-K') Neuroblasts are sometimes at the center of rosettes more basally, white arrow. Scale bars = 10μm.

References

Bertet, C., L. Sulak, and T. Lecuit. 2004. Myosin-dependent junction remodelling controls planar cell intercalation and axis elongation. *Nature*. 429:667-71.

Blankenship, J.T., S.T. Backovic, J.S. Sanny, O. Weitz, and J.A. Zallen. 2006. Multicellular rosette formation links planar cell polarity to tissue morphogenesis. *Dev Cell*. 11:459-70.

Buszczak, M., S. Paterno, D. Lighthouse, J. Bachman, J. Planck, S. Owen, A.D. Skora, T.G. Nystul, B. Ohlstein, A. Allen, J.E. Wilhelm, T.D. Murphy, R.W. Levis, E. Matunis, N. Srivali, R.A. Hoskins, and A.C. Spradling. 2007. The carnegie protein trap library: a versatile tool for Drosophila developmental studies. *Genetics*. 175:1505-31.

Campos-Ortega, J. 1993. Early Neurogenesis in Drosophila melonogaster. *In* The Development of Drosophila melanogaster. Vol. II. M. Bate and A. Martinez Arias, editors. Cold Spring Harbor Laboratory Press, New York. 1091-1129.

Dawes-Hoang, R.E., K.M. Parmar, A.E. Christiansen, C.B. Phelps, A.H. Brand, and E.F. Wieschaus. 2005. folded gastrulation, cell shape change and the control of myosin localization. *Development*. 132:4165-78.

Drees, F., S. Pokutta, S. Yamada, W.J. Nelson, and W.I. Weis. 2005. Alpha-catenin is a molecular switch that binds E-cadherin-beta-catenin and regulates actin-filament assembly. *Cell*. 123:903-15.

Gates, J., and M. Peifer. 2005. Can 1000 reviews be wrong? Actin, alpha-Catenin, and adherens junctions. *Cell*. 123:769-72.

Harris, T.J., and M. Peifer. 2004. Adherens junction-dependent and -independent steps in the establishment of epithelial cell polarity in Drosophila. *J Cell Biol*. 167:135-47.

Harris, T.J., and M. Peifer. 2005. The positioning and segregation of apical cues during epithelial polarity establishment in Drosophila. *J Cell Biol*. 170:813-23.

Harris, T.J., and M. Peifer. 2007. aPKC controls microtubule organization to balance adherens junction symmetry and planar polarity during development. *Dev Cell*. 12:727-38.

Martin, A.C., M. Gelbart, R. Fernandez-Gonzalez, M. Kaschube, and E.F. Wieschaus. 2010. Integration of contractile forces during tissue invagination. *J Cell Biol*.

Martin, A.C., M. Kaschube, and E.F. Wieschaus. 2009. Pulsed contractions of an actin-myosin network drive apical constriction. *Nature*.

Muller, H.A., and E. Wieschaus. 1996. armadillo, bazooka, and stardust are critical for early stages in formation of the zonula adherens and maintenance of the polarized blastoderm epithelium in Drosophila. *J Cell Biol*. 134:149-63.

Peifer, M., S. Orsulic, D. Sweeton, and E. Wieschaus. 1993. A role for the Drosophila segment polarity gene armadillo in cell adhesion and cytoskeletal integrity during oogenesis. *Development*. 118:1191-207.

Quinlan, M.P., and J.L. Hyatt. 1999. Establishment of the circumferential actin filament network is a prerequisite for localization of the cadherin-catenin complex in epithelial cells. *Cell Growth Differ*. 10:839-54.

Roeth, J.F., J.K. Sawyer, D.A. Wilner, and M. Peifer. 2009. Rab11 helps maintain apical crumbs and adherens junctions in the Drosophila embryonic ectoderm. *PLoS One*. 4:e7634.

Sawyer, J.K., N.J. Harris, K.C. Slep, U. Gaul, and M. Peifer. 2009. The Drosophila afadin homologue Canoe regulates linkage of the actin cytoskeleton to adherens junctions during apical constriction. *J Cell Biol*. 186:57-73.

Sweeton, D., S. Parks, M. Costa, and E. Wieschaus. 1991. Gastrulation in Drosophila: the formation of the ventral furrow and posterior midgut invaginations. *Development*. 112:775-89.

Tepass, U., E. Gruszynski-DeFeo, T.A. Haag, L. Omatyar, T. Torok, and V. Hartenstein. 1996. shotgun encodes Drosophila E-cadherin and is preferentially required during cell rearrangement in the neurectoderm and other morphogenetically active epithelia. *Genes Dev*. 10:672-85.

Yamada, S., S. Pokutta, F. Drees, W.I. Weis, and W.J. Nelson. 2005. Deconstructing the cadherin-catenin-actin complex. *Cell*. 123:889-901.

Zallen, J.A., and J.T. Blankenship. 2008. Multicellular dynamics during epithelial elongation. *Semin Cell Dev Biol*. 19:263-70.

Zallen, J.A., and E. Wieschaus. 2004. Patterned gene expression directs bipolar planar polarity in Drosophila. *Dev Cell*. 6:343-55.

Zallen, J.A., and R. Zallen. 2004. Cell-pattern disordering during convergent extension in Drosophila. *Journal of Physics: Condensed Matter*:S5073-S5080.

CHAPTER 4

DISCUSSION

Building an animal is a truly remarkable process. We all begin as one cell that then divides to create more cells, which act as building blocks. These building blocks then must be shaped into a form in the process of morphogenesis. While we have made leaps and bounds in our understanding how we build an animal, we still have a relatively poor understanding of morphogenesis itself (Fraser and Harland, 2000; Wieschaus, 1997). A catalog of beautiful descriptive work detailing various morphogenetic processes in several model organisms has been built. Additionally, great progress has been made in discovering what genes are required for specific morphogenetic events. We now have a catalog of what cells do and understand many of the tools cells use during morphogenesis. But the question remains, how do cells use these tools to change shape, move, bend, and all the other amazing things they do? This understanding of how cells coordinate their movements will give us greater insight into how birth defects arise and how things go wrong in human developmental diseases, including cancer. Many aspects of morphogenesis are conserved across the animal kingdom. For example, apical constriction is used in *Drosophila* to internalize the mesoderm and in mammals to form the neural tube (Sawyer et al., 2009b). Defects in forming the neural tube occurs in one in a thousand human births (Copp et al., 1990; Golden and Chernoff, 1995). Still relatively little is known about the molecular mechanisms that underlie neurulation defects in humans (Greene et al., 2009). Studying morphogenesis in model systems will

give us important insight into human morphogenesis. In my dissertation research, I investigated how cell-cell adhesion is coupled to cell shape change during morphogenesis.

Adherens Junctions: Not your average glue

Cell-cell adhesion is critical for development. Classical cadherins and their associated catenins play central roles in morphogenesis of many tissues. The cadherin-catenin complex is thought to form mechanical attachments between cells by linking actin in neighboring cells. This specialized structure, the adherens junctions (AJs), is found at the apical ends of cells and helps cells stick together. AJs are not merely glue; cells and tissues must change their shape in a coordinated way (Nishimura and Takeichi, 2009). Quite a lot is known about the proteins that constitute the AJs and it was long believed there was a direct linkage between AJs and actin, with the transmembrane protein E-cadherin bound to ß-catenin, ß-catenin to α-catenin, and α-catenin to F-actin. Recent biochemical work demonstrated that linking AJs to F-actin is not that simple. α-catenin monomers bind to AJs, while α-catenin dimers bind to F-actin (Drees et al., 2005; Gates and Peifer, 2005; Yamada et al., 2005). This was surprising to many in the field, but it remains clear that AJs play important roles in morphogenesis, as their loss leads to early embryonic lethality in both flies and mice (Cox et al., 1996; Larue et al., 1994; Muller and Wieschaus, 1996; Torres et al., 1997). Now the challenge is to understand how junctions are dynamically regulated and linked to the actin cytoskeleton.

In the past decade there has been great progress in understanding how AJs are modulated during morphogenesis. Roles for Rho-family small GTPases and their regulators were known to be important for establishing and maintaining AJs, and now the

list is growing with the addition of other small GTPases (reviewed in Nishimura and Takeichi, 2009). Endocytosis has also emerged as an important way to modulate junctions (reviewed in Nishimura and Takeichi, 2009). Finally, there are other proteins found at AJs whose functions are less well understood. For example, recent studies have revealed the importance of nonclassical cadherins and nectins in AJ modulation (reviewed in Nishimura and Takeichi, 2009).

My dissertation research addressed the function of afadin/Canoe(Cno), a protein that localizes to AJs, whose role in adhesion and morphogenesis was unclear. In mammals, afadin and the cell-cell adhesion molecules nectins form a novel intracellular cell adhesion system that works in concert with cadherin-catenins. Further, studies in mammalian systems suggested that afadin played an essential role in the establishment of AJs and polarity (Takai and Nakanishi, 2003). Studies in *Drosophila* told a different story, in which Cno works to coordinate signaling pathways during morphogenesis (Boettner et al., 2003; Matsuo et al., 1999; Miyamoto et al., 1995). In both invertebrates and mammals, it is clear that afadin/Canoe plays an essential role in morphogenesis and embryos lacking its function fail early in development (Ikeda et al., 1999; Zhadanov et al., 1999). We hypothesized that Cno may act to regulate junctional plasticity by regulating connections to actin and to signal transduction machinery. We tested this hypothesis using *Drosophila* as a model system to define the function of Canoe (Cno) in cell-cell adhesion and morphogenesis by completely removing its function.

Canoe: A helping hand

My dissertation research revealed that Cno is not essential for establishment of adhesion or polarity, but is required for morphogenesis. In fact, it is required right from

the start of the first dynamic morphogenetic event, gastrulation. At the beginning of gastrulation, the mesoderm is internalized in a process called ventral furrow formation (Chapter 1, Chapter 2). In the absence of Cno, ventral furrow formation fails because cell shape change is no longer coupled to actomyosin constriction. Cno is also required in another morphogenetic event, germband elongation (Chapter 1, Chapter 3). As gastrulation proceeds, cells must intercalate to extend the epithelium. To do this, junctional proteins became enriched along the DV axis and cytoskeletal proteins along the AP axis. This planar polarity is thought the drive the process of intercalation and in turn elongation (Harris et al., 2009; Zallen and Blankenship, 2008). In the absence of Cno, germband elongation is impaired. Enrichment of junctional proteins on DV borders becomes more enhanced, while cytoskeletal protein enrichment does not. Again, cell shape change is uncoupled from the actomyosin network changes. Myosin is no longer tightly associated with the cortex on DV borders and gaps in its localization appear. Interestingly, Cno is normally enriched along AP borders with the cytoskeletal proteins. This suggested that in germband elongation, as in ventral furrow formation, Cno is required to maintain linkages between AJs and the actomyosin network during dynamic morphogenesis. Indeed, Cno is also required later in morphogenesis as cells begin to divide and delaminate (Chapter 3). Taken together, this suggests that during dynamic morphogenesis, AJs need a "helping hand" with their connections to the actomyosin network to ensure precise coordination.

How Can-oe(you) do it?

The challenge now is to understand how Cno can facilitate this linkage between AJs and the actomyosin network at the molecular level. We gained some insight into this

problem. First, Cno can bind directly to F-actin, like its homolog Afadin (Mandai et al., 1997; Sawyer et al., 2009a). Previous studies revealed that Cno can bind direclty to Echinoid, a nectin-like protein, that is present at AJs (Wei et al., 2005). Cno can also bind directly to Polychaetoid (Pyd/ZO-1); Pyd is mammalian tight junction protein, but in *Drosophila* associates with AJs (Takahashi et al., 1998). Studies in mammals, revealed that Afadin can bind α-catenin directly (Pokutta et al., 2002). We added to this list by finding that the PDZ domain of Cno could bind directly the C-terminus of DEcad (Sawyer et al., 2009a). However, Cno does not immunoprecipitate with other proteins in the AJ complex (DEcad, β-catenin, and α-catenin). Further, Cno does not require the AJ complex or Echinoid for its localization. We found that F-actin and the small GTPase Rap1 are important for its localization. This led us to the hypothesis that Cno is normally in an inactive state when not bound to Rap1, and when Rap1 bound Cno can open and become active and interact with F-actin and the AJs.

However, it is still unclear whether Cno interacts with AJs either directly or indirectly. In the future, it will be important to test these hypotheses directly. To that end, we have established a collaboration with Kevin Slep, an assistant professor at UNC-Chapel Hill, who is an expert in crystallography and biochemistry. Kevin Slep, Wangsun Choi, a new postdoctoral fellow in our lab, and Kuo-Chen Jung, a graduate student in out lab, are dissecting Cno and trying to determine if there are portions of Cno that can self-interact using yeast two-hybrid and biochemical strategies. If there are portions that can self-interact, this would support the hypothesis that Cno is a closed state, until a binding partner binds and changes its conformation.

We know relatively little about what proteins bind to Cno or the function of the suite of protein interaction domains in Cno. One strategy to learn more about binding partners is to use purified Cno domains for mass spectrometry analysis. If successful, this would help us to understand how Cno is interacting with both the cytoskeleton and AJs. Is Cno a direct link with other proteins bound to Cno to modify how it links AJs and the actomyosin network? Alternatively, does Cno modify the cytoskeleton so that other proteins can stabilize the link between AJs and the actomyosin network? Our work supports the idea that the link could be direct, since Cno can bind both the C-terminus of DEcad and F-actin directly (Sawyer et al., 2009a). However, in mammals Afadin can bind Ponsin and Profilin directly and α-actinin indirectly, which are proteins that can modify to the cytoskeletal network (Asada et al., 2003; Boettner et al., 2000; Mandai et al., 1999), suggesting that afadin may modify the cytoskeleton and this in turn could modulate AJs during morphogenesis. These two ideas need not necessarily be mutually exclusive: one can imagine a scenario in which afadin/Cno links AJs and the actomyosin network directly, and while in this conformation other cytoskeletal proteins bind afadin/Cno and modify the actomyosin network around AJs. This might allow the actomyosin network and/or the junctions to relax to allow for cell shape changes experienced during morphogenesis, while still maintaining a connection.

Once we have a more complete list of Cno binding partners, it would be fascinating to investigate the function of Cno's protein binding domains. Recently, several members of our lab have established structure-function assays, using the Gateway® Cloning (Invitrogen) system to generate transgenes missing protein domains of interest. Using a similar strategy to dissect the function of Cno would give us valuable

information. We have carefully characterized how loss of Cno affects early morphogenesis; therefore we can gain insight on which protein domains are required for Cno's function. Almost certainly particular domains will be required for specific events at specific time points. Cno is a complex scaffolding protein; discovering which protein domains are important for what function and when will be important to understanding how Cno regulates AJ-actomyosin linkages at the molecular level.

Staying tense

Over the past several years, it has become increasingly clear that forces play an important role in morphogenesis (reviewed in Paluch and Heisenberg, 2009). *Drosophila* has been a leading model system for understanding more about forces in morphogenesis. Apical constriction during mesoderm invagination and dorsal closure both involve pulsed constrictions of the actomyosin network. In apical constriction these pulsed constrictions are reinforced by a stiff edge, or ratchet. During mesoderm invagination, the transcriptional regulator Twist, regulates the stability of constricting cells, creating a ratchet (Martin et al., 2009). In dorsal closure, this ratcheting mechanism is provided by the actomyosin cable assembled by the leading edge cells (Solon et al., 2009). Interestingly, when adhesion is reduced during mesoderm invagination, large epithelial tears arise in the epithelium as cells invaginate (Martin et al., 2010). Further, recent work in germband elongation demonstrated that tension is necessary and sufficient for Myosin's cortical localization (Fernandez-Gonzalez et al., 2009). Adhesion is also important for maintaining tension during dynamic morphogenesis. During mesoderm invagination, in embryos with reduced adhesion, tears arise in the epithelium. Even more interesting, it appears that spot-AJs are important for transmitting and balancing tension

across the apical plasma membrane (Martin et al., 2010). It is tempting to speculate that Cno plays an important role in balancing apical tension. Indeed, the loss of epithelial integrity in ventral epithelium of *cno* mutants has similarities to these epithelial tears seen in embryos with reduced adhesion (Chapter 3; Fig. 9). In addition, Cno is enriched at tricellular junctions along with a pool of F-actin (Sawyer et al., 2009a). One hypothesis is that Cno facilitates connections from tricellular junctions to the supracellular actomyosin network, helping to maintain tension across the apical surface of cells.

Morphing backward and forward

Fifteen years ago, the molecular mechanisms of morphogenesis was thought to be one of developmental biology's unresolved mysteries, but one in which we would make rapid progress (Barinaga, 1994). Indeed, we have come a long way in furthering our understanding of the molecular mechanisms of morphogenesis and I feel that my dissertation research has contributed to that knowledge. At the same time, we still have much learn about how cells coordinate the complex dance of morphogenesis. Once we understand how cells do things right during normal development, we will have greater insight in how to correct problems when cells do things wrong.

References

Asada, M., K. Irie, K. Morimoto, A. Yamada, W. Ikeda, M. Takeuchi, and Y. Takai. 2003. ADIP, a novel Afadin- and alpha-actinin-binding protein localized at cell-cell adherens junctions. *J Biol Chem*. 278:4103-11.

Barinaga, M. 1994. Looking to development's future. *Science*. 266:561-4.

Boettner, B., E.E. Govek, J. Cross, and L. Van Aelst. 2000. The junctional multidomain protein AF-6 is a binding partner of the Rap1A GTPase and associates with the actin cytoskeletal regulator profilin. *Proc Natl Acad Sci U S A*. 97:9064-9.

Boettner, B., P. Harjes, S. Ishimaru, M. Heke, H.Q. Fan, Y. Qin, L. Van Aelst, and U. Gaul. 2003. The AF-6 homolog canoe acts as a Rap1 effector during dorsal closure of the Drosophila embryo. *Genetics*. 165:159-69.

Copp, A.J., F.A. Brook, J.P. Estibeiro, A.S. Shum, and D.L. Cockroft. 1990. The embryonic development of mammalian neural tube defects. *Prog Neurobiol*. 35:363-403.

Cox, R.T., C. Kirkpatrick, and M. Peifer. 1996. Armadillo is required for adherens junction assembly, cell polarity, and morphogenesis during Drosophila embryogenesis. *J Cell Biol*. 134:133-48.

Drees, F., S. Pokutta, S. Yamada, W.J. Nelson, and W.I. Weis. 2005. Alpha-catenin is a molecular switch that binds E-cadherin-beta-catenin and regulates actin-filament assembly. *Cell*. 123:903-15.

Fernandez-Gonzalez, R., M. Simoes Sde, J.C. Roper, S. Eaton, and J.A. Zallen. 2009. Myosin II dynamics are regulated by tension in intercalating cells. *Dev Cell*. 17:736-43.

Fraser, S.E., and R.M. Harland. 2000. The molecular metamorphosis of experimental embryology. *Cell*. 100:41-55.

Gates, J., and M. Peifer. 2005. Can 1000 reviews be wrong? Actin, alpha-Catenin, and adherens junctions. *Cell*. 123:769-72.

Golden, J.A., and G.F. Chernoff. 1995. Multiple sites of anterior neural tube closure in humans: evidence from anterior neural tube defects (anencephaly). *Pediatrics*. 95:506-10.

Greene, N.D., P. Stanier, and A.J. Copp. 2009. Genetics of human neural tube defects. *Hum Mol Genet*. 18:R113-29.

Harris, T.J., J.K. Sawyer, and M. Peifer. 2009. How the cytoskeleton helps build the embryonic body plan: models of morphogenesis from Drosophila. *Curr Top Dev Biol*. 89:55-85.

Ikeda, W., H. Nakanishi, J. Miyoshi, K. Mandai, H. Ishizaki, M. Tanaka, A. Togawa, K. Takahashi, H. Nishioka, H. Yoshida, A. Mizoguchi, S. Nishikawa, and Y. Takai. 1999. Afadin: A key molecule essential for structural organization of cell-cell junctions of polarized epithelia during embryogenesis. *J Cell Biol*. 146:1117-32.

Larue, L., M. Ohsugi, J. Hirchenhain, and R. Kemler. 1994. E-cadherin null mutant embryos fail to form a trophectoderm epithelium. *Proc Natl Acad Sci U S A*. 91:8263-7.

Mandai, K., H. Nakanishi, A. Satoh, H. Obaishi, M. Wada, H. Nishioka, M. Itoh, A. Mizoguchi, T. Aoki, T. Fujimoto, Y. Matsuda, S. Tsukita, and Y. Takai. 1997. Afadin: A novel actin filament-binding protein with one PDZ domain localized at cadherin-based cell-to-cell adherens junction. *J Cell Biol*. 139:517-28.

Mandai, K., H. Nakanishi, A. Satoh, K. Takahashi, K. Satoh, H. Nishioka, A. Mizoguchi, and Y. Takai. 1999. Ponsin/SH3P12: an l-afadin- and vinculin-binding protein localized at cell-cell and cell-matrix adherens junctions. *J Cell Biol*. 144:1001-17.

Martin, A.C., M. Gelbart, R. Fernandez-Gonzalez, M. Kaschube, and E.F. Wieschaus. 2010. Integration of contractile forces during tissue invagination. *J Cell Biol*.

Martin, A.C., M. Kaschube, and E.F. Wieschaus. 2009. Pulsed contractions of an actin-myosin network drive apical constriction. *Nature*.

Matsuo, T., K. Takahashi, E. Suzuki, and D. Yamamoto. 1999. The Canoe protein is necessary in adherens junctions for development of ommatidial architecture in the Drosophila compound eye. *Cell Tissue Res*. 298:397-404.

Miyamoto, H., I. Nihonmatsu, S. Kondo, R. Ueda, S. Togashi, K. Hirata, Y. Ikegami, and D. Yamamoto. 1995. canoe encodes a novel protein containing a GLGF/DHR motif and functions with Notch and scabrous in common developmental pathways in Drosophila. *Genes Dev*. 9:612-25.

Muller, H.A., and E. Wieschaus. 1996. armadillo, bazooka, and stardust are critical for early stages in formation of the zonula adherens and maintenance of the polarized blastoderm epithelium in Drosophila. *J Cell Biol*. 134:149-63.

Nishimura, T., and M. Takeichi. 2009. Remodeling of the adherens junctions during morphogenesis. *Curr Top Dev Biol*. 89:33-54.

Paluch, E., and C.P. Heisenberg. 2009. Biology and physics of cell shape changes in development. *Curr Biol*. 19:R790-9.

Pokutta, S., F. Drees, Y. Takai, W.J. Nelson, and W.I. Weis. 2002. Biochemical and structural definition of the l-afadin- and actin-binding sites of alpha-catenin. *J Biol Chem*. 277:18868-74.

Sawyer, J.K., N.J. Harris, K.C. Slep, U. Gaul, and M. Peifer. 2009a. The Drosophila afadin homologue Canoe regulates linkage of the actin cytoskeleton to adherens junctions during apical constriction. *J Cell Biol*. 186:57-73.

Sawyer, J.M., J.R. Harrell, G. Shemer, J. Sullivan-Brown, M. Roh-Johnson, and B. Goldstein. 2009b. Apical constriction: A cell shape change that can drive morphogenesis. *Dev Biol*.

Solon, J., A. Kaya-Copur, J. Colombelli, and D. Brunner. 2009. Pulsed forces timed by a ratchet-like mechanism drive directed tissue movement during dorsal closure. *Cell*. 137:1331-42.

Takahashi, K., T. Matsuo, T. Katsube, R. Ueda, and D. Yamamoto. 1998. Direct binding between two PDZ domain proteins Canoe and ZO-1 and their roles in regulation of the jun N-terminal kinase pathway in Drosophila morphogenesis. *Mech Dev*. 78:97-111.

Takai, Y., and H. Nakanishi. 2003. Nectin and afadin: novel organizers of intercellular junctions. *J Cell Sci*. 116:17-27.

Torres, M., A. Stoykova, O. Huber, K. Chowdhury, P. Bonaldo, A. Mansouri, S. Butz, R. Kemler, and P. Gruss. 1997. An alpha-E-catenin gene trap mutation defines its function in preimplantation development. *Proc Natl Acad Sci U S A*. 94:901-6.

Wei, S.Y., L.M. Escudero, F. Yu, L.H. Chang, L.Y. Chen, Y.H. Ho, C.M. Lin, C.S. Chou, W. Chia, J. Modolell, and J.C. Hsu. 2005. Echinoid is a component of adherens junctions that cooperates with DE-Cadherin to mediate cell adhesion. *Dev Cell*. 8:493-504.

Wieschaus, E. 1997. From Molecular Patterns to Morphogenesis: The Lessons from Drosophila. *In* Nobel Lectures: Physiology or Medicine 1991-1995. N. Ringertz, editor. World Scientific Publishing Co., Singapore.

Yamada, S., S. Pokutta, F. Drees, W.I. Weis, and W.J. Nelson. 2005. Deconstructing the cadherin-catenin-actin complex. *Cell*. 123:889-901.

Zallen, J.A., and J.T. Blankenship. 2008. Multicellular dynamics during epithelial elongation. *Semin Cell Dev Biol*. 19:263-70.

Zhadanov, A.B., D.W. Provance, Jr., C.A. Speer, J.D. Coffin, D. Goss, J.A. Blixt, C.M. Reichert, and J.A. Mercer. 1999. Absence of the tight junctional protein AF-6

disrupts epithelial cell-cell junctions and cell polarity during mouse development. *Curr Biol*. 9:880-8.